NATIONAL BUREAU OF STANDARDS REPORT

4444

FIRST PROGRESS REPORT ON HYDRAULICS OF SHORT PIPES

HYDRAULIC CHARACTERISTICS OF COMMONLY USED PIPE ENTRANCES

by John L. French

TO
BUREAU OF PUBLIC ROADS
U. S. DEPARTMENT OF COMMERCE

December 28, 1955

U. S. DEPARTMENT OF COMMERCE
NATIONAL BUREAU OF STANDARDS

U. S. DEPARTMENT OF COMMERCE

Sinclair Weeks, *Secretary*

NATIONAL BUREAU OF STANDARDS

A. V. Astin, *Director*

THE NATIONAL BUREAU OF STANDARDS

The scope of activities of the National Bureau of Standards is suggested in the following listing of the divisions and sections engaged in technical work. In general, each section is engaged in specialized research, development, and engineering in the field indicated by its title. A brief description of the activities, and of the resultant reports and publications, appears on the inside of the back cover of this report.

Electricity and Electronics. Resistance and Reactance. Electron Tubes. Electrical Instruments. Magnetic Measurements. Process Technology. Engineering Electronics. Electronic Instrumentation. Electrochemistry.

Optics and Metrology. Photometry and Colorimetry. Optical Instruments. Photographic Technology. Length. Engineering Metrology.

Heat and Power. Temperature Measurements. Thermodynamics. Cryogenic Physics. Engines and Lubrication. Engine Fuels.

Atomic and Radiation Physics. Spectroscopy. Radiometry. Mass Spectrometry. Solid State Physics. Electron Physics. Atomic Physics. Nuclear Physics. Radioactivity. X-rays. Betatron. Nucleonic Instrumentation. Radiological Equipment. AEC Radiation Instruments.

Chemistry. Organic Coatings. Surface Chemistry. Organic Chemistry. Analytical Chemistry. Inorganic Chemistry. Electrodeposition. Gas Chemistry. Physical Chemistry. Thermochemistry. Spectrochemistry. Pure Substances.

Mechanics. Sound. Mechanical Instruments. Fluid Mechanics. Engineering Mechanics. Mass and Scale. Capacity, Density, and Fluid Meters. Combustion Controls.

Organic and Fibrous Materials. Rubber. Textiles. Paper. Leather. Testing and Specifications. Polymer Structure. Organic Plastics. Dental Research.

Metallurgy. Thermal Metallurgy. Chemical Metallurgy. Mechanical Metallurgy. Corrosion.

Mineral Products. Porcelain and Pottery. Glass. Refractories. Enameled Metals. Concreting Materials. Constitution and Microstructure.

Building Technology. Structural Engineering. Fire Protection. Heating and Air Conditioning. Floor, Roof, and Wall Coverings. Codes and Specifications.

Applied Mathematics. Numerical Analysis. Computation. Statistical Engineering. Mathematical Physics.

Data Processing Systems. Components and Techniques. Digital Circuitry. Digital Systems. Analogue Systems.

Cryogenic Engineering. Cryogenic Equipment. Cryogenic Processes. Properties of Materials. Gas Liquefaction.

Radio Propagation Physics. Upper Atmosphere Research. Ionospheric Research. Regular Propagation Services.

Radio Propagation Engineering. Frequency Utilization Research. Tropospheric Propagation Research.

Radio Standards. High Frequency Standards. Microwave Standards.

- Office of Basic Instrumentation
- Office of Weights and Measures

NATIONAL BUREAU OF STANDARDS REPORT

NBS PROJECT
0603-10-3586

December 28, 1955

NBS REPORT
4444

FIRST PROGRESS REPORT ON HYDRAULICS OF SHORT PIPES

HYDRAULIC CHARACTERISTICS OF COMMONLY USED PIPE ENTRANCES

by John L. French
Fluid Mechanics Section
Mechanics Division

TO
BUREAU OF PUBLIC ROADS
U. S. DEPARTMENT OF COMMERCE
Appropriation 13X0221 Federal Aid Highways

NBS

U. S. DEPARTMENT OF COMMERCE
NATIONAL BUREAU OF STANDARDS

TABLE OF CONTENTS

FIRST PROGRESS REPORT ON HYDRAULICS OF SHORT PIPES

HYDRAULIC CHARACTERISTICS OF COMMONLY USED PIPE CULVERT ENTRANCES

by John L. French

1. SCOPE OF REPORT

This report is a progress report issued to the sponsoring agency to summarize the completed experimental work of the investigation. The analysis of the data presented and the conclusions drawn from the data are tentative and subject to change as the continuing experimental work of the project makes further data available. In this connection this first progress report presents data only for various culvert inlets to short smooth culverts of length 12 diameters. Further, the experimental data presented are limited only to the head-discharge relationship and to regime of flow in the culvert and the important collateral data regarding pressures in the culvert and at its outlet are not yet available. It is therefore likely that future experimental data regarding the location of pressure lines, increased length, diameter and roughness of barrel, the effect of approach and outlet conditions and other developments will possibly significantly modify or alter the interpretation of the data presented herein.

For these reasons, the present report is to be considered only as an internal progress report to the sponsoring agency.

2. AUTHORIZATION OF PROJECT

The problems to be investigated in this project were formulated by the staff of the Hydraulic Research Branch, Bureau of Public Roads, Carl F. Izzard, Chief. The project was initiated by a letter of authorization dated June 25, 1954 from Mr. C. D. Curtiss, Acting Commissioner of Public Roads to Dr. A. V. Astin, Director of the National Bureau of Standards, and funds for the support of the project were subsequently transferred.

3. SCOPE OF INVESTIGATION

The specific objectives of the project are: (1) to determine the head-discharge relationship of commonly used non-rectangular culvert inlets under various conditions regarding slope, length, and roughness of the culvert barrel; (2) to determine the factors controlling regime change from sluice type flow to full conduit flow and the reverse; and to quantitatively define, for selected inlets the range of operation in each regime of flow; and (3) to develop improved types of culvert inlets of increased hydraulic efficiency.

The major portion of the experimentation will be done at small model sizes corresponding to a culvert barrel of 5.5 inches diameter. However, sufficient work will be done with 12-inch and 30-inch models to adequately determine model scale effect on some of the complex phenomena of culvert flow.

4. EXPERIMENTAL APPARATUS

The experimental apparatus used in the tests reported here consisted essentially of a 6-foot wide by 12-foot long by 4-foot high tank which served as the upstream approach channel for the model culvert; and a cantilevered truss 30 feet long for supporting the culvert barrel.

A sketch of the structure is shown in figure 1. The 6- by 12-foot tank was supported at 3 points. The two upstream supports consisted of pin connections to the supporting structure, allowing rotation in a vertical plane, and variation in slope of the approach channel and culvert barrel was conveniently obtained by adjusting the hydraulic jack at the third support point. In figure 2 is shown a photograph of the apparatus.

The pipe culvert barrel was made of lucite tubing with a nominal inside diameter of 5.5 inches. Maximum variation in tubing diameter was plus or minus 1/32 inch and the entrance section of the barrel was from selected stock with an actual diameter of 5.5 inches plus or minus 0.003 inches.

The pipe-arch barrel was molded from 1/4-inch thick lucite sheet. The dimensions of the pipe-arch section are shown in table 1. The dimensions shown were obtained by scaling down from a section of commercial 36-inch by 22-inch pipe-arch section. Unfortunately, the particular section used to obtain the model dimensions did not comply with the manufacturer's commercial tolerances as to cross-sectional dimensions and hence was not deemed a typical product by the manufacturer. Further, in scaling down the dimensions from the commercial pipe-arch section to a model size with a 5.5-inch vertical rise, the shape as indicated by the maximum outside dimensions of the corrugations were used. Inasmuch as the dimensions of the corrugations remain constant for all sizes of corrugated pipe-arch sections an error was thus involved. The error thus introduced had the effect of making the span to height ratio 1.45 for the lucite model as compared to a corresponding ratio of 1.47 for the prototype. The corrugations were not modeled, and the pipe-arch sections used in the tests reported here were made entirely with smooth boundaries.

The rate of discharge through the model culvert was measured by means of an orifice meter in a 4-inch diameter supply line for low rates of supply and by an orifice meter in an 8-inch diameter supply line for the larger rates of flow. The orifice meters were calibrated in place. The height of the water surface in the upstream pool, above the culvert invert at the inlet, was measured by means of a 1-inch diameter manometer tube, located two feet upstream from the headwall and near the wall of the approach channel as indicated in figure 1.

LIST OF FIGURES

Table 1

Dimensions of Model Pipe-Arch Section

x inches	y_1 inches	y_2 inches	x inches	y_1 inches	y_2 inches
0	0.0	5.50	2.450	.332	4.76
.175	.004	5.49	2.625	.402	4.65
.350	.013	5.47	2.800	.481	4.50
.525	.022	5.45	2.975	.586	4.35
.700	.035	5.42	3.150	.709	4.20
.875	.048	5.40	3.325	.856	3.99
1.050	.061	5.38	3.412	.995	3.92
1.225	.088	5.34	3.500	1.06	3.78
1.400	.105	5.29	3.587	1.172	3.65
1.575	.131	5.22	3.675	1.31	3.50
1.750	.157	5.15	3.762	1.47	3.32
1.925	.193	5.05	3.850	1.67	3.14
2.100	.228	4.97	3.937	2.01	2.84
2.275	.271	4.88	3.990	2.45	

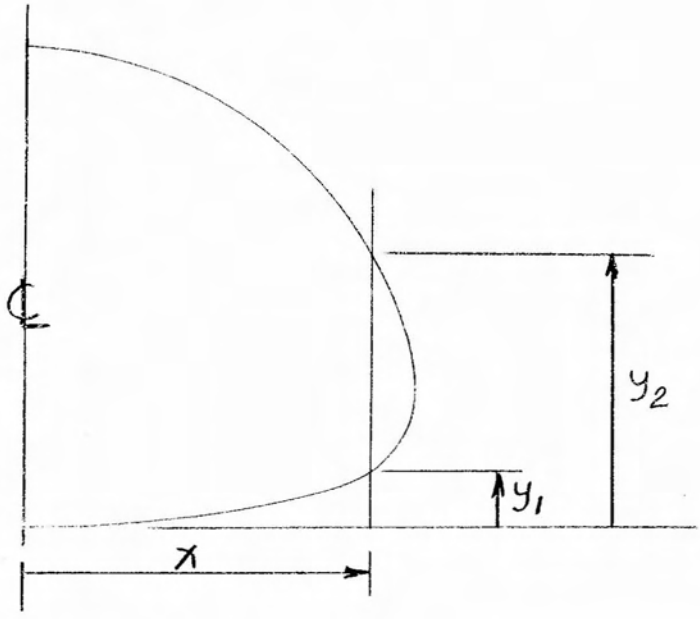

Slopes were measured by means of a graduated scale at a point on the cantilevered truss approximately 28 feet from the pin connection support. The zero slope reading on the scale was obtained by means of an engineer's level and the other slopes were computed from the scale readings.

The culvert headwall, embankment slope, wingwalls, and spill cones were modeled in lucite with the dimensions shown in figure 3. For ease in making setup changes the various inlets were designed to be installed in a 3/4-inch socket built into the headwall at the upstream end of the culvert barrel. Model changes involving typical headwall inlets could be made conveniently by installing a lucite ring of the appropriate shape, for example, a square edge, or socket inlet, in the 3/4-inch by 3/4-inch recessed groove. Sufficient care was taken in the machining of the various inlets and in their installation in the groove to insure proper alingment of the inlet with the culvert barrel. The joint between the inlet and culvert and between the inlet and headwall was in each case filled with sealing wax and sanded smooth.

5. FLOW CHARACTERISTICS OF COMMONLY USED CULVERT INLETS

Experimental data on 27 different culvert inlet models or modification of inlets were obtained during the course of that part of the investigation being reported here. These inlet models included several which were designed expressly for installation in a headwall, as well as many of the projecting type. A few of the inlets were tested with parallel and 45° wingwalls as well as with spill cones. A few of the inlets were also tested in narrow approach channels, as well as the relatively wide approach channel of the apparatus shown in figure 1. The detailed dimensions of the various model inlets tested are shown in figures 3, 4, 5, and 6, and a listing of the inlets is given in table 2.

Table 2

Model Numbering Schedule

By Type:

Type 1 - Culverts with right angle headwall, wall height 1.33D, length 6.25D, embankment spill cones. Number series 1 to 99 assigned.

Type 2 - Culverts with flared or parallel wingwalls. Number series 51 to 79 assigned.

Type 3 - Culverts without headwall or wingwall, barrel cut on a bevel to fit flush with embankment slope. Number series 81 to 99 assigned.

Type 4 - Culverts with barrel projecting to toe of embankment slope, no headwall. Number series 101 to 139 assigned.

Table 2 (continued)

Model Numbers of Each Type for Which Tests are Reported

Type 1, Circular Barrel

Model 1: square edge entrance profile

1.1: slightly rounded edge

2: pipe joint groove 0.042D by 0.083D

3: pipe joint groove 0.083D by 0.083D

4: pipe joint groove 0.05D by 0.07D

5: entrance profile rounded, radius 0.15D

6: entrance profile rounded, radius 0.25D

7: beveled edge entrance 0.0083D by 0.022D

4-B: same as 4 above, with trapezoidal restricted approach channel

Type 1, Pipe-Arch Barrel

Model 21: square edge entrance profile

22: beveled edge entrance 0.0083D by 0.022D

Type 2, Circular Barrel

Model 51: 45° wingwall angle, square edge entrance

52: 45° wingwall angle, pipe joint groove entrance, 0.05D by 0.07D

61: parallel wingwalls, square edge entrance

62: parallel wingwalls, pipe joint groove entrance, 0.05D by 0.07D

62.1: parallel wingwalls of height 2D

Type 3, Circular Barrel

Model 81: flush with embankment 2 to 1 slope, sharp edge entrance profile

Type 3, Pipe-Arch Barrel

Model 91: flush with embankment 2 to 1 slope, sharp edge entrance profile

Table 2 (continued)

Type 4, Circular Barrel

Model 101: square end, wall thickness 0.09D, square edge entrance profile

102: pipe joint groove 0.05D by 0.07D, wall thickness 0.09D

103: pipe joint groove 0.083D by 0.083D, wall thickness 0.12D

111: thin wall, inside bevel 0.0083 x 0.0220D

112: thin wall, inside bevel 0.0035 x 0.0092D

113: inclined plane bevel, top projection D/2, thin wall, no inside bevel

102-B,111-B: same as above with trapezoidal restriction approach channel

Type 4, Pipe-Arch Barrel

Model 126: thin wall, inside bevel 0.0083 x 0.0220D

5.1 Non-Submerged Flow

When the culvert inlet is non-submerged the flow controlling section will be either near the culvert inlet or culvert outlet, depending upon whether the slope of the culvert is greater or less than critical. If the slope is subcritical, the flow will pass through critical depth a relatively short distance upstream from the outlet. If the culvert slope is supercritical the control section will move upstream to the inlet as shown in figure 7. Analysis of this type of flow from the viewpoint of critical depth theory yields useful and convenient results.

Applying the energy principle we have, referring to figure 7

$$\frac{H}{D} + S_o \frac{L'}{D} + \frac{V_o^2}{2gD} = \frac{d_c}{D} + \frac{V_c^2}{2gD} , \qquad (1)$$

where S_o is the culvert barrel slope, V_o is the approach velocity, d_c is critical depth, V_c is critical velocity, L' is the distance downstream from the culvert entrance of the control section of critical depth, D is the diameter of the culvert barrel and H is the elevation of the upstream pool with reference to the invert of the culvert at the inlet section. In equation (1) energy losses between the upstream pool and the control section have been assumed to be negligible and the kinetic energy factor α, has been assumed to be one.

The sum of the terms on the right side of equation (1) is commonly designated the specific energy at critical depth and is computable. Analysis of tabulated values of the specific energy at critical depth for circular pipe indicate that to a close approximation in the range, $0.4 < \frac{d_c}{D} + \frac{V_c^2}{2gD} < 1.0$,

$$\frac{d_c}{D} + \frac{V_c^2}{2gD} = 0.58 \left(\frac{Q}{D^{5/2}}\right)^{0.57}, \qquad (2)$$

where Q is the rate of discharge. In equation (2) Q and D are required to be expressed in terms of feet and seconds.

Letting,

$$\frac{H_a}{D} = \frac{H}{D} + S_o \frac{L'}{D} + \frac{V_o^2}{2gD}, \qquad (3)$$

we have from equation (1) and (2)

$$\frac{H_a}{D} = 0.58 \left(\frac{Q}{D^{5/2}}\right)^{0.57}. \qquad (4)$$

Equation (4) is of the form

$$\frac{H_a}{D} = k \left(\frac{Q}{D^{5/2}}\right)^{n}, \qquad (5)$$

and the experimental work reported herein on non-submerged flow will be presented in the form of equation (5). Since equation (4) has been derived on the basis of no energy loss and an assumed value of $\alpha = 1$, deviations of k and n from the values of equation (4) will reflect non-conformance to the assumption made, and inaccuracies in the determination of L'.

Experimental data for non-submerged flow at supercritical slope for 21 models are shown in figures 8 to 14. Reference to these figures will show that for all the inlets tested, the experimental data can be adequately represented within the range of experimentation by a relation of the type of equation (5). The values of the constants k and n for the various inlets tested are given in table 3.

Table 3

Values of the Constants k and n of equation (5) for Supercritical Slopes (Non-Submerged Flow)

Model Number	k	n
1	0.592	0.615
1.1	.592	.615
2	.574	.600
3	.574	.600
4	.574	.600
5	.570	.595
6	.570	.595
7	.592	.615
51	.575	.615
52	.574	.600
61	.582	.600
62	.574	.600
81	.602	.575
101	.600	.620
102	.579	.615
102-B	.579	.615
103	.579	.615
111	.630	.615
111-B	.610	.615
112	.641	.620
113	.621	.620

It is to be noted that equation (5) was derived on the basis of an approximation valid only in the range $0.4 < H_a/D < 1.0$. Hence, the tabulated values of k and n in table 3 are valid only in the same range of H_a/D.

Of interest is the fact that the value of n is so nearly constant for all the inlets tested, and it is evident from table 3 that for inlets in a headwall with spill cones, 45° wingwalls or parallel wingwalls, or for projecting type inlets cut off perpendicular to the axis of the culvert, or of the overhanging type such as Model 113 that the value of n may be assumed constant and equal to 0.61 with only small error.

The experimental results reported here indicate in general, a small but definite and consistent slope effect for non-submerged flow. This effect was consistently apparent in the plotting of the data and could be readily detected in the laboratory by changing the culvert slope while the rate of discharge was held constant. This result was to have been expected from the data reported by Shoemaker and Clayton [1] to the effect that on a 4-inch square model box culvert the location of critical depth in non-submerged flow was a short distance downstream from the culvert entrance. A similar channel slope effect of approximately the same order of magnitude has been shown by Woodburn to exist in experimental studies of critical depth flow over broad crested weirs [2].

The effect of slope on non-submerged supercritical culvert flow can be accounted for, as indicated in the derivation of equations (4) and (5) by assuming that the control section of critical depth is located a distance L' downstream from the inlet and in the culvert barrel. Shoemaker and Clayton [1] have experimentally determined the length L' for certain types of box culvert inlets for a culvert slope of 4%, and have found that it varies with the rate of discharge through the box culvert as well as being dependent on the geometry of the inlet.

Since no direct measurements in the tests of this investigation were made on the magnitude of L' and since the slope effect is small, the length L' used in plotting the data of figures 8 to 14 was assumed for each inlet to be constant for all rates of discharge and for all supercritical slopes; and a value was assigned to L' which most nearly made the experimental data for all supercritical slopes form a common curve. This computational method is illustrated in figure 16 for Model 1. This procedure has the advantage of simplicity and at the same time is sufficient because the relative smallness of the slope effect does not affect to any appreciable degree the usefulness of figures 8 to 14 as engineering design curves for non-submerged flow conditions on supercritical slopes. Nevertheless it is apparent that a definitive determination of L' cannot be made in this manner. Indeed, in addition to the data of Shoemaker and Clayton [1], indicating that L'/D varies with $Q/g^{1/2} D^{5/2}$ and the geometry of the inlet, there is evidence from the data reported herein that for at least some of the inlets that L'/D varies with the slope.

Referring to figure 8 it is evident that the slight bevel of Model 7 produces no apparent improvement in hydraulic characteristics as compared with Model 1 for non-submerged flow. The data of Schiller [3] on a square edge pipe culvert inlet with spill cones agrees well with the data for Models 1 and 7 given in figure 8. Schiller's data on the square edge entrance with 30° wingwalls and with a barrel slope of 0.84% are slightly to the right of the data presented in figure 8 for Model 51, the square edge entrance with 45° wingwalls. Both investigations are in agreement that the wingwall construction is slightly, but not significantly more efficient than the spill cone type of construction.

Mavis [4] and Straub, Anderson and Bowers [5] have tested the circular square edge inlet in an experimental setup where the floor of the approach channel was substantially below the level of the culvert invert, rather than at the same level as was the case in the present experimental setup. Because of this difference in setup geometry it would be expected that separation effects would be greater in the experimental setup of Mavis and of Straub, Anderson and Bowers than in the present investigation and that consequently their results would be expected to plot to the left of those shown in figure 8 for Model 1. Also to be considered in this connection is that Mavis as well as Straub, Anderson and Bowers did not use spill cones or wingwalls in their model construction. Presumably because of these differences in geometry the experimental results of these investigations plot appreciably to the left of the data shown in figure 8 for Model 1. At an H_a/D of 0.8 the difference is approximately 10% with regard to the value of $Q/D^{5/2}$.

Karr [6] has also investigated the square edge pipe inlet experimentally. In his investigation the floor of the approach channel was at the same elevation as the culvert inlet. Karr's rates of discharge for a given water surface elevation are substantially greater than those obtained in the tests reported here, being approximately 12% greater at a value of H_a/D of 0.8.

Referring to figure 9 for pipe socket inlets in a headwall, Ree [7] has published fragmentary data on a pipe socket used on a pipe-outlet spillway. Ree's data agrees fairly well with that of figure 9 being approximately 4% to the left at a value of H_a/D of 0.8. All of the details of Ree's experimental setup are not available but the invert of the inlet was a distance $D/4$ above the floor of the approach channel. This factor, as indicated by the comparison of the data of Mavis [4] and Straub, Anderson and Bowers [5] on square edge inlets with the results for Model 1, would have the effect of causing Ree's data to plot to the left of that shown in figure 9.

Straub, Anderson and Bowers [5] were the first, to the writer's knowledge, to suggest rounding of a culvert inlet to improve its efficiency and they have reported data on a culvert inlet with radius of rounding of 0.15D corresponding to Model 5. The same experimental setup was used by these investigators with the rounded inlet as with the square edge inlet. That is, the floor of the approach channel was appreciably lower than the culvert invert and spill cones or wingwalls were not used. As was the case with the square edge inlet, these differences in inlet geometry as compared with that of the present investigation have caused the data of these investigators to plot appreciably to the left of the data reported here, being approximately 11% to the left at $H_a/D = 0.8$, with a rapidly increasing deviation as H_a/D becomes smaller.

Ree [7] has published data on an inlet rounded to a radius of 0.125D on a pipe-outlet spillway. His data is substantially the same as that of Straub, Anderson and Bowers [5] for H_a/D values greater than approximately 0.8 but plot increasingly to the right of the data of Straub, Anderson and Bowers [5] as H_a/D is decreased below 0.8. This effect would be expected from the fact that in Ree's setup the invert was 0.25D above the approach channel floor while in the setup of Straub, Anderson and Bowers this dimension was 0.437D.

Schiller [3] did not investigate the rounded entrance in a headwall but did test the projecting rounded inlet. In Schiller's test the radius of rounding was 0.15D, the length of culvert was 13 diameters, and the invert of the culvert was above the approach channel floor an unreported distance equal to the pipe wall thickness of the pipe used in the model study. The slope of the culvert in Schiller's test was zero. Schiller's data for this inlet appears to be substantially identical with the data of Models 5 and 6 in figure 10, although it might have been expected to plot to the left. The coincidence of Schiller's data for a projecting inlet with data for a similar inlet in a headwall indicates, as will presently be illustrated again, that for some inlets there is little or no difference in rating curves between the two types of installations.

In figure 11 are given data for three projecting type inlets; Model 101, square edge; Model 112, a sharp edge; and Model 113, the sharp edged overhanging type of projecting inlet developed by Karr [6]. As was the case for Model 1 of figure 8, Karr's data plots substantially to the right of that shown in figure 11 for Model 113, being approximately 10% to the right at $H_a/D = 0.8$. No immediate explanation of this deviation is apparent.

Schiller lists three points in the non-submerged range for a sharp edge thin walled projecting inlet. These three points agree quite closely with the data plotted in figure 11 for Model 112.

The data of figure 12 for Models 102, 103, and 102-B are in close agreement with Schiller's data on a pipe socket inlet of approximate dimensions 0.056D radial by 0.1D axial, and with a pipe wall thickness of 0.126D. These dimensions are comparable to the 0.05D by 0.07D and 0.083D by 0.083D pipe sockets used in this investigation. In Schiller's experimental setup the invert of the culvert model was 0.126D above the floor of the approach channel and the slope used was 0.2%. The subcritical slope used by Schiller and the fact that the invert was above the approach channel floor would be expected to cause Schiller's data to plot to the left of the data for Models 102, 103, and 102-B of figure 12. It is to be concluded that the culvert length of 13D used by Schiller was sufficiently short and smooth so that negligible energy losses occurred on subcritical slopes between the inlet and outlet; and in addition that separation effects with the socket inlets are substantially equal whether the inlet is flush with the approach channel floor or a pipe wall thickness above it.

In figure 13 are given data for the square edge model flush with the embankment slope, Model 81. Schiller's data plot appreciably to the left of the data shown. Schiller's data were for an embankment slope of 1-1/2 to 1 while the embankment slope used in the experiments reported here was 2 to 1. Whether the difference in test results noted is due to unequal embankment slopes or to differences in edge condition such as caused the difference in test results between Models 1 and 1.1 is not known.

It has been noted that Schiller's results with the projecting rounded inlet of radius 0.15D was substantially identical with the results of these tests with a similar inlet in a headwall. Referring to table 3 it will be noted that k and n of equation (5) are substantially the same for Models 1 and 101. In like manner the constants k and n are approximately equal for inlets 3 and 4 in a headwall and the similar projecting type inlets, Models 102, 102-B, and 103. This phenomena appears to be identical to that investigated by Harris [8] with re-entrant pipes flowing full. Harris concluded from his investigation that the entrance loss for re-entrant pipes of 0.05D or greater wall thickness was identical with the entrance loss for a flush type inlet. It is to be similarly concluded from the data presented here for non-submerged flow, together with Schiller's data, that for commercial type pipes, with wall thickness approximating 0.1D that the hydraulic efficiency of the projecting square end type inlet is substantially the same as a similar inlet ending in a headwall.

In figure 14 are shown data for Model 61, a square edge entrance with parallel wingwalls. These data are in substantial agreement with the data of Schiller for the same inlet on a slope of 0.84%.

In figure 15 are shown data for Models 2, 3, and 5 on zero slope. The control section for zero slope is near the outlet, and the data shown are, of course, valid only for the barrel roughness and length used in the tests.

5.2 Submerged Entrance - Entrance Control

As first pointed out by Mavis [4] submergence of a culvert inlet does not necessarily insure that a culvert will flow full. On the contrary Mavis found, with submerged square edge inlets connected to relative short culverts and with free outfall, that the typical regime of flow in the culvert was part full with a free surface.

Mavis' observation of part full culvert flow with submerged entrance has been amply confirmed by subsequent investigators and Shoemaker and Clayton [1] have aptly applied the term sluice flow to this type of flow.

Referring to figure 17 separation of the flow at the entrance from the upper surface of the pipe has occurred with consequent formation of a free surface. From analogy with sluice flow phenomena we may consider that the vena-contracta has formed at section 2. The profile of the free surface

downstream for the vena-contracta will depend upon downstream conditions as well as the rate of discharge through the culvert. These factors would include slope, length, diameter, and roughness of the culvert barrel as well as outlet conditions relating to tail water elevation or type of support of the issuing jet. Although the resemblance of this type of flow to conventional sluice flow has been cited the analogy is limited in certain important aspects of the phenomena by the circular culvert conduit confining the flow downstream of the headwall. Most importantly, it may be observed that if the slope is sufficiently flat and if the culvert is sufficiently long and rough, the free surface of the flow will rise to the top of the pipe culvert and the free-surface type sluice flow shown in figure 17 will not occur.

The existence of the closed conduit within which the sluice type flow occurs, affects the flow phenomena also owing to air entrainment by the free surface. Because of air entrainment it is necessary that air circulation as shown in figure 18 occur. Such air circulation has been repeatedly observed in these tests. Air circulation of this nature can be expected to have the effect of lowering the air pressure over the free surface at the inlet to a subatmospheric value. Further, since increasing degrees of submergence can be expected to be accompanied with increased mean water velocities in the conduit with consequent increase in air entrainment, together with an increase in water depth at the culvert outlet, it is to be expected that the pressure reduction above the water surface at the inlet will increase as H/D or $Q/D^{5/2}$ increases. Hence, although the flow of water under a sluice gate is subject to only the constant normal atmospheric pressure, it is evident that such is not necessarily the case for so-called sluice flow in a culvert inlet.

Throughout certain ranges of H/D, vortices form in the upstream pool through which air is discharged into the culvert through the inlet. This phenomenon is more pronounced with full conduit flow than with sluice type flow, but nevertheless appears to be a significant aspect of the latter type of flow. Because of the flow of air into the culvert through vortex action the fluid in the culvert near the inlet in sluice type flow is not necessarily water alone, but in certain ranges of H/D is an air-water mixture. It is also apparent that the air introduced to the culvert inlet through vortex action will have the effect of reducing the subatmospheric pressure differential that air entrainment along the free surface could be expected to cause. The relative magnitudes of these compensating factors are as yet unknown.

Sluice type flow rather than full conduit flow is characterized by gross separation of the main flow from the boundary surface near the inlet. This separation, of course, occurs around the periphery of the inlet as well as at the top of the inlet. In this connection reference to figure 19 indicates separation to be occurring around the full periphery of the projecting inlet, except near the bottom. The drops of water visible in the photograph are adhering to the inside surface of the pipe and indicate separation around practically the full periphery of the inlet. Upon close

examination of the photograph of figure 19a it will be observed that spiral counter clockwise flow of water along the inside pipe boundary is occurring a short distance downstream from the inlet. This aspect of the flow is also clearly seen in figure 19b which is a view of the inlet looking vertically downward. The spiral flow phenomenon illustrated by the photographs of figures 19a and 19b is somewhat unstable. The situation shown in figure 19b was observed frequently, but equally as often the direction of the spiral motion was reversed, or spiral motion was initiated on each side and met at the top of the culvert and then plunged vertically downward to the water surface as indicated in figure 20.

For the above reasons, although the analogy to sluice flow is most useful in analysis of the problem, it is evident that as regards important details of submerged but not full conduit flow the sluice flow analogy must be used with a degree of caution.

Referring to figure 17 and assuming uniform flow at sections 1 and 2, we may write from energy consideration

$$\frac{\rho v_o^2}{2} + \rho g\,(H + S_o L') = p_a + \rho \alpha \frac{v^2}{2} + \rho g h + \rho g h_e, \qquad (6)$$

where v_o is the approach velocity, v is the mean velocity at section 2 associated with the depth h, α is the kinetic energy factor, h_e is the head lost between section 1 and 2, and p_a the difference between atmospheric pressure and the air pressure over the free surface at section 2.

The energy head loss, h_e, between sections 1 and 2 of figure 17 may in general result from two causes; first from energy losses associated with separation effects in the immediate neighborhood of the entrance and secondly from energy losses associated with boundary drag. We assume that the first, commonly termed an entrance loss, predominates and that L' is sufficiently short so that the latter type of loss is negligible. Entrance losses are commonly expressed in terms of the velocity head in the barrel thus

$$h_e = k_e \frac{v^2}{2g}.$$

Substituting in equation (6),

$$\frac{\rho v_o^2}{2} + \rho g\,(H + S_o L') = p_a + \rho \alpha \frac{v^2}{2} + \rho g h + k_e \rho \frac{v^2}{2}, \qquad (7)$$

and letting $H' = H + \frac{v_o^2}{2g} + S_o L'$, (8)

and $v = Q/A_2$,

where Q is volume rate of flow and A_2 is the cross-sectional area occupied by water at section 2, we have, after rearranging

$$H' - (h + p_a/\rho g) = \frac{Q^2}{2gA_2^2}(\alpha + k_e),$$

or

$$Q = \frac{1}{(\alpha + k_e)^{1/2}} A_2 \sqrt{2g\left[H' - (h + \frac{p_a}{\rho g})\right]},$$

which may be put in the form

$$Q = \frac{1}{(\alpha + k_e)^{1/2}} \frac{A_2}{A} A\sqrt{2g\left[H' - (h + \frac{p_a}{\rho g})\right]} \qquad (9)$$

where A is the area of the culvert barrel. It is apparent that

$$\frac{1}{\sqrt{\alpha + k_e}} \frac{A_2}{A}$$

is of the nature of a discharge coefficient and we may write,

$$Q = C_D A\sqrt{2g\left[H' - (h + \frac{p_a}{\rho g})\right]} \qquad (10)$$

where the discharge coefficient is defined by,

$$C_D = \frac{1}{\sqrt{\alpha + k_e}} \frac{A_2}{A}. \qquad (11)$$

Equation (10) can be put in the convenient form

$$\frac{H'}{D} = \frac{Q^2}{2C_D^2 A^2 gD} + \frac{h}{D} + \frac{p_a}{\rho gD}, \qquad (12)$$

or giving A its value in terms of barrel diameter,

$$\frac{H'}{D} = \frac{0.812}{C_D^2}\left(\frac{Q}{g^{1/2} D^{5/2}}\right)^2 + \frac{h}{D} + \frac{p_a}{\rho gD}. \qquad (13)$$

Equation (13) will be of utility in analyzing the experimental data only if, for a given inlet geometry and for a given culvert barrel, C_D, and

$$\left(\frac{h}{D} + \frac{p_a}{\rho g D}\right)$$

are substantially constant throughout the major part of the range of experimentation, and only if the length L' which enters into H'/D through equation (8) is either negligible or constant. That such is the case is indicated by the experimental data of figures 21 to 32, and we can write for equation (13)

$$\frac{H'}{D} = k_1 \left(\frac{Q}{D^{5/2}}\right)^2 + k_2, \qquad (14)$$

where k_1 and k_2 are constants for a particular model installation. Equation (14) has served as a guide in the plotting of all the experimental data on sluice type flow. That is H'/D has been plotted against $(Q/D^{5/2})^2$.

The experimental results for Model 1 under sluice type flow are given in figure 21. The experimental results of Straub, Anderson and Bowers [5] check the data of figure 21 for Model 1 quite closely, indicating that the differences in experimental setup described in the discussion of the results for non-submerged flow, have little apparent effect for sluice type flow. As indicated previously the various models of inlets in a headwall were obtained by inserting an appropriately shaped lucite ring into a socket in the headwall. In the case of Model 1, the square edged inlet in a headwall, the ring was symmetrical and the correct geometry of the inlet could be obtained by inserting the ring in such a manner that either face was flush with the headwall. Thus the ring made it possible to obtain Model 1 with either of the ring edges forming the "square edge" of the model. Casual examination of the ring would indicate that both edges were equally square and would serve satisfactorily. However, a more careful examination indicated an extremely slight rounding of one of the edges, such as might be formed by the machinist smoothing the edge with a few strokes of emery cloth. This rounding was not uniform around the circumference of the ring but was estimated to average approximately 0.1 mm in radius. Although the difference in the two edges of the ring was visually barely perceptible, the hydraulic effect was sufficiently large to cause Model 7 (beveled edge) to indicate consistently smaller discharges for a given headwater elevation than the square edge with the extremely small rounding stated above.

Use of the squarest edge of the ring gave results which caused the head-discharge curves of Model 1 and Model 7 to have the proper qualitative relationship to each other. It is to be concluded that results on some of the various sharp and square edged inlets obtained by different investigators may differ by several percent unless the control edges of the models are made to extremely close tolerances.

The square edge with the extremely small rounding referred to above has been designated Model 1.1 and the experimental data obtained with this inlet are shown in figure 21. Schiller's [3] data for the square edge inlet with spill cones plots slightly to the right of the data in figure 21 giving approximately 4% greater values of $Q/D^{5/2}$ than Model 1 and 2% greater than Model 1.1 at H/D = 3.0. This divergence of experimental results is apparently due in part at least to differences in the location of the spill cones. In the tests reported here the spill cones were 1.25D apart at the headwall at the elevation of the channel floor, while in Schiller's investigation the spill cones were sufficiently close together to be substantially tangent to the circular inlet at a point approximately 1/8 D above the culvert invert. Schiller's arrangement of the spill cones would be expected to decrease contraction and it is to be concluded that a small increase in capacity will result from locating the spill cones as near the culvert inlet as scour and erosion effects will permit.

In figures 22 and 24 are given data for the socket and rounded inlets in a headwall, under sluice flow conditions. Insofar as the writer is aware data directly applicable to the inlets of figures 22 and 24 under sluice flow conditions have not be published. Reference to figure 22 will show that Models 3 and 4, the pipe socket inlets of dimensions 0.083D by 0.083D and 0.05D (radial) by 0.07D gave identical results while Model 2 with socket dimension of 0.042D by 0.083D gave slightly smaller discharges at corresponding degrees of submergence. It is to be concluded that the pipe sockets of Models 3 and 4 are equally effective in suppressing contraction when mounted in a headwall. It is of interest to note from figure 29 that the data for similar sockets mounted in projecting inlets, Models 102 and 103 indicate that Model 103 (0.083D by 0.083D) gives appreciably greater discharges at corresponding levels of the upstream pool than does Model 102 (0.05D by 0.07D). In this connection comparison of the data of figure 29 for Model 103 with the data of figure 22 for Model 3 will show that the two inlets are substantially equivalent. Comparison of the data of figure 29 for Model 102 with the data of figure 22 for the corresponding socket in a headwall, Model 4, will indicate that the projecting inlet, Model 102, gives appreciably less discharge for equivalent degrees of submergence.

In figure 25 are given data for the square edge inlet in a headwall with two types of wingwalls and with the edge beveled to simulate in an approximate manner the type of inlet obtained with a corrugated pipe culvert in a headwall. The data for this latter inlet, Model 7, are to be compared with the data of figure 21, for Model 1, square edge in a headwall, and with the data of figure 22 for the socket inlets in a headwall. It will be noted that Model 7 gives somewhat greater discharges than Model 1 at comparable values of H/D, but is substantially less efficient than any of the three socket inlets tested.

Comparison of the data of figure 25 for Models 1, 51, and 61, indicate that the effect with regard to the square edge inlets of spill cones and the type of parallel wingwalls used here is substantially the same, while 45° wingwalls have the effect of slightly increasing the rate of discharge for a given upstream pool level. In this connection it is to be noted that Schiller [3] obtained substantially identical results on a square edge inlet, with spill cones, 30° wingwalls and parallel wingwalls. Schiller's results for these three inlet variations agree closely with the data shown in figure 23 for the square edge with 45° wingwalls. It is to be noted in this connection that the data presented here is not precisely comparable to Schiller's results for any of the three inlets. In the case of Model 1, as indicated previously, the spill cones in Schiller's tests were somewhat nearer the inlet, being substantially tangent to the circular inlet a short distance above the invert. With regard to the parallel wingwalls, they were placed a distance D apart in Schiller's tests and a distance 1.25D apart in the tests reported here. In the case of the flared wingwalls, Schiller's angle of flare was 30° as compared with 45° in the tests reported here. It is to be inferred from a comparison of Schiller's results with those reported here for Models 1, 51, and 61 that (a) 30° and 45° wingwall flares are substantially equivalent in their effect on inlet efficiency, (b) that parallel wingwalls are more efficient when placed tangent with the circular inlet than with a spacing greater than D, and (c) that spill cones produce greater discharges for sluice type flow at a given degree of submergence when placed as close to the inlet as possible.

From figure 22 it will be noted that the rating curve for Model 4 and Model 52 are identical, indicating that spill cones and 45° wingwalls are substantially equivalent to each other for the .05D by .07D socket inlet. This result is to be compared with the experimental data for the square edge inlet in which the use of 45° wingwalls produced a slight increase in capacity as compared with spill cones. Reference to figure 33 will show that Model 4, the .05D by .07D socket inlet in a headwall, is substantially more efficient hydraulically than Model 1 and it is to be inferred that while the 45° wingwall produces an upstream flow pattern or a turbulence level less conducive to separation in the inlet than spill cones that the effect is sufficiently small to be negligible for inlets such as Model 4, of such shape to, of themselves, produce only relative small contraction effects. In the case of such inlets as Model 1, in which severe contraction of the flow occurs, the relatively minor improvement in the upstream flow pattern caused by the 45° wingwall as compared with spill cones is sufficient to be detected experimentally as a small increase in discharge, being in the tests reported here approximately 4% at $H/D = 4.0$. It is to be inferred that the 45° wingwalls as compared to the spill cones used here will produce a relatively small improvement in rate of discharge for those inlets subject to relatively high degree of contraction in sluice type flow such as Model 1, and that the magnitude of the improvement decreases as the efficiency of the inlet increases and will be negligible for those inlets of relatively low contraction effects such as Models 3, 4, and 5.

With regard to parallel wingwalls comparison of the data of figure 25 for Models 51 and 61 and comparison of the data of figure 22 for Model 52 with the data of figure 26 for Model 62 indicates that for both the square edge inlet and the .05D by .07D socket inlet that the parallel wingwalls are to a small degree less efficient than 45° wingwalls. As indicated in figure 25 Model 61, the square edge inlet with parallel wingwalls, is substantially the equivalent of the square edge with spill cones. Similar comparison of the data of figure 26 for Model 62 with the data for Model 4 shown in figure 22 indicates that the parallel wingwalls are appreciably less efficient with the 0.05D by 0.07D socket inlet than spill cones. It is to be concluded that, insofar as the rating curve for sluice type flow is concerned that the parallel wingwalls used in these tests are less efficient than spill cones. The above conclusions regarding the relative merits of 45° wingwalls, parallel wingwalls, and spill cones apply only to the relative efficiency of these inlet modifications in sluice type flow. A more significant and important measure of inlet efficiency under certain field conditions is the point at which a particular model causes change from sluice type flow to full conduit flow. With this criterion of inlet efficiency it will be shown shortly that the test results indicate certain advantages of parallel wingwalls over either spill cones or 45° wingwalls.

In figure 27 are given data for the square edge inlet flush with the embankment slope. Schiller's data for a similar inlet on an embankment of slope 1-1/2 to 1 rather than the 2 to 1 slope used here are also shown. Comparison of the data of figure 27 for Model 81 with the data of figure 21 for Model 1 will show that Model 81 is substantially less efficient than the corresponding inlet in a headwall, insofar as the sluice type rating curves are concerned. However, data to be presented shortly will show that Model 81 will produce full conduit flow at appreciably lower degrees of submergence than will Model 1.

Data on the square edge projecting inlet, Model 101 are given in figure 28. It will be noted that with this inlet as with several others tested that the rating curve appears to have a change in slope in the neighborhood of H/D = 2.0. It is not immediately clear why this should be so, but it may be noted that Addison [9] in tests of model sluices has observed the same effect. Comparison of the data for this model with the data of figure 21 for the square edge inlet in a headwall will show that the two inlets are substantially equivalent, indicating that the pipe wall thickness of the projecting inlet was sufficiently large to cause the re-entrant inlet to have substantially the same flow characteristics as a flush inlet.

In figure 30 are given data on the thin walled projecting inlets tested. Schiller's data on a thin wall projecting inlet are also plotted. The change in slope of the rating curves at an approximate value of H/D of 2.3 is to be noted. Comparison of the data of this figure with the data of figure 29 for Models 102 and 103 will show that the projecting

thin wall models have substantially less capacity than the projecting pipe socket inlets. Reference to the data of figure 25 for Model 7 will show that the projecting thin wall inlets for Models 111 and 112 have also substantially less capacity than the corresponding model in a headwall, Model 7.

Comparison of the data of figures 22 and 23 for Models 4 and 4-B with the data of figures 29 and 31 for the corresponding projecting inlets, Models 102 and 102-B will show that the projecting type inlets are appreciably less efficient. Comparison of the data of figure 22 for Model 3 with the data of figure 29 for Model 103 will indicate that, for the 0.083D by 0.083D socket inlet with a pipe wall thickness of 0.12D, there is no appreciable difference in performance between the projecting and headwall inlets.

It is to be concluded that the projecting inlets are uniformly less efficient than the corresponding inlet in a headwall, except in those cases where the pipe wall thickness of the projecting inlet is sufficiently large to cause the projecting inlet to have substantially the same hydraulic characteristics as a flush type inlet.

In figure 31 are shown the sluice flow data for Model 111-B; a thin wall inlet in the trapezoidal channel with flood plain shown in figure 6. For convenience, the rating curve for Model 111 has also been shown. It will be observed that essentially identical results were obtained for the higher degrees of submergence; the difference in rating curves being sufficiently small to warrant a single rating curve for the two models for the higher degrees of submergence.

Comparison of the data of figures 22 and 23 for Models 4 and 4-B and of figures 29 and 31 for Models 102 and 102-B indicates that the effect of the restricted trapezoidal channel with flood plain shown in figure 6 is to consistently reduce the rate of discharge for the higher degrees of submergence. However, detailed comparison of the data of these figures will show that for sluice type flow the magnitude of the difference in discharge rate at corresponding values of H/D does not exceed approximately 6% for the two types of channels, and it is to be concluded from the data for Models 4-B, 102-B, and 111-B that insofar as the sluice type flow rating curves are concerned that the two types of channels are substantially equivalent for the higher degrees of submergence.

For the lower degrees of submergence it will be observed that for Models 102-B and 111-B that the effect of the constricted trapezoidal channel is to increase the rate of discharge as compared with the wide rectangular channel, and in the case of Model 4-B, to cause full conduit flow as shown in figure 47.

The depth of water H over the invert of the inlet was obtained in the case of the models with the constricted trapezoidal channel by means of a manometer opening located in the bottom of the channel 30 inches

upstream from the headwall. The manometer opening was located on the centerline of the channel. For low rates of flow a hydraulic jump sometimes formed in the channel. The location of the jump was in all cases upstream for the manometer opening. For the lower rates of flow the approach velocity was sufficiently high to warrant inclusion of the approach velocity head in the computed values of H'/D. That is, in figure 31, as well as in figure 23,

$$\frac{H'}{D} = \frac{H}{D} + S_o \frac{L'}{D} + \frac{v_o^2}{2gD} .$$

In figure 32 are given data on sluice type flow in inlet Model 113. In Karr's original development tests [6] on this model full conduit flow was obtained for values of H/D above approximately 1.2 and hence data for sluice type flow was not reported.

All the data of figures 21 to 32 can be represented to a close approximation by a relation of the type of equation (14). In table 4 are given experimentally determined values of k_1 and k_2 of equation (14) and values of the discharge coefficient C_D of equation (11) for the various models. It is to be noted that the discharge coefficient C_D and k_2 for Models 1 and 101 and for Models 3 and 103 are substantially equal, illustrating the effect of pipe wall thickness on the efficiency of projecting type inlets as reported by Harris [8].

For ease in comparing the results for the various models, the rating curves for representative inlets have been plotted in figure 33.

In the plotting of the data of figures 21 to 32 that value of L' was used which most nearly brought the data for the various slopes for a particular inlet into coincidence. This method has the obvious advantage of simplicity but as indicated in the discussion of the same problem in non-submerged flow, cannot serve as a definitive determination of the dimension. In this connection there is evidence in the plotting of the data that L' varies with H/D as well as with the inlet geometry; the slope effect appearing to be less pronounced for higher values of H/D than for the lower values. However, because of the general smallness of the effect and the lack of direct measurements on the length L', the dimension was assumed for simplicity to be constant throughout the range of experimentation for a given inlet. Reference to the data of figures 21 to 32 will show that this assumption of a constant L' for each inlet yields, within the range of experimentation sufficiently consistent results.

The effect of the vena contracta of figure 17 being located the distance L' downstream is, of course, that for a given value of H, the effective head $H + S_o L'$ increases as the slope increases with a consequent increase in Q. This relatively small but consistent effect of increasing slope causing an increase in Q for a given H has also been observed by Shoemacher and Clayton [1] with box culverts.

The lack of direct measurements on the length L' of figure 17 has been mentioned. In this connection it may be noted that direct measurement of L' for many of the inlets is an experimental task of considerable difficulty. Figures 19 and 20 indicate one aspect of flow condition near the inlet section for some of the inlets. A further difficulty in this connection is the transverse as well as longitudinal wave action occurring in general with sluice type flow. Typical conditions are as shown in figure 34. Under these conditions direct experimental measurements of L' as well as the depth h of figure 17 for some of the models is virtually impossible in certain ranges of H/D.

Thus while the sluice flow analogy has been useful in the development of equations (13) and (14) and in the handling of the data, it is apparent that the phenomena involved in closed pipe culverts deviate appreciably from that encountered in the flow of water under a conventional sluice gate.

In connection with the applicability of the sluice flow analogy to pipe culvert flow one further limitation of the conventional two-dimensional sluice analogy leading to equations (13) and (14) deserves mention.

From equation (13) and (14) it is apparent that

$$k_2 = \frac{h}{D} + \frac{p_a}{\rho g D} \cdot \qquad (15)$$

It is evident that if, as appears reasonable, $p_a/\rho gD$ is assumed for low rates of flow to be negligibly small that k_2 may be assumed equal to h/D, the relative depth of water at the vena contracta. Hence, A_2/A may be computed and $(\propto + k_e)$ determined for each inlet model from equation (11). If values of $(\propto + k_e)$ are computed in this manner from the values of k_1 and k_2 given in table 4 it will be found that for low values of H/D two inlets show $(\propto + k_e)$ to be less than 1, indicating, (1) experimental error, or (2) insufficient data to adequately define the rating curve for low values of H/D, or (3) that the assumption of negligible air pressure in the inlet, even for low values of H/D is unwarranted, or (4) that the simple two-dimensional sluice flow analogy used in the analysis leading to equation (13) does not adequately represent the culvert phenomena insofar as $(\propto + k_e)$ is concerned. In connection with this last possibility it is to be noted that the assumption was made in the analysis leading to equation (15) that hydrostatic pressure conditions prevail at the vena contracta, section 2 of figure 17. Owing to wave formation with consequent curvilinear flow, such as shown in figure 34 this is not necessarily the case for all models.

Assuming curvilinear flow at the control section, and referring to figure 35 we have along the streamline c, for the counterpart of equation (6),

$$\frac{\rho v_o^2}{2} + \rho g\,(H + S_o L') = p_y + \rho g y + \frac{\rho v_y^2}{2} + \rho g h_y\,, \qquad (16)$$

where p_y and v_y are respectively the pressure and velocity on the streamline c at the control section a distance y above the invert, and h_y is the energy head loss along the streamline between the upstream pool and the control section.

Integrating equation (16) over the whole flow

$$\int_A \left[\frac{\rho v_o^2}{2} + \rho g\,(H + S_o L')\right] v_o dA = \int_a \left(p_y + \rho g y + \frac{\rho v_y^2}{2} + \rho g h_y\right) v_y da,$$

where A is the area of the approach channel, and a is the area of flow at the control section. Assuming for simplicity that v_o is constant, and rearranging,

$$\frac{\rho v_o^2}{2} + \rho g\,(H + S_o L') = \frac{1}{Q}\int_a \rho \frac{v_y^3}{2}\, da + \frac{1}{Q}\int_a \rho g h_y\, v_y da +$$

$$+ \frac{1}{Q}\int_a (p_y + \rho g y)\, v_y\, da, \qquad (17)$$

from which

$$\frac{\rho v_o^2}{2} + \rho g\,(H + S_o L') = \frac{\rho \alpha v^2}{2} + \rho g h_e + \frac{1}{Q}\int_a (p_y + \rho g y)\, v_y\, da, \qquad (18)$$

and it is apparent from consideration of equations (8), (14), (15), and (18) that

$$k_2 = \frac{1}{Q}\int_a (p_y + \rho g y)\, v_y\, da. \qquad (19)$$

If hydrostatic pressure distribution prevails at the control section

$$p_y = p_a + \rho g\,(h - y), \qquad (20)$$

and equations (18) and (19) reduce respectively to equations (6) and (15). However, if curvilinear flow prevails at the control section it is at once obvious from equation (19) that k_2 is not the equivalent of h/D, even for low rates of flow with short culverts, where p_a can be expected to be negligible. It follows that values of $(\propto + k_e)$ computed from experimental results by means of equations (11) and (13) for low rates of flow on the assumption that p_a will then be negligibly small will be in error if curvilinear flow due to wave action such as indicated by figure 34 prevails at the control section.

The presence in general of curvilinear flow at the control section appears to cause the computed values of $(\propto + k_e)$ determined from equations (11) and (13) to be less than 1 for some of the models, and indicates the doubtful validity of computing $(\propto + k_e)$ in that manner. It is of interest to note in this connection that values of $(\propto + k_e)$ computed in the manner of equations (11) and (13) from the data of Addison [9] on certain of the sluice models of the Assuan Dam also indicate values of $(\propto + k_e)$ less than 1, and thus suggesting curvilinear flow at the control section.

The principal conclusions of the experimentation with regard to the sluice flow rating curves may be summarized as follows:

1. The beveled edge inlet in a headwall, Model 7, is somewhat more efficient than the square edge inlet in a headwall, Model 1.

2. The socket inlets in a headwall, Models 2, 3, and 4 are appreciably more efficient than Model 1 or Model 7.

3. The rounded inlets tested here, Models 5 and 6 are more efficient than the other models tested.

4. The projecting inlets are less efficient than corresponding inlets in a headwall, except for those inlets in which the pipe wall thickness is sufficiently great to cause the projecting inlet to perform essentially as an inlet in a headwall.

5. The projecting thin wall inlets are less efficient than the projecting square edge or socket inlets.

6. Model 81, the square edge inlet flush with the embankment slope is less efficient than any of the inlets tested with the exception of the thin wall projecting inlet.

7. Comparison of Schiller's data on Model 1 with the data reported here indicates (a) that relatively minor differences in location of spill cones and parallel wingwalls with reference to the inlet exert small but consistent effects upon the efficiency of the inlet, and (b) that wingwalls of 30° and 45° angle of flare are substantially equivalent.

8. While consistent differences in results were observed with some of the model inlets in the trapezoidal channel with flood plain, as compared with the wide rectangular approach channel, the effects were in general small and to an approximation the two channels may be considered substantially equivalent, insofar as the sluice flow rating curves are concerned.

Table 4

Experimentally Determined Values of C_D, k_1, and k_2 of Equation (14) for Sluice Type Flow in Circular Pipe Culverts

Model	Range	C_D	k_1	k_2
1	*	0.624	0.0648	0.663
1.1	*	.643	.0610	.683
2	*	.696	.0522	.691
3, 4 and 52	H/D<1.9	.716	.0489	.700
3, 4 and 52	H/D>1.9	.738	.0463	.757
4-B	*	.710	.0501	.780
5	*	.779	.0415	.740
6	*	.899	.0312	.973
7	*	.635	.0624	.672
51	*	.651	.0594	.691
61	*	.640	.0612	.820
62	*	.696	.0521	.688
81	H/D<2.2	.543	.0856	.571
81	H/D>2.2	.590	.0727	.815
101	H/D>2.4	.611	.0673	.600
101	H/D<2.4	.625	.0643	.680
102	*	.700	.0514	.688
102-B	*	.668	.0567	.578
103	*	.732	.0468	.757
111	H/D<2.2	.564	.0826	.646
111	H/D>2.2	.528	.0906	.490
111-B	*	.521	.0922	.440
112	H/D<2.2	.544	.0854	.650
112	H/D>2.2	.518	.0938	.488
113	*	.578	.0755	.665

* full range of experimentation

5.3 Full Conduit Flow

Transition from part full to full conduit flow occurs for most of the inlets tested in this investigation, if the relative degree of submergence is increased sufficiently.

The application of the energy principle leads to

$$\frac{H}{D} + S_o \frac{L}{D} - \frac{\beta}{D} = \left(\frac{4}{\pi}\right)^2 \frac{Q^2}{2gD^5} \left(\alpha + k_e + f_1 \frac{L}{D} \right), \qquad (21)$$

where S_o is the slope of the culvert, β is the elevation above the outlet invert at which the pressure line or hydraulic gradient pierces the plane of the outlet, Q is the culvert discharge, α is the kinetic energy correction factor and f_1 is the effective Darcy-Weisback resistance coefficient over the entire length of the culvert, which, from the work of Keulegan [13] can be expected to vary with L, when L is comparatively short. Letting

$$C_1 = \left(\frac{4}{\pi}\right)^2 \frac{\left(\alpha + k_e + f_1 \frac{L}{D}\right)}{2g}, \qquad (22)$$

and

$$\frac{H'}{D} = \frac{H}{D} + S_o \frac{L}{D} - \frac{\beta}{D}, \qquad (23)$$

we have

$$\frac{H'}{D} = C_1 \left(\frac{Q}{D^{5/2}}\right)^2. \qquad (24)$$

All the terms in equations (23) and (24) are observed quantities of the experimentation except β/D and C_1. The term β/D for the apron-type support used here can be evaluated from the data of Li [10] shown in figure 35. Li's data were obtained with a conduit and apron slope of 2.5%. However, Li has also shown experimentally that in the case of the free outlet that substantially the same values of β/D prevail for slopes of zero and 2.5%. In the absence of specific data on the effect of slope on β/D it has been assumed in the reduction of the full conduit flow data of this report that Li's conclusion regarding negligible slope effect with free outlets is also valid with respect to the outlet jet supported by an apron.

With regard to equation (22) Morris [11] has presented limited data indicating that α and k_e vary with Reynolds number. For the smooth lucite culvert barrels used in this investigation it is to be expected that f_1 will also vary with Reynolds number. Hence it would be expected

that for smooth culvert barrels, such as used here, that C_1 will in general be a function of the Reynolds number as well as L/D. However, in this connection, it is to be noted that in the derivation of equation (24) the effect of vortex action on full conduit culvert flow has been neglected. Vortex action over the culvert inlet was frequently observed in full conduit flow, as well as with sluice type flow, and has the effect of decreasing the rate of discharge, Q, through the culvert, as compared with full conduit flow under similar conditions with no vortex. Since vortex action over a culvert inlet varies with the degree of submergence, and hence with Q, it would be expected that vortex action will cause a corresponding variation of C_1 with Q.

In figures 37 and 38 the full conduit data of the investigation have been plotted in accordance with equation (24) with the term β/D appearing in equation (23) being evaluated for all slopes from Li's data of figure 36 for a 2.5% slope. Unfortunately, it was necessary to extrapolate Li's data beyond the range of his experimental data in plotting the data of figures 37 and 38 for values of $Q/D^{5/2}$ below 4.5. Hence corrections in these figures may become necessary when experimental work now scheduled on the location of the pressure line is completed.

With the exception of the data for low values of H'/D for Model 113, it will be noted from figures 37 and 38 that a mean curve based upon the assumption of a constant C_1 in equation (24) adequately represents the data throughout the range of experimentation. In this connection it is to be noted that with most of the inlets a consistent tendency is apparent for values of $Q/D^{5/2}$ below 4.0, for the data to plot to the right of the mean curve. This is in the range of $Q/D^{5/2}$ for which Li's data on β/D was extrapolated, and is, of course, subject to error.

It will also be noted that the experimental data for many of the inlets consistently plot to the left of the linear mean curve in the range $1.5 < H'/D < 3.0$. As will be indicated by reference to the tables of appendix B this is in the range of maximum vortex action and a portion of the deviations of the plotted data from the mean curve is attributable to this factor.

It appears evident that owing to the effect of vortex action and to the uncertainties introduced by the extrapolation of Li's data beyond his experimental range that conclusions from the data of figures 37 and 38 regarding the variation of C_1 with Reynolds number are unwarranted.

Comparison of the data of figures 37 and 38 with the data of figure 47 will indicate, for several of the model inlets, that experimental points have been plotted in figures 37 and 38 which are outside the range of full conduit flow indicated in figure 47. This results from the hysteresis effect previously mentioned, owing to which full conduit flow after once being established will persist to lower values of H/D than the value of H/D at which regime change from sluice type to full conduit flow occurs as the upstream pool level is increased.

Reference to the data of figure 37 for Model 113 will indicate a break in slope of the rating curve at a value of H'/D of approximately 1.8, with the experimental data of this investigation plotting appreciably above the data obtained by Karr [6]. Reference to table 32 of Appendix B will show that vortex action in this range of H'/D was exceptionally strong and it is to be inferred that deviation of the experimental data of this investigation from Karr's results for the lower values of H/D is attributable to vortex action.

In table 5 are given the experimentally determined values of C_1 of equation (24) for the various inlets tested, determined from the mean curves of figures 36 and 37. Also given in table 5 are values of $k = (\propto + k_e + f_1 L/D)$ computed from equation (22).

Table 5

Experimentally Determined Values of C_1 and k
For Full Conduit Flow
(Smooth Lucite Culvert Barrel of Length 12D)

Model	C_1	$k = (\propto + k_e + f_1 \frac{L}{D})$
5	0.0324	1.28
6	.0324	1.28
51	.0400	1.58
61	.0436	1.73
81	.0518	2.05
3	.0360	1.43
2	.0365	1.45
4	.0340	1.35
4-B	.0340	1.35
62	.0405	1.60
62.1	.0340	1.35
102	.0338	1.34
102-B	.0338	1.34
103	.0338	1.34
113	.0520	2.06

The data of this investigation are not sufficient to separate for each inlet the losses in column 3 of table 5, or to assign a value to the kinetic energy factor α. However, with regard to Models 5 and 6, it will be observed from table 5 that $k = \alpha + k_e + f_1 L/D = 1.24$ for both inlets. Since the radius of rounding for Models 5 and 6 are respectively 0.15D and 0.25D it is to be assumed that the increased radius of curvature of Model 6, in no way affects the hydraulic characteristics of the inlet under full flow conditions, and hence that α, k_e and f_1 for the two models are the same. Further, from the work of Hamilton [12] it would be expected that the entrance loss under full flow conditions for these inlets would be negligible. Morris [11] has obtained limited experimental data on the variation of α with distance from the entrance for a rounded inlet of 0.156D radius of curvature. Morris' data indicate a Reynolds number effect, and in the range of Reynolds numbers used in the tests reported here the value of α obtained by Morris is approximately 1.01 at a distance of 12 diameters from the entrance. Assuming this determination of α to hold for both models, $f_1 L/D$ for Models 5 and 6 is 0.23 and the mean value of f_1 over the range of Reynolds numbers used in the experimentation is 0.0192.

These tests were made at Reynolds numbers varying from 1.37 to 4.64×10^5, with corresponding resistance coefficients for fully developed turbulent flow ranging from approximately 0.017 to 0.0135, based on the assumption of hydraulically smooth pipe. It is probable that the higher value of f_1, inferred from the experimental data reported here, as compared with the value of f determined on the basis of hydraulically smooth pipe is the result as pointed out by Keulegan [13] of the higher resistance coefficient to be expected in the "entrance length" of a conduit where an expanding boundary layer is developing with consequent increased boundary resistance as compared with the region of fully developed flow. However, it is also to be noted that the pipe used in this investigation was assembled from smooth lucite tubing in lengths of approximately 5 feet. Tolerances on the nominal 5.5 inch diameter tubing were plus or minus 1/32 inch on any diameter; hence while the pipe material itself may be considered smooth, the joints constituted a roughness element of presently unknown importance insofar as the resistance coefficient is concerned. Presently scheduled tests include determination of the resistance coefficient for fully developed turbulent flow.

It is apparent from the foregoing that assignment of precise values to the individual terms making up k of table 5 requires further experimental work. The kinetic energy factor α may be determined readily from velocity traverses for each individual inlet, although the data of Morris [11] for the square edge and 0.15D radius rounded inlets indicate that the range in value of α for smooth culverts of lengths 12 to 15 diameters (which is of perhaps minimum practical length) will be sufficiently small for all types of inlets ranging from those with sufficient rounding or tapering to completely suppress contraction, to those with square edges, to warrant the use of an engineering estimate. However, it is to be noted in this connection that Streeter's [14] data on the relation of α to conduit roughness in the fully developed flow ranges indicates that an increase in α will accompany an increase in conduit roughness.

It is apparent that the values of $k = (\propto + k_e + f_1 L/D)$ listed in table 5 for the various inlets apply only to a culvert barrel of the length and roughness used, both as regards f_1 and $\propto$ as well as L/D; and that precise assignment of values to the individual terms $\propto$, k_e, and $f_1 L/D$ cannot now in general be made, even for the particular culvert barrel used in the tests.

5.4 Pipe-Arch Section

The pipe-arch section used in these tests was molded from 1/4-inch lucite sheets to the form indicated by the coordinates of table 1. The cross-sectional area of the modeled section was 34.65 square inches with a hydraulic radius of 1.62 inches for the full section. The length of the pipe-arch section tested was 77.8 inches, or in terms of the hydraulic radius for the full section, 47.9R; as was the case for the circular pipe used in these tests.

Computation by the usual methods, of the specific energy at critical depth from the cross-section of the pipe-arch model given in table 1, leads to the approximate relation for the pipe-arch section under non-submerged flow conditions of,

$$\frac{d_c}{D_1} + \frac{v_o^2}{2gD} = 0.56 \left(\frac{Q}{BD_1^{3/2}}\right)^{0.58} , \qquad (26)$$

where B is the maximum horizontal dimension of the section and D_1 is the maximum vertical dimension.

Reference to equation (2) for non-submerged flow for circular cross section indicates a close similarity in the critical flow relations for the two cross sections.

Following the method used for circular pipe sections, the data for the pipe-arch sections under non-submerged flow have been presented in figures 39, 40, 41, and 42 in the form of

$$\frac{H_a}{D_1} = k \left(\frac{Q}{BD_1^{3/2}}\right)^n . \qquad (27)$$

In figure 39 are given data for a square edge pipe-arch section in a headwall, Model 21, under non-submerged flow conditions. This inlet is not comparable to field conditions inasmuch as the pipe-arch section is made commercially of corrugated metal and field installation of this section in a headwall are more nearly equivalent to Model 22. Nevertheless, the pipe-arch square edge inlet was tested because of its ease in construction and because it would give an additional model for comparing

the relative efficiency of the pipe arch and circular pipe culvert cross-section.

In figures 40, 41, and 42 are given experimental data for non-submerged flow conditions for pipe-arch Models 22, 91, and 126.

With regard to sluice type flow, the area of the pipe-arch section used in these tests can be expressed as

$$A = 0.789\ B\ D_1 . \tag{28}$$

Substituting this relation in equation (12) and simplifying we have

$$\frac{H'}{D_1} = \frac{0.808}{C_D^2}\left(\frac{Q}{g^{1/2} B\ D_1^{3/2}}\right)^2 + \frac{h}{D_1} + \frac{p_a}{\rho g D_1} , \tag{29}$$

from which

$$\frac{H'}{D_1} = k_1\left(\frac{Q}{B\ D_1^{3/2}}\right)^2 + k_2 , \tag{30}$$

where k_1 and k_2 are constants for a particular model installation. Equation (30) is to be compared with equation (14) the corresponding relation for circular pipe culverts.

Reference to equations (13) and (29) indicates that to a close approximation that a comparison of the hydraulic performance of the two sections under sluice type flow can be obtained by the simple expedient of considering the circular section to be a pipe-arch section in which $B = D_1$.

In figures 43, 44, and 45 are given sluice flow data on pipe-arch Models 21, 22, 91, and 126. In each case the mean curve for the corresponding circular pipe model has also been shown and it will be noted that there is a consistent deviation between the two types of barrel sections with the pipe-arch section giving a slightly larger rate of discharge than a circular section of the same area. This was expected owing to the fact that with sluice type flow the barrel is flowing only partially filled with the unsymmetrical section of the pipe arch providing a greater proportion of its total area for conducting the water flow at a given depth than the circular section.

In table 6 are given computed values of C_D, k_1, and k_2, for the pipe-arch models.

With regard to full conduit flow in the pipe-arch section, application of the energy principle leads to

$$\frac{H'}{D} = C_1 \left(\frac{Q}{BD_1^{3/2}}\right)^2, \qquad (31)$$

which is analogous to equation (24) for circular pipe sections.

In figure 46 are given data on Model 91 for full conduit flow. The value of C_1 of equation (31) for Model 91 with the particular length of barrel used is 0.0515, which on reference to table 5 will be seen to be substantially the same as that determined for Model 81, the corresponding inlet for the circular cross section. In the plotting of the data of figure 46 the assumption has been made that Li's data of figure 36 on the location of the pressure line at the outlet is applicable to pipe-arch sections as well as to circular sections.

Table 6

Experimentally Determined Values of C_D, k_1, and k_2 of Equations (29) and (30) for Sluice Type Flow in Pipe-Arch Section

Model	C_D	k_1	k_2
21	0.635	0.062	0.66
22	.657	.058	.73
91	.585	.0731	.695
126	.542	.0849	.59

5.5 Regime of Flow in Culverts

As has been indicated, submergence of the inlet of a culvert is not ordinarily sufficient to guarantee that the culvert will flow full. For many inlets submergence of the inlet causes only a contracted type of flow similar in many respects, as has been stated, to the flow occurring at a sluice gate. Owing to the fact that full conduit flow results in greater rates of discharge through the culvert for a given degree of submergence, particularly for long culverts on steep slopes, it is of importance from the design engineer's viewpoint to define with some precision the range of relative pool depth H/D associated with each regime of flow for certain of the commonly used inlets, and to determine the effect of upstream conditions such as turbulence level, and width of the approach stream, as well as the effects of slope, length and roughness of the culvert barrel on flow regime in the culvert. The detailed experimental study of flow regime change in a culvert is reserved for a later phase of the investigation and will be reported in a subsequent progress report. Nevertheless certain of the experimental results on small culvert models of length 12D will be presented in the present progress report.

A resumé of the type of flow prevailing in the conduit for submerged entrance conditions is given in figure 47 for the various inlets tested. These limits of sluice type and full conduit flow are given in terms of the H/D value existing before a change in the regime of flow occurred. For example, with Model 4 on zero slope, figure 47 indicates full conduit flow prevailing from an H/D value of 1.22 to 2.08; sluice flow from 2.08 to 2.88 and full conduit flow above 2.88. These ranges of H/D for the various regimes of flow are to be interpreted to mean that as the value of $Q/D^{5/2}$ is gradually increased, sluice type or slug type flow existed up to a value of H/D = 1.22, full conduit flow then occurred and continued until a value of H/D = 2.08 was reached, as read with the conduit flowing full, whereupon reversion to sluice type flow occurred, with a consequent immediate increase in H/D, and such flow continued until a value of H/D = 2.88 was reached, as read with the culvert operating as a sluice, and then reversion to full conduit flow occurred.

The data in figure 47 was obtained by slowly increasing the rate of flow into the upstream pool. In this connection it was observed that the regime of flow in the culvert, that is whether the culvert operated as a sluice or with full conduit flow, was somewhat sensitive to the rate of increase of flow. For example, if the water was introduced in such fashion as to cause H/D to increase at a relatively rapid rate, it was observed that full conduit flow often resulted, while if the water surface was raised more slowly sluice type flow persisted. An interpretation of this experimental observation, in terms of upstream approach flow turbulence level will be given shortly in the discussion of the effect of upstream turbulence level on regime of culvert flow.

In these tests the rate at which the water surface was raised approximated 0.2 cm or less per minute over the critical range where a change in flow regime appeared imminent. At this rate of increase in water surface elevation there was no apparent tendency of the rising water surface to artificially induce full conduit flow.

It is proper to note that the data of figure 47 are not in all cases strictly comparable as between the several inlets. The pneumatic and hydraulic processes causing changes in flow regime, either from sluice type flow to full conduit flow, or the reverse, are not necessarily in a steady state. For example, it was repeatedly observed that for certain inlets and for certain degrees of submergence that vortex action above the inlet varied with time. That is, on occasion a vortex would form, increase in strength until air was flowing from the water surface into the culvert inlet, then decrease in strength and intensity to the point where air was no longer being drawn into the inlet, and then the cycle would be repeated. The effect of this phenomenon on the height of the water surface above the invert of the culvert could readily be detected and variation in H/D because of variation in vortex strength amounted to as much as 0.14D on occasion.

In like manner and possibly owing to the variation in vortex strength described above, separation at the inlet was frequently not in a steady state. For relatively high degrees of submergence with sluice type flow, many of the inlets flowed with complete gross separation around the inlet except at the invert where the floor of the approach channel was flush with the inlet. That is, the area of gross separation was characterized by an air pocket between the flowing water and the culvert inlet, except of course, at the leading edge of the inlet. This phenomenon is illustrated by the photograph of figure 19a where the drops of water adhering to the inside surface are clearly visible, indicating the presence of nearly a complete annular air space around the flowing jet of water.

For lower degrees of submergence the area of separation did not extend completely around the inlet and the location and extent of the area of gross separation were observed on occasion to vary appreciably with time. These variations in separation were also reflected in corresponding changes in the observed values of H/D.

Because of the variation of vortex action with time and no doubt because of the variation with time of other significant factors affecting the regime of flow, it was observed in many instances that changes in regime occurred during the 15 to 20 minute waiting period required for the water surface to become stable when an experimental run was being made. When this occurred the change in flow regime was taken to occur at the H/D observed during the waiting period. It is apparent that the regions of various flow regimes as determined in this manner will to a degree be affected by the length of the waiting period for each run and also by the number of waiting periods throughout the rating range.

Inasmuch as substantially the same number of experimental points were obtained on each inlet of figure 47 and the waiting period for each point was substantially the same, it is believed, from a statistical viewpoint that the data are substantially comparable among the various inlets with one exception. In the case of Model 5 on zero slope the tests extended over a period of approximately 5 days, amounting to approximately 5 times the period over which any other inlet on a given slope was tested. On only a very few occasions during the 5-day period was sluice type flow obtained and it is therefore highly probable that if this inlet had been tested at the slope indicated for approximately the same length of time as the other inlets that full conduit flow would have been obtained over the full range of H/D and would have been so recorded in figure 47.

Reference to several of the rating curves for full conduit flow will indicate points on these curves which lie outside the range of full conduit flow given in figure 47. As stated previously, this results from a hysterisis effect observed in the operation of most of the inlets. It was observed that the value of H/D at which change from sluice flow to full conduit flow occurred as the water surface was raised was consistently higher than the corresponding value of H/D for change from full flow to sluice flow as the water surface was lowered.

Referring to figure 47 it is noteworthy that the inlets which provided an increased area at the face of the inlet as compared with the area of barrel, in general operated in the full conduit condition at lower values of H/D than did those inlets which did not provide an entrance section of increased area. This result is in agreement with the results of Shoemaker and Clayton [1] for box culverts and Straub, Anderson and Bowers [15] for circular culverts and forcibly illustrates the very strong influence of separation effects on the ability of a culvert to flow full.

The appreciable effect of barrel slope in increasing the value of H/D at which the change from sluice type flow to full conduit flow occurs is consistently apparent. For Models 51 and 61 the effect of slope on flow regime is quite marked, full conduit flow being obtained for $H/D \geq 1.5$ for zero slope and sluice type flow being obtained throughout most of the experimental range, on 0.5% slope. The experimental work reported here has repeatedly shown that the slope of the culvert barrel influences the ability of a culvert to flow full and that general conclusions based upon experimental work at mild slopes that a given inlet geometry will produce full conduit flow are not necessarily valid at slopes near or greater than critical slopes.

Comparison of the data of figure 47 for Models 1 and 51 indicate an increased tendency for the 45° wingwalls to produce full conduit flow at zero slope, as compared with spill cones. In like manner comparison of the data of Model 62 with the data of Model 4 at the higher slope indicate a somewhat increased efficiency of the parallel wingwalls in producing full conduit flow as compared with spill cones. It is to be concluded from the limited data available that 45° and parallel wingwalls are somewhat more efficient in producing full conduit flow than a headwall and spill cones.

Comparison of the data for Model 62.1 with the data of Models 62 and 52 indicate that the wingwalls of this model are more efficient in producing full conduit flow than either the conventional type 45° or parallel wingwalls. The increased efficiency of Model 62.1 in producing full conduit flow apparently results from its ability to induce a higher turbulence level in the approach flow. In this connection it was noted that flow conditions immediately upstream from the inlet were substantially altered by the wingwalls of Model 62.1 With this model it was observed that the flow accelerated at the upstream entrance to the channel caused by the vertical parallel wingwall, passed through critical depth and formed a jump immediately upstream of the inlet. It was observed that vortex action was noticeably decreased and that it never existed until the water surface overtopped the wingwalls. The jump formed by the wingwalls immediately upstream from the inlet will have the effect of increasing the scale and intensity of turbulence in the approach stream entering the inlet, and as will be indicated later, such approach stream turbulence appears to have a marked effect in causing full conduit flow.

The projecting types of inlets were in general less efficient in producing full conduit flow than similar models in a headwall. However, in this connection, attention is directed to Model 113. The results of Karr [6] in regard to the ability of this type of inlet to produce full conduit flow were corroborated. Karr infers from photographs of flow through this inlet that its ability to produce full conduit flow stems from an upward component of the mean entrance velocity which, according to Karr, reduces separation effects. It will be noted from figure 37 that the data of these tests deviate appreciably to the left from the data of Karr for low values of H/D. Reference to table 26 of Appendix B will show that strong vortex action with consequent large amounts of air flow in the culvert were present in the lower range of H/D. It is to be inferred that the approach channel of this investigation was more subject to vortex action than Karr's channel and that the recorded difference in experimental results is owing to the presence of the excessively strong vortex action in the tests reported here for Model 113.

Reference to figure 47 will indicate that the pipe-arch Model 91 broke into full conduit flow at consistently lower values of H/D than did Model 81.

The sometimes pronounced effect of roughening the surface of the rounded inlets on their ability to flow full is illustrated by the results obtained with Model 6. This model, as well as Models 4 and 5 were tested with and without a sand coating on the inside surface of the inlet. The limited data obtained with Model 4 indicated no substantial effect upon the value of H/D at which transition from sluice type to full conduit flow occurs. The sand coating used with the roughened models consisted of sand grains with a mean diameter of 0.1 mm.

Model 6 exhibited a surface tension effect which is worthyof note. When the model was tested, after a sufficiently long period of disuse to insure that the inside surface of the inlet and the culvert barrel was dry, sluice type flow prevailed for a considerable range in relative depths of submergence, H/D. The tests referred to here were made with a culvert slope of 4.77% and in the smooth condition without a coating of sand. After full flow had been obtained by increasing H/D sufficiently, and hence after the inside surface had become wet, repeated tests invariably indicated full conduit flow at a slope of 4.77% for submerged inlet conditions. With the sand coating referred to previously no surface tension effect was exhibited and the culvert invariably flowed full for all slopes used. The implications with regard to turbulence of the effect of surface roughness recorded here on the ability of an inlet to cause full conduit flow will be discussed in Section 6 of this report.

It will be noted from figure 47 that Model 51, the square edge inlet with 45° wingwalls flowed full on zero slope while the corresponding Model 1 with spill cones did not. This result leads to the conclusion, as have other phases of the experimentation, that the physical

phenomena determining whether a culvert will flow full or as a sluice, are in such delicate balance that apparently minor and seemingly inconsequential changes in upstream conditions sometimes become decisive in flow regime determination.

A series of tests was also made with Model 4 with a reduced width of approach channel and with the culvert barrel above the approach channel floor. In these tests the false bottom of the tank used for the approach channel was removed giving the situation shown in figure 3. The approach channel was reduced to a width of 3 feet for a distance of 6 feet immediately upstream from the inlet by the installation of wood partition walls. On a slope of 1% Model 4 flowed full throughout the range tested. Since the removal of the false bottom would increase rather than decrease separation effects, it is to be concluded that the improvement observed was due to the reduced approach channel width with consequent increase in approach velocity, and turbulence generation in the separation area near the upstream end of the narrow channel.

Similar tests in a 3-foot wide approach channel were made with Model 5 at a slope of 6%. In these tests the effect of approach channel width was less pronounced, and sluice type flow was obtained except when the water surface in the pool above the inlet was rapidly raised. The conclusion to be drawn from these test results appears to be that a narrow channel is conducive to full conduit flow but is not of itself, at the higher slopes at least, the controlling factor involved. It is to be regretted that the pressure of other phases of the investigation prevented the systematic exploration of the effect of channel width on flow regime changes.

The above described test results were obtained in narrow rectangular approach sections. Further tests to determine the effect of channel shape on flow regime change were obtained in the trapezoidal channel with simulated flood plain shown in figure 4. Reference to figure 47 will show that full conduit flow was obtained with the .05D by .07D socket inlet in this channel (Model 4-B) until H/D became sufficiently high to cause appreciable submergence of the flood plain. This result of full conduit flow for flow confined to the trapezoidal section of the channel was to have been expected from the test results described above for the same socket inlet in a 3-foot wide rectangular section. The change to sluice type flow accompanying appreciable submergence of the flood plain is apparently owing to the less favorable flow pattern thus caused with consequent increased separation effects and resulting sluice type flow.

Comparison of the data of figure 47 for Models 4, 4-B, 102, and 102-B suggests that the excessively narrow trapezoidal section of bottom width 1D delays regime change to full conduit flow at the higher values of H/D.

In the above discussion of the test results reference has been made on several occasions to turbulence in the approach stream. Experimental work, to be described shortly has shown that the effects of turbulence in the approach stream or turbulence generated in the throat of the inlet by roughening elements such as sand grains and trip wires exert a substantial effect on the ability of a culvert inlet to establish and sustain full conduit flow.

The experimental data given above on various aspects of the phenomena relating to change in regime from sluice type to full conduit flow are not sufficiently complete in many cases to warrant general conclusions. Nevertheless, the implications to be drawn from the experimental data cited can be summarized as follows:

1. Increasing the radius of curvature of rounded inlets or securing equivalent effects by means of sockets at the inlet section decreases the value of $H/D = H_1D$ at which sluice flow changes to full conduit flow.

2. Increasing the slope causes an increase in H_1/D.

3. On a rising stage the value of H_1/D is larger than the value of H/D at which full conduit flow changes to sluice flow on a falling stage.

4. The regime changing phenomena is sensitive to the rate at which the water surface is raised; a rapidly rising water surface being conducive to full conduit flow.

5. Limited experimental data indicate that H_1/D is less for a narrow approach channel of rectangular shape than for a wider one.

6. The regime changing phenomena is sensitive to the upstream turbulence level.

6. EFFECT OF APPROACH CHANNEL TURBULENCE ON REGIME OF FLOW IN CULVERTS

In addition to the tests previously reported a short series of tests was made on the effect of upstream turbulence level on regime change in a culvert at 4% slope with Model 5 inlet.

Reference to figure 47 will show that sluice type flow occurred with Model 5 on supercritical barrel slopes at low or moderate values of H/D. These data were obtained with an approach channel width of 6 feet, corresponding to 13.1 pipe diameters. The culvert inlet ended flush with a headwall and a gravel stilling baffle was located 6.88 feet upstream of the inlet, and flow conditions in the approach channel above the inlet were relatively smooth and non-disturbed. The width of the approach channel for a distance 8.5 diameters upstream was then reduced to 4 diameters, care being taken to reduce flow disturbance at the entrance to the narrow channel by gently rounding the entrance from the wider channel to the constricted channel. A wood slat stilling grid made of vertical

1 1/2-inch slats spaced 1 inch apart was placed in the channel 3.5 feet upstream from the culvert inlet. Under these conditions the culvert on a 4% slope with 0.15D radius rounded inlet in a headwall flowed full when the entrance was appreciably submerged. Significantly, the inlet did not produce full conduit flow when the baffle was removed. These observations strongly imply that the ability of Model 5 to produce full conduit flow is substantially influenced by the turbulence level in the approach stream. The importance of upstream turbulence was further demonstrated by using three other types of turbulence stimulators. The first consisted of simply placing vertically a 1 1/2-inch thick wooden slat against each of the vertical side walls of the narrow approach channel, 3.5 feet upstream from the inlet. With the two wooden slats in place full conduit flow occurred. With the slats removed strong separation at the inlet occurred with consequent part full or sluice type flow.

The second type of turbulence stimulator consisted of cementing sand particles of 0.1 mm mean diameter to the inlet surface and for a distance of approximately one diameter downstream. These tests were made in the 6-foot wide approach channel. The effect of the sand coating was ordinarily to cause full conduit flow up to $H/D = 1.7$, with a change in regime at this point to sluice type flow. The effect of sand coatings of larger grain size was not pursued further, but it appears probable that such coatings would have further improved the performance of the inlet. However, as previously mentioned, a sand coating of 0.1 mm mean grain size was applied to Model 6 with the result that the inlet produced full conduit flow for all slopes tested (maximum slope of 9.31%) while the uncoated model at 1% slope produced sluice type flow up to $H/D = 3.1$.

The third type of turbulence stimulator used with Model 5 in the wide approach channel consisted of cementing to the rounded inlet surface small wires bent to form circles of such diameter that the wires were located slightly downstream from the leading edge of the inlet. These tests with trip wire stimulators were made on a Model 5 inlet which had been coated with the sand referred to previously. The first wire installed was 0.5 mm in cross-sectional diameter and was formed to a circle of 6.75 inches diameter. The wire was fastened to the inlet surface at 4 or 5 points around its circumference by means of sealing wax. With this wire full conduit flow was obtained up to $H/D = 1.9$. The wire ring was then replaced with a 0.5 mm ring of 6.5 inch diameter and full conduit flow was obtained up to $H/D = 2.4$. This ring was in turn replaced with a 0.5 mm wire ring of 6 inch diameter and sluice flow occurred at $H/D = 1.5$. With a 0.5 mm ring of 6.25 inch diameter full conduit flow was obtained up to $H/D = 2.1$.

The cross-sectional diameter of the wire rings was then increased to 1 mm, and a ring of 6.5 inch diameter was installed. Full conduit flow was obtained at $H/D = 2.5$. The cross-sectional diameter of the wire was further increased to 1.5 mm with a circle diameter of 6.5 inches, and full conduit flow was obtained up to $H/D = 3.4$; sluice flow prevailed from $H/D = 3.4$ to $H/D = 4.5$, at which point change to full

conduit flow occurred. With the preceding wire in place a quarter of a 1.5 mm wire ring of 6.25 inches in diameter was placed on the topmost quadrant of the inlet surface and full conduit flow was obtained for all degrees of submergence greater than H/D = 1.2.

The inlet is extremely sensitive to small deviations in location of the wires and methods of fastening the wires to the inlet surface; and difficulty in reproducing these results with any precision was experienced.

The significance of the above tests is that turbulence generated by boundary roughness on the inlet surface, as well as approach stream turbulence level is capable of producing very substantial improvement in the ability of the rounded inlets to produce full conduit flow.

The physical phenomena involved here is of course, separation of the main flow from the inlet boundary surface. The effect of turbulence both in the upstream approach stream and that generated in the throat of the inlet by such stimulators as trip wires and boundary roughness suggests similarity to the separation effects found on spheres and cylinders. For such bodies the location of the point of separation, and consequently the magnitude of its effect, depends upon the shape and roughness of the boundary, the Reynolds number, and the intensity and scale of upstream turbulence. It is known, in the case of such curved spherical and cylindrical boundaries, that the onset of turbulence in the boundary layer will permit the boundary layer to advance farther against an adverse pressure gradient before separation occurs, and hence enable the separation point to be located farther downstream with consequent decrease in separation effects. It has been repeatedly shown that such apparently unimportant circumstances as a slight surface roughness or turbulence in the approach stream have a marked effect upon the onset of turbulence in the boundary layers of such bodies, and hence upon the location of the separation point, the size of the wake and consequently upon the drag coefficient. For these reasons roughening the boundary by means of cemented sand grains, trip wires or pins has become a common means of decreasing separation effects. That such means would also be effective in decreasing to some degree the effects of separation in culvert inlets of curved boundaries was to be expected.

The demonstrated sensitivity of the rounded culvert inlet models to upstream turbulence implies that scale effects will exist between small and large model sizes. Further, since transition to turbulent flow in the boundary layer of the curved inlet shapes will occur with natural roughness as the Reynolds number increases with increased model size, it would be expected that the larger scale culvert models would not be as sensitive to separation effects and to the effect of approach stream turbulence on separation in the culvert model as the smaller models heretofore tested. Under these circumstances it would be expected that for certain of the model inlets that the value of H/D at which sluice flow changes to full conduit flow would decrease as the model scale were increased.

In this connection, preliminary tests at a 12-inch diameter barrel size for Model 5 (3% slope and barrel length of 12D) consistently indicates transition from sluice type flow to full conduit flow at a value of H/D ranging from 2.7 to 3.1. In this case the curved inlet ring was made of a cement-sand mixture with a relatively smooth neat cement surface finish, but nevertheless with a natural roughness considerably greater than the lathe-turned lucite entrance of the 5.5-inch diameter model. Upstream turbulence level was controlled by a wood slat stilling grid of 1 3/4-inch mesh located 40 feet upstream from the inlet.

As was the case with Model 5 at the 5.5-inch diameter size the larger model is sensitive to approach channel turbulence level. A slat grid placed 6 feet upstream from the inlet and made of vertical 3 3/4-inch wide slats placed perpendicular to the approach flow and spaced 1 1/2 inches apart invariably produced full conduit flow on submergence of the inlet.

The sensitivity of Model 5 at the 12-inch size to approach channel turbulence indicates that scale effects for the rounded inlet models can be expected between the 12-inch and larger models.

The question of approach channel turbulence level assumes importance, in regard to culvert model testing only because of the diversity of possible field installation conditions. At full scale with a relatively deep narrow approach channel of natural roughness the turbulence level can be expected to be sufficiently high to insure full conduit flow for the rounded inlets as well as others investigated here. With the wider approach channel characteristic of a comparatively shallow stream with a flood plain, it is not equally evident from data presently available that such would be the case.

In connection with the foregoing direct observations of the effect of approach channel turbulence on regime flow, two other manifestations of the phenomena may be noted. During the course of the tests reported here it was repeatedly observed that full conduit flow could, with certain inlet models, be artificially induced by rapidly raising the water surface in the upstream pool. This result has been observed at both the 5.5-inch and 12-inch model sizes. This phenomenon may be readily explained in terms of turbulence effect. The Reynolds number formed by the approach velocity and a characteristic dimension of the upstream stilling grid will at a given H/D be higher on a rising stage than on a stationary or falling stage; hence the intensity of approach channel turbulence will be higher with consequent decrease in separation effects and increase in tendency toward regime changes to full conduit flow.

The second manifestation of turbulence noted during the normal course of the tests was in connection with the formation of a hydraulic jump immediately upstream of the inlet. Reference to figure 47 will indicate that Model 62.1 flowed full for the 1% and 6% slopes for all appreciable degrees of submergence. The only essential difference between Model 62.1 and Model 62 was that the parallel wingwalls did not slope downward with

the embankment but continued upstream at a horizontal elevation of 2D above the channel floor as shown in figure 5. The effect of this alteration in wingwalls was to form a hydraulic jump immediately upstream from the inlet with consequent increase in turbulence level because of the jump roller. The turbulence level increase was sufficient to cause the culvert to flow full for all appreciable degrees of submergence when tested on the 1% and 6% slopes. This inlet was also tested on a 8.9% slope. At this slope sluice flow developed.

7. FACTORS AFFECTING REGIME OF FLOW IN SUBMERGED CULVERTS

The fundamental cause of sluice type flow in a culvert is of course, separation of the flow from the inlet boundaries, and the phenomena causing boundary separation is known to be a sufficiently high adverse pressure gradient along the boundary surface. That is, if the bounding surfaces of an inlet are contoured in such fashion that an adverse pressure gradient along the boundary does not exist, then reversal of flow near the boundary and hence separation cannot occur. With such an inlet the culvert will flow full immediately after submergence of the inlet and will continue to flow full as the upstream pool level is increased regardless of admission of air by vortex action, provided only the bounding surfaces are so contoured that the pressure does not increase along the inlet boundaries in the direction of flow for any value of H/D.

Although the absence of an adverse pressure gradient is sufficient to insure full conduit flow it is apparent that energy transfer by turbulent mixing of the high velocity main flow with the slow moving fluid near the wall can prevent flow reversal and hence separation even in the presence of an adverse pressure gradient provided the turbulence level is sufficiently great and provided the gradient is sufficiently small. It is, of course, this effect of turbulence level on flow reversal and separation which as described previously caused full conduit flow to occur when trip wires were installed in the inlet, or when a grid was placed in the approach stream.

In a conduit transition, such as an inlet, in which only one fluid is involved, separation ordinarily persists only a short distance downstream from the point of generation, owing to turbulent mixing with consequent expansion of the high velocity core into the region of slower moving liquid. For this reason, while the process is not as efficient as would be the case in a properly contoured conduit transition, it nevertheless causes less loss of efficiency than if the area of separation had continued undiminished in size throughout the length of the conduit.

However, in a conduit, such as a culvert, in which two fluids, air and water are involved, the effect of flow reversal with consequent separation can become far more pronounced. In this case, as the upstream pool level is gradually increased from a non-submerged inlet condition to a submerged condition, the culvert inlet would be expected to flow with the water in contact with the boundary surface up to a point where turbulent

mixing was no longer able to supply the energy necessary to overcome the adverse pressure gradient along the boundary. At this point the flowing water would be expected to leave the boundary and the reversal of flow normally accompanying separation in a one fluid system would be evidenced in the culvert inlet by an air flow towards the point of separation from the downstream portion of the conduit. Air flow would be expected to be somewhat as shown in figure 18, and in this connection air inflow upstream into the culvert from the outlet has been repeatedly observed in the tests reported here.

It appears evident from the foregoing that the solution to the problem of designing an improved culvert inlet that will produce full conduit flow consists only of contouring the boundaries of the inlet in such fashion that adverse pressure gradients along the boundaries do not occur. This problem of designing an improved inlet which will produce full conduit flow under all operating conditions is, of course, of practical importance and will constitute a subsequent phase of this investigation.

In addition, the problem of change in regime of flow in commonly used culvert inlets, as the upstream pool level is progressively increased constitutes a second important culvert problem connected with separation phenomenon. Two aspects of this problem have been observed in the tests reported here. In the first, full conduit flow is initiated very shortly after the inlet is submerged and continues until a value of H/D of 2 or 3 is reached whereupon regime change to sluice type flow occurs. In the second type of regime change the culvert inlet ordinarily operates in a sluice flow condition until a large value of H/D is reached whereupon the flow changes to full conduit flow.

With regard to the first case, change from full conduit flow to sluice type flow, it was observed that flow regime change was invariably associated with an air carrying vortex over the culvert inlet. Since in this case full conduit flow ordinarily was initiated very shortly after submergence, it is to be inferred that inlets which behaved in this manner (Model 5, for example) were contoured in such fashion that the adverse pressure gradient along the inlet boundaries was sufficiently small and that the turbulence level was sufficiently high so that flow reversal and separation did not occur at the lower values of H/D. It appears equally clear that as H/D was increased that the stream line pattern immediately upstream of the inlet or the turbulence level changed sufficiently so that separation along the upper boundary was established. Introduction of sufficient air, through vortex action into this region of single fluid separation permitted the gross type of air-water separation associated with sluice type flow.

The action of the air carrying vortex in permitting access of air to the sensitive region of adverse pressure gradient and separation illustrates the sometimes decisive nature of vortex action in transforming a small region of comparatively unimportant separation in a single fluid

system to a flow limiting region of gross separation extending throughout the length of the conduit simply by the introduction of sufficient air to the sensitive region.

The remedy for this type of regime change from full conduit flow to sluice type flow may take two forms. First, the vortex for a given culvert installation may be eliminated by proper design of the inlet or approach channel; or second, the undesirable effects of the vortex can be eliminated by contouring the inlet boundaries so that regions of separation do not occur for any degree of submergence of the inlet. This latter method is illustrated by the work of Shoemaker and Clayton [1] in which they remark with reference to the effect of vortex action on a tapered box culvert inlet: "The absence - of contraction allowed the culvert barrel to remain full even upon the admission of air to the entrance -."

The above discussion of regime change refers to change from full conduit flow to sluice type flow. Of perhaps more importance is the regime change in which sluice type flow changes to full conduit flow. This type of regime change was observed with most of the inlets tested. For low degrees of submergence the inlet operated as a sluice and for high degrees of submergence the conduit flowed full; at some intermediate value of H/D the flow regime changed from sluice type to full conduit flow. The precise mechanism causing the relatively large and rapid decrease in separation effects involved in the change from sluice type to full conduit flow is unknown. However, referring to figure 18, the air circulation initiated by friction as well as by air entrainment across the air-water interface will have the effect of creating a sub-atmospheric pressure in the air space within the conduit and in the inlet. This subatmospheric pressure within the inlet could be expected to influence the separation phenomena at the inlet possibly through decreasing the adverse pressure gradient along that portion of the inlet boundary in contact with the water and hence permit the point of separation to advance farther downstream. As the level in the upstream pool is increased with consequent increase of velocity and depth of water in the conduit, it would be expected that air entrainment across the air-water interface and air inflow from the culvert outlet would be such as to cause a progressive decrease in the pressure over the water surface at the inlet, and that eventually the pressure would become sufficiently small and subatmospheric so that separation in the inlet would cease and the culvert would thus flow full.

That such negative air pressures exist in sluice type flow is shown by the data of figure 48 for Model 4 at the 12-inch diameter model size. These pressures were measured through a manometer located one diameter downstream from the face of the inlet and at the crown of the barrel. Full conduit flow for the run shown in figure 48 occurred at H/D = 3.95, and the rapid decrease in the air pressure in the inlet, as this value of H/D is approached is to be noted. Negative air pressures in the inlet during sluice type flow have also been observed by Straub, Anderson

and Bowers [5]. For example, with a square edge inlet to a model culvert 4 inches in diameter and 105 diameters long on a 4% slope, negative air pressures of 0.005 and 0.008 feet of water were observed with sluice type flow at discharges of 0.451 and 0.500 cubic feet per second, respectively. The same culvert flowed full at Q = 0.600 cubic feet per second. Further in run 460 of the same investigation, the culvert was ventilated presumably by opening the manometer taps along the crown of the culvert, and the model flowed only part full at the same rate of discharge Q = 0.600 cubic feet per second. It appears evident that the negative air pressure in the culvert, caused by the relative magnitudes of air inflow from the outlet and from vortex action over the inlet; and air outflow through entrainment or drag at the air-water interface exerts an important effect upon the separation phenomena controlling change from sluice type to full conduit flow.

8. DEVELOPMENT OF IMPROVED INLETS

From the foregoing it would appear that efforts to improve the ability of a given culvert model to produce full conduit flow should be confined to four basic avenues of approach as follows: (1) reduce separation effects through inlet and approach channel geometry changes, (2) reduce vortex formation, (3) increase air entrainment in the culvert inlet and barrel, and (4) reduce air inflow into the culvert from the barrel outlet.

With regard to (1) above, separation effects can be reduced by two methods; (a) the use of rounded inlet sections or equivalent means such as groove and socket joint inlets or tapered transition sections and (b) geometry changes in the inlet itself or in the approach channel to increase the scale and intensity of turbulence. With regard to (a) the basic approach to securing minimum separation effects is of course proper contouring of the inlet section. With regard to (b) experimental results have shown that roughening of the inlet surface is effective and desirable. The implication of presently available experimental data also is that the design engineer should not aim to secure approach channels of highly engineered smooth boundaries and perhaps precise alignment. The aim of the design engineer in this respect should be to obtain insofar as practical, high approach velocities with consequent high turbulence level due to natural roughness.

With regard to reduction in vortex action above the culvert inlet, it would appear that future experimental work could with profit proceed in two directions. First, preliminary and fragmentary experimental results now available on 12-inch diameter models indicate that gross unsymmetry of approach flow acts as an inhibitor of vortex action over the culvert. It would appear that future experimental work could with possibly fruitful results explore this aspect of vortex phenomena more thoroughly. The second possibility of reducing the strength of vortex action over the culvert inlet appears to be through sufficient rounding of the inlet or the use of an equivalent transition section to secure sufficiently high

pressures in the approach channel over the inlet so that vortex formation is decreased.

Air entrainment in the inlet and in the culvert barrel will be increased by whatever means are taken to increase upstream approach flow turbulence or a higher turbulence level in the inlet section. It would also appear reasonable to expect that any means within the culvert barrel which caused an agitated or violently disturbed water surface in the culvert barrel would increase air entrainment. In this connection it has been observed that rifling the inside surface of a pipe has increased the capacity of the pipe to transport suspended sediment. Since suspended sediment transport and air entrainment are both manifestations of turbulence phenomena, it might be expected that rifling, or appropriately located segments of rifling in the culvert inlet section and barrel might be effective in increasing the transport of air out of the culvert by the entrainment process.

Practical means of reducing air inflow into the culvert from the outlet are not immediately apparent. The problem here is in essence a priming problem similar in many respects to the problem of priming a siphon spillway. In such structures abrupt changes in slope, installation of steps, lips, and sealing basins have become common means of securing effective priming through preventing air inflow from the downstream end of the siphon [16]. Whether similar means could be employed for reducing or eliminating the entrance of air from the culvert outlet is a question outside the scope of the present project.

9. REFERENCES

1. Model Studies of Tapered Inlets for Box Culverts, Roy H. Shoemaker and Leslie A. Clayton, Research Report 15-B, Highway Research Board, Washington, D. C., 1953.

2. Tests on Broad Crested Weirs, J. G. Woodburn, Transactions American Society of Civil Engineers, Vol. 96, 1932.

3. Tests of Circular Pipe Culvert Inlets, R. E. Schiller, Jr., manuscript copy of paper to appear as a research report of the Highway Research Board.

4. Hydraulics of Culverts, F. T. Mavis, Pennsylvania State College Engineering Experiment Station Bulletin 56, 1942.

5. Effect of Inlet Design on Capacity of Culverts on Steep Slopes, Lorenz G. Straub, Alvin G. Anderson, and Charles E. Bowers, St. Anthony Falls Hydraulic Laboratory, University of Minnesota, Project Report 37, April 1954.

6. Model Studies of Inlet Designs for Pipe Culverts on Steep Slopes, Malcolm H. Karr, Oregon State College, Engineering Experiment Station, Unpublished report on Project 145.

7. Discussion of Importance of Inlet Design on Culvert Capacity, Lorenz G. Straub, Alvin G. Anderson and Charles E. Bowers, Research Report 15-B, Highway Research Board, Washington, D. C., 1953, by W. O. Ree.

8. The Influence of Pipe Thickness on Re-Entrant Intake Losses, Charles W. Harris, University of Washington Engineering Experiment Station, Bulletin No. 48, 1928.

9. Supplementary Notes on Flow Through Model Sluices, Herbert Addison, Paper No. 5081, Jour. Institution of Civil Engineers, Vol. 8, 1937-38.

10. Hydraulic Behavior of Culverts, Wen-Hsiung Li, Unpublished manuscript.

11. Preliminary Flow Tests on a Model Culvert, Henry M. Morris, Project Report No. 7, St. Anthony Falls Hydraulic Laboratory, University of Minnesota, May 1949.

12. Suppression of Pipe Intake Losses by Various Degrees of Rounding, J. B. Hamilton, University of Washington Engineering Experiment Station Bulletin No. 51, November 1929.

13. Friction Losses in Short Pipes and Culverts Flowing Full, Garbis H. Keulegan, Unpublished manuscript, National Bureau of Standards, 1948.

14. The Kinetic Energy and Momentum Correction Factors for Pipes and for Channels of Great Width, V. L. Streeter, Civil Engineering, April 1942.

15. Importance of Inlet Design on Culvert Capacity, Lorenz G. Straub, Alvin G. Anderson and Charles E. Bowers, Research Report 15-B, Highway Research Board, Washington, D. C., 1953.

16. Siphon Spillways, A. H. Naylor, Edward Arnold and Co., London, 1935.

ACKNOWLEDGMENT

The problems investigated here have been formulated by the staff of the Hydraulic Research Branch, Bureau of Public Roads. The writer is particularly indebted to Mr. Herbert C. Bossy of the Hydraulic Research Branch for valuable suggestions regarding the writing of the progress report and the conduct of the experimentation.

FIGURE 1

EQUIPMENT SET-UP
5.5 INCH DIAMETER MODEL

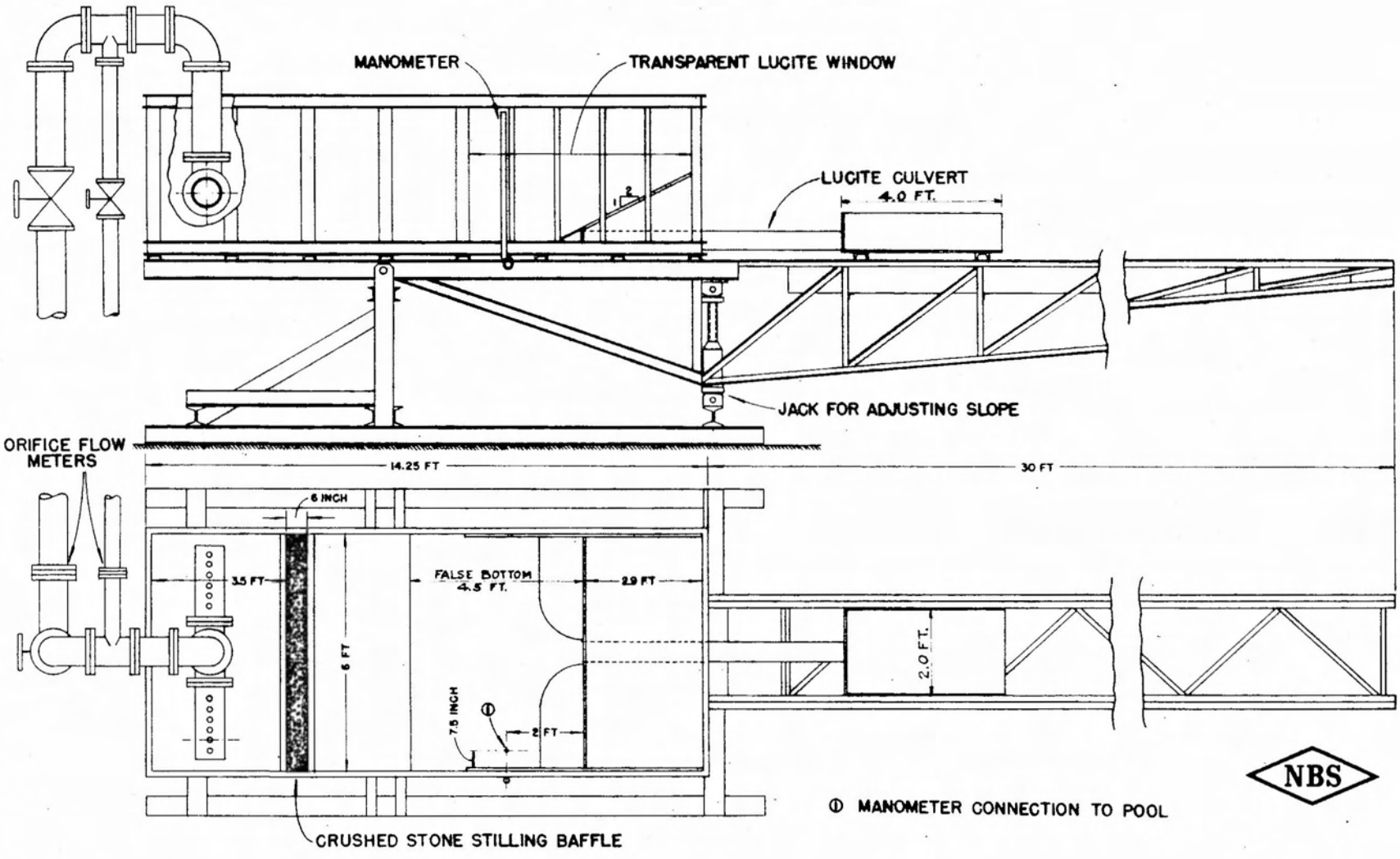

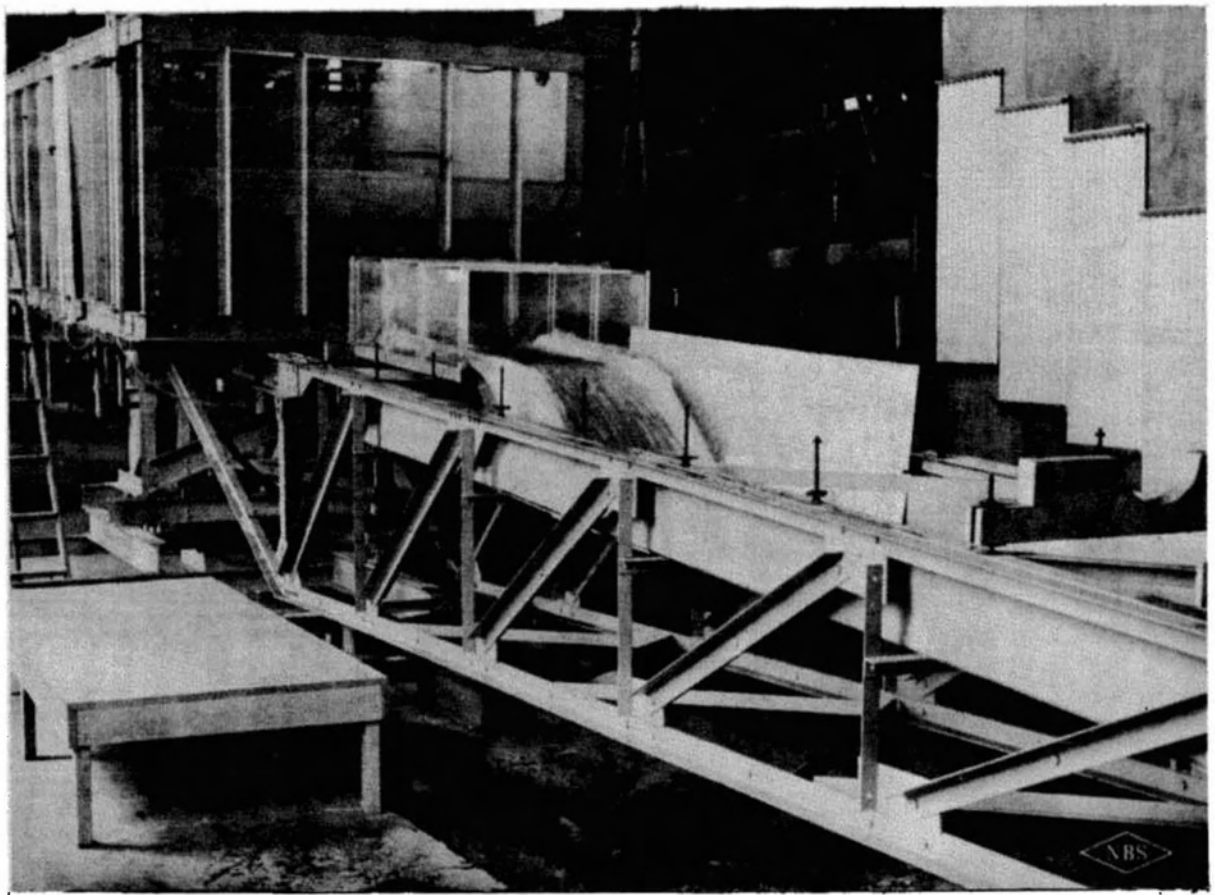

FIGURE 2 ADJUSTABLE SLOPE CHANNEL

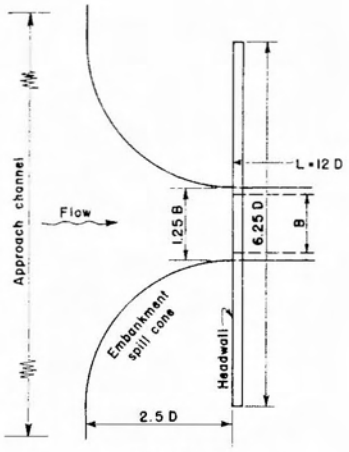

PLAN

HEADWALL AND EMBANKMENT SPILL CONES

TYPE 1

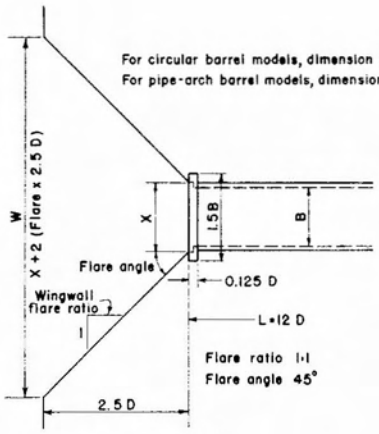

PLAN

FLARED WINGWALLS MODELS 51-52

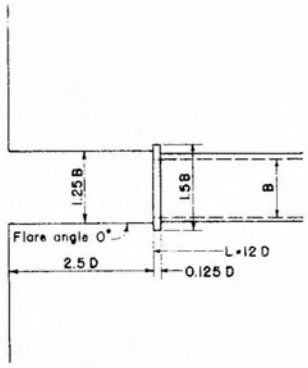

PLAN

PARALLEL WINGWALLS MODELS 61-62

TYPE 2

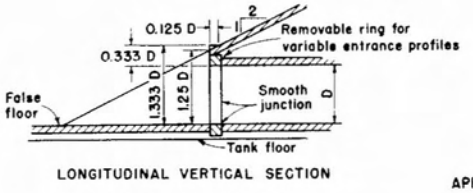

LONGITUDINAL VERTICAL SECTION

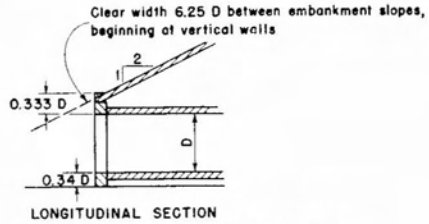

LONGITUDINAL SECTION APPROACH CHANNEL FLOOR BELOW MODEL FLOWLINE

TYPES 1 AND 2

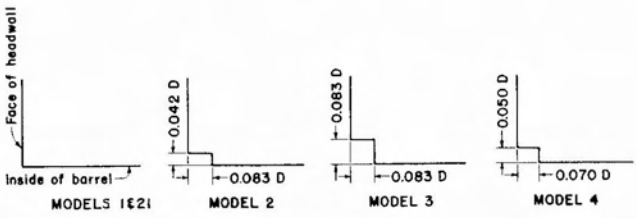

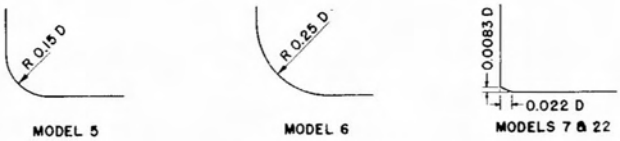

ENTRANCE DETAILS

TYPE 1

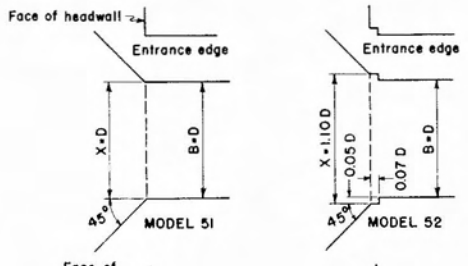

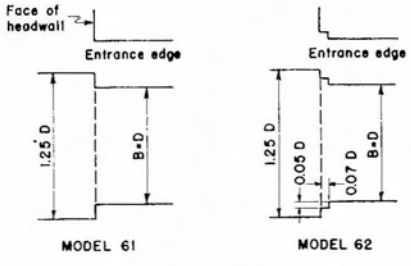

ENTRANCE DETAILS

TYPE 2

FIGURE 3

CULVERT MODEL ENTRANCES

NBS

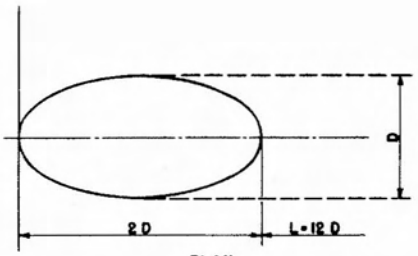

PLAN
MODEL 81
CIRCULAR PIPE

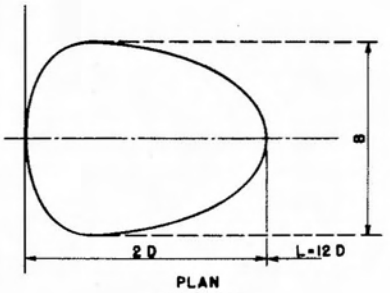

PLAN
MODEL 91
PIPE-ARCH

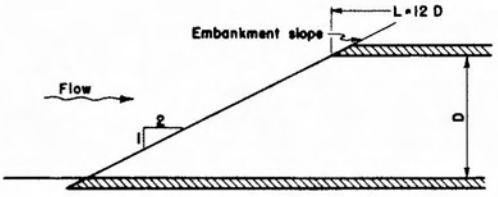

LONGITUDINAL VERTICAL SECTION
MODELS 81 & 91

TYPE 3 MODELS

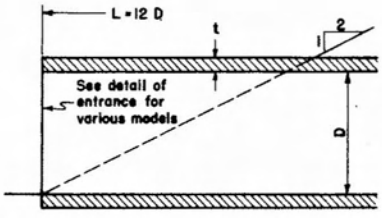

MODELS 101 TO 108 CIRCULAR
121 TO 125 PIPE-ARCH
131 TO 139 ARCH

NORMAL-WALL, VARIOUS ENTRANCES

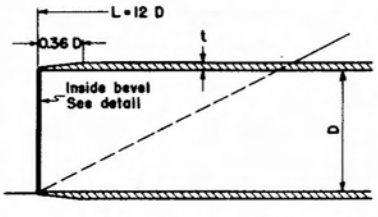

MODELS 111-112 CIRCULAR
126 PIPE-ARCH

THIN-WALL

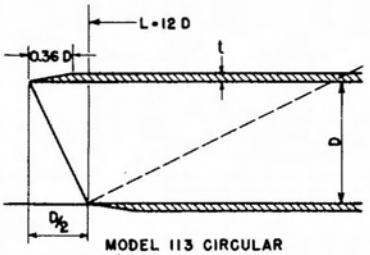

MODEL 113 CIRCULAR
INCLINED PLANE BEVEL

THIN-WALL

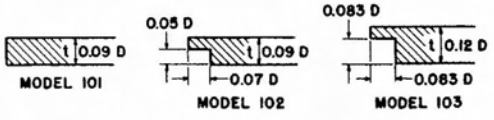

ENTRANCE DETAILS

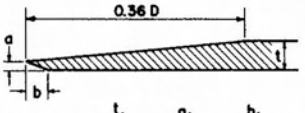

MODEL	t/D	a/D	b/D
111	0.0227	0.0083	0.0220
112	0.0227	0.0035	0.0092
126	0.045	0.0083	0.0220

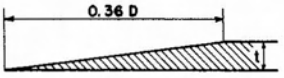

MODEL	t/D
113	0.045

BEVEL DETAILS

TYPE 4 MODELS

NBS

FIGURE 4
CULVERT MODEL ENTRANCES

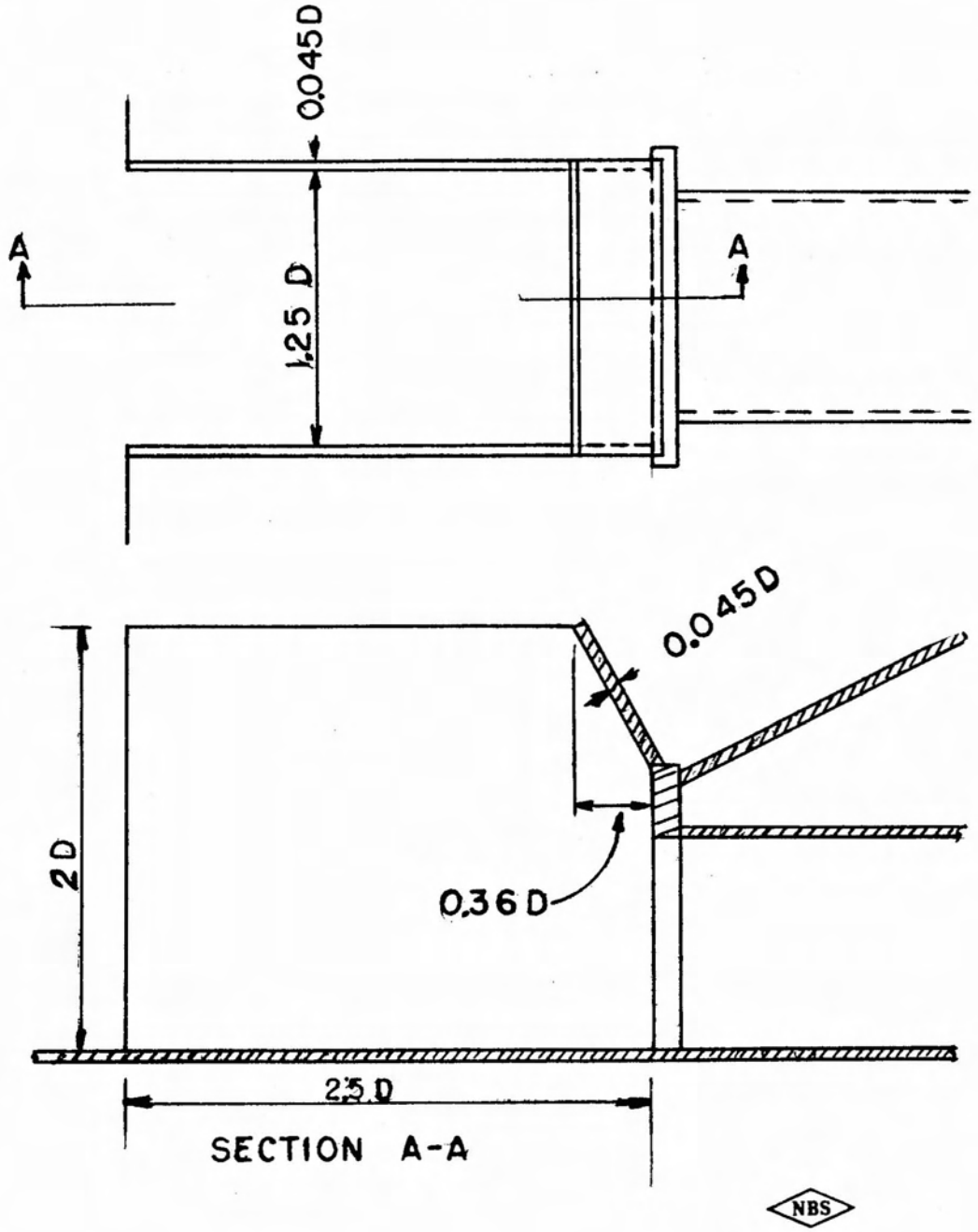

FIGURE 5
MODEL 62.1

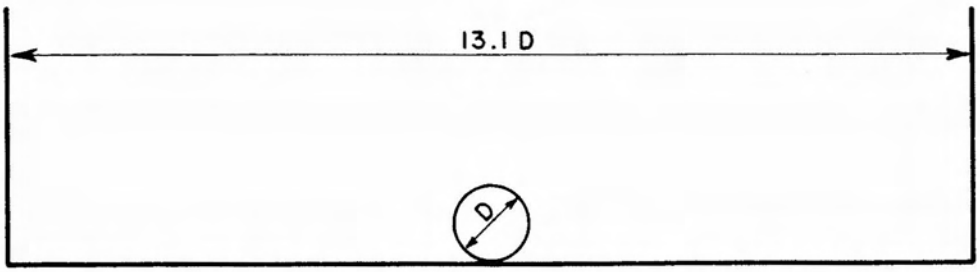

WIDE RECTANGULAR APPROACH CHANNEL
Used with all model tests except those for which a special approach channel section is specified

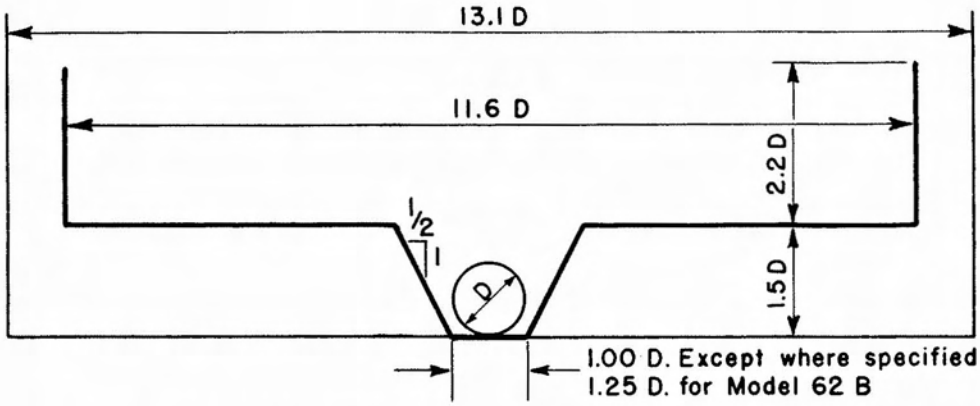

TRAPEZOIDAL RESTRICTED APPROACH CHANNEL
Used with models designated by suffix "B"

CIRCULAR PIPE ARCH

BARREL SECTIONS

FIGURE 6

UPSTREAM APPROACH CHANNELS AND CULVERT MODEL BARRELS

MAY 1955

NATIONAL BUREAU OF STANDARDS
RESEARCH PROJECT 0603-10-3586

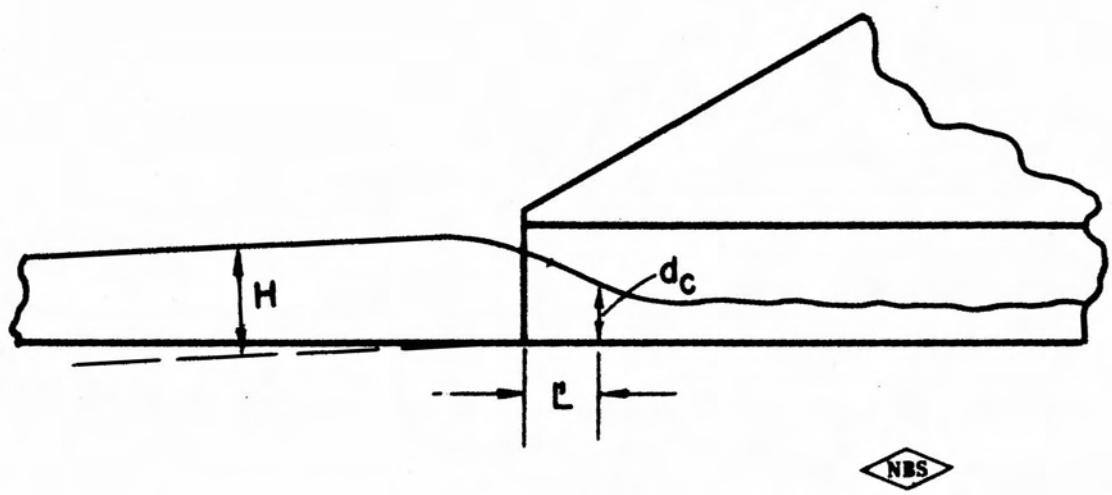

FIGURE 7
NON-SUBMERGED INLET — SUPERCRITICAL SLOPE

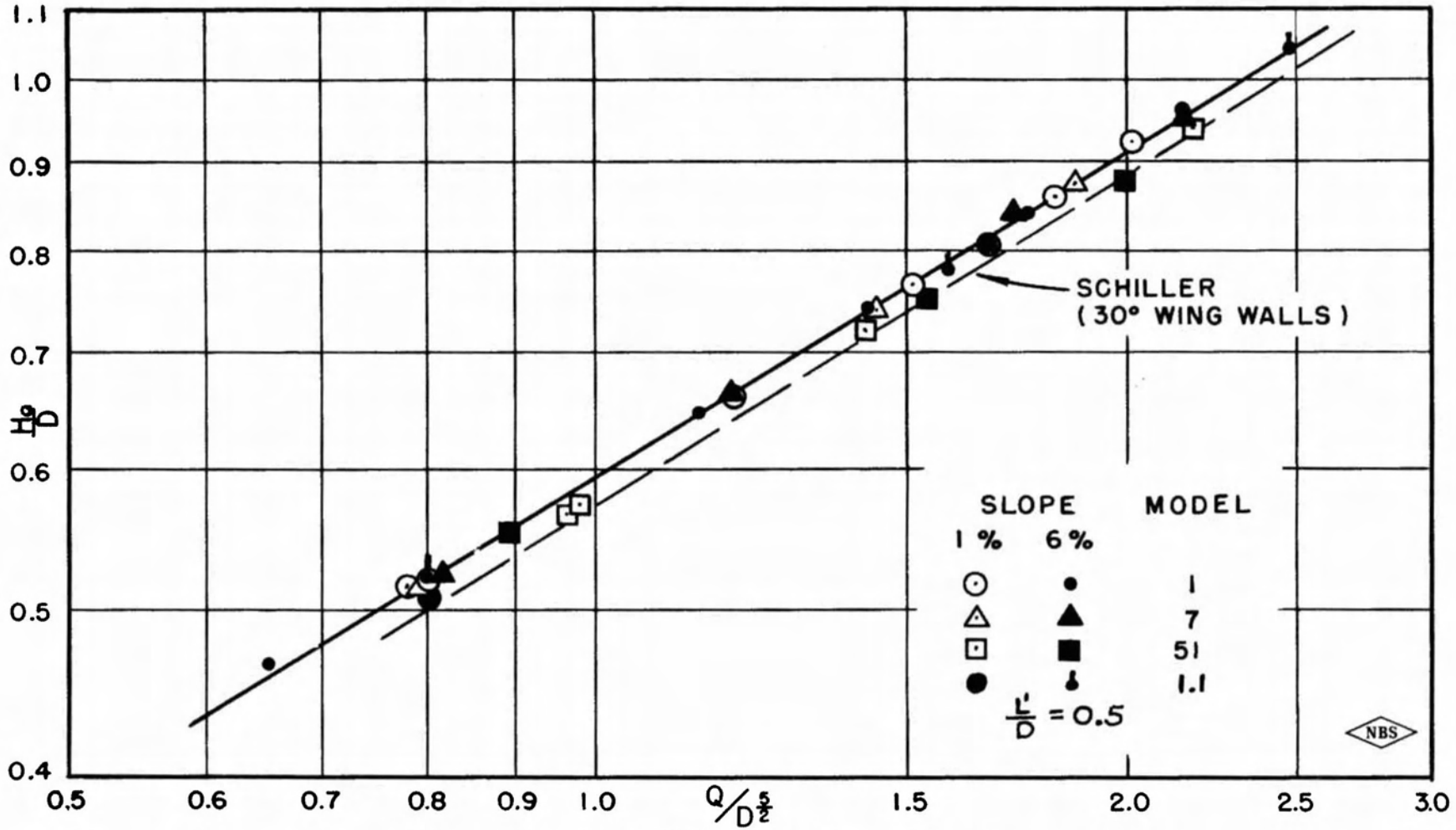

FIGURE 8
NON-SUBMERGED ENTRANCE – ENTRANCE CONTROL
MODELS 1, 7 AND 51

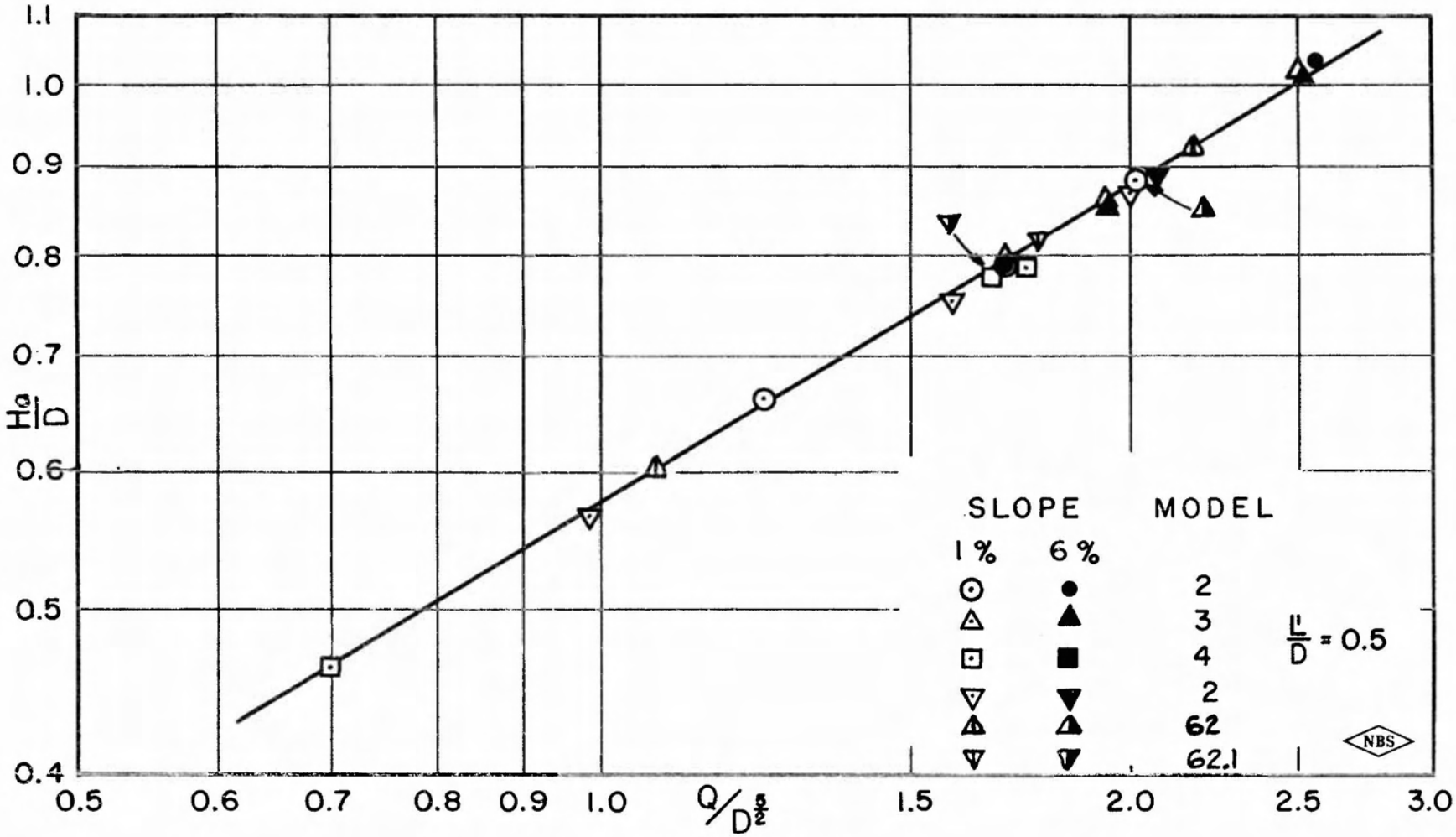

FIGURE 9
NON-SUBMERGED ENTRANCE-ENTRANCE CONTROL
HEADWALL-SOCKET INLETS

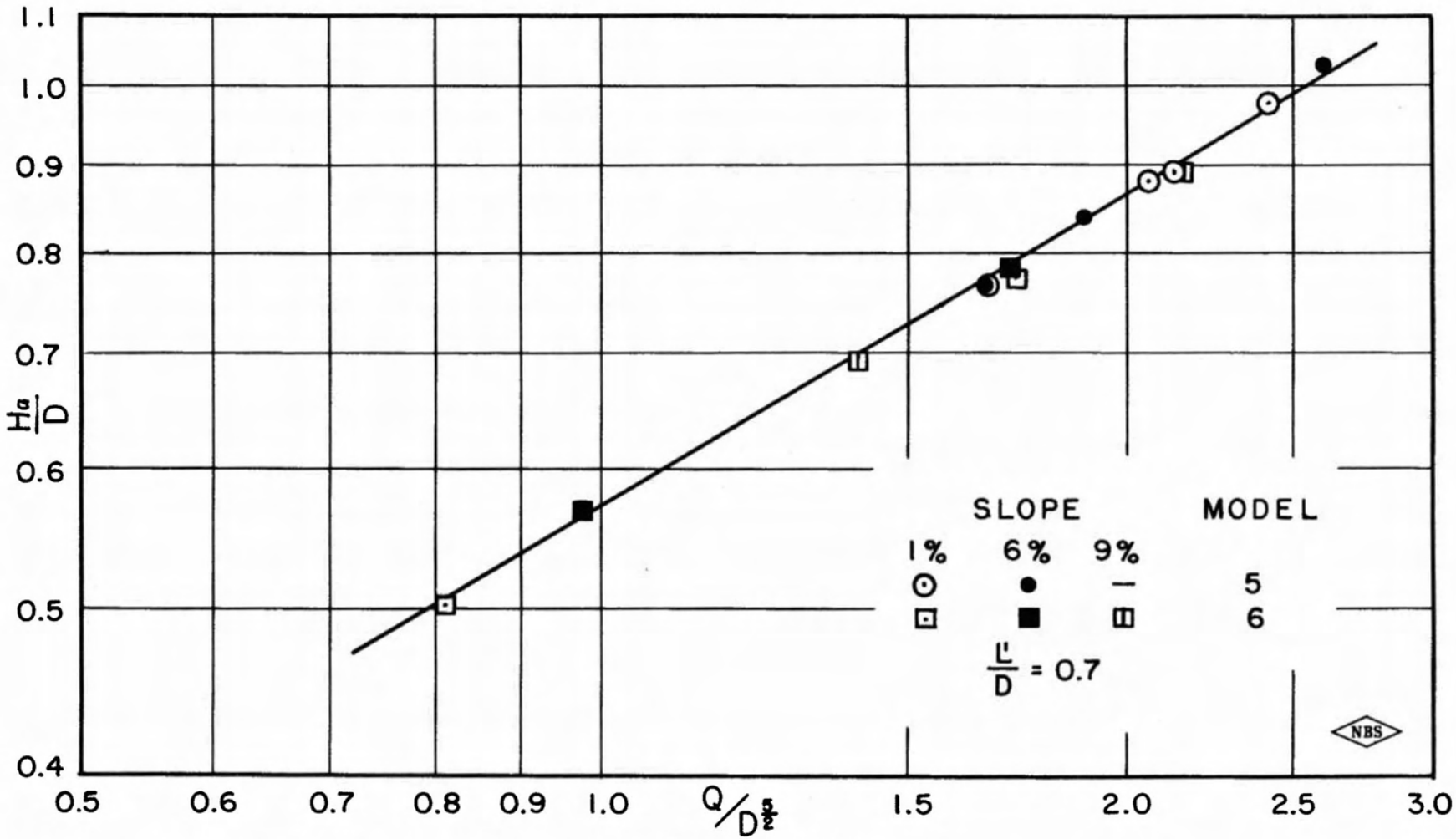

FIGURE 10
NON-SUBMERGED FLOW – ENTRANCE CONTROL
MODELS 5 AND 6

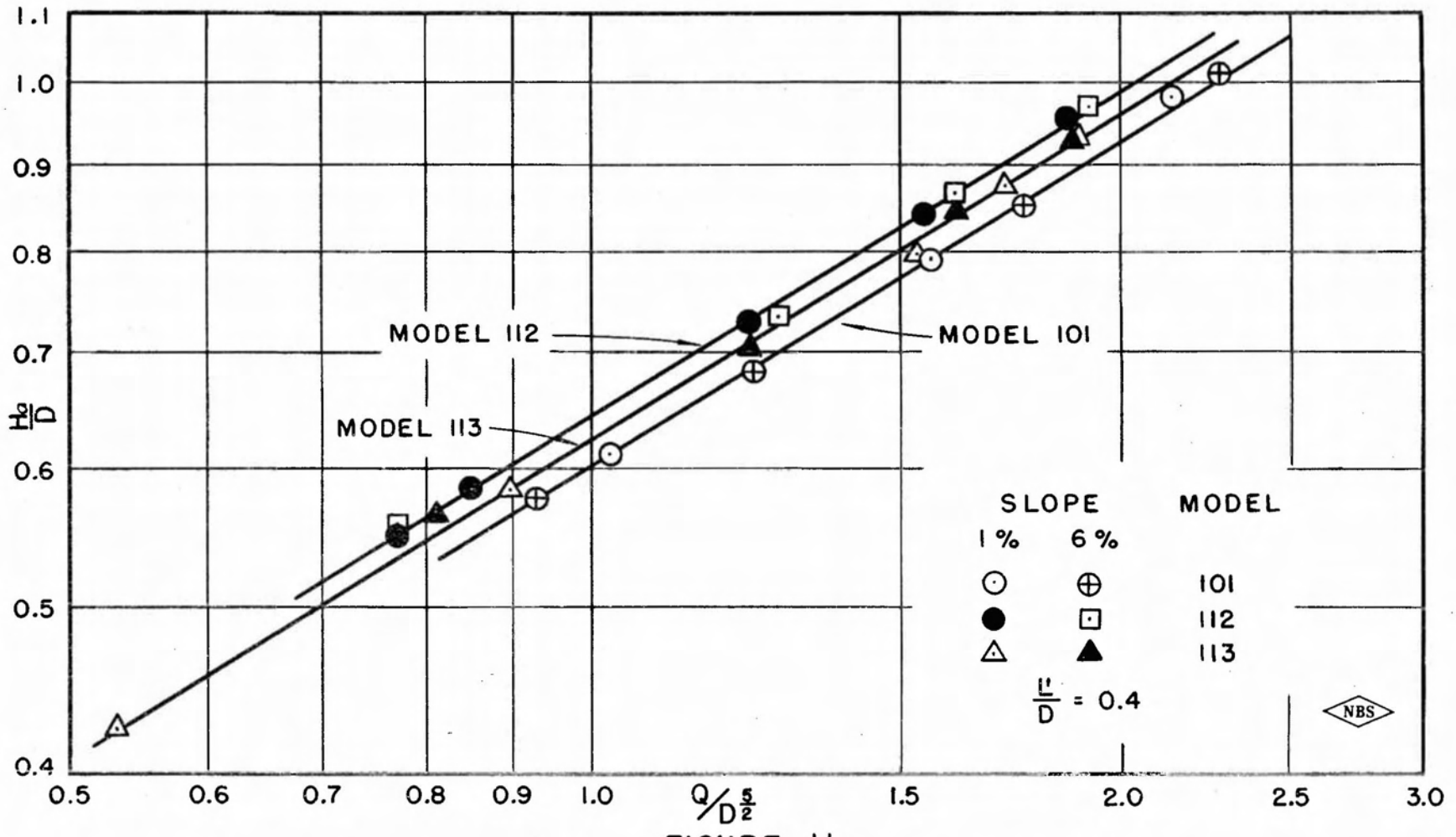

FIGURE 11
NON-SUBMERGED ENTRANCE-ENTRANCE CONTROL
MODELS 101, 112 AND 113

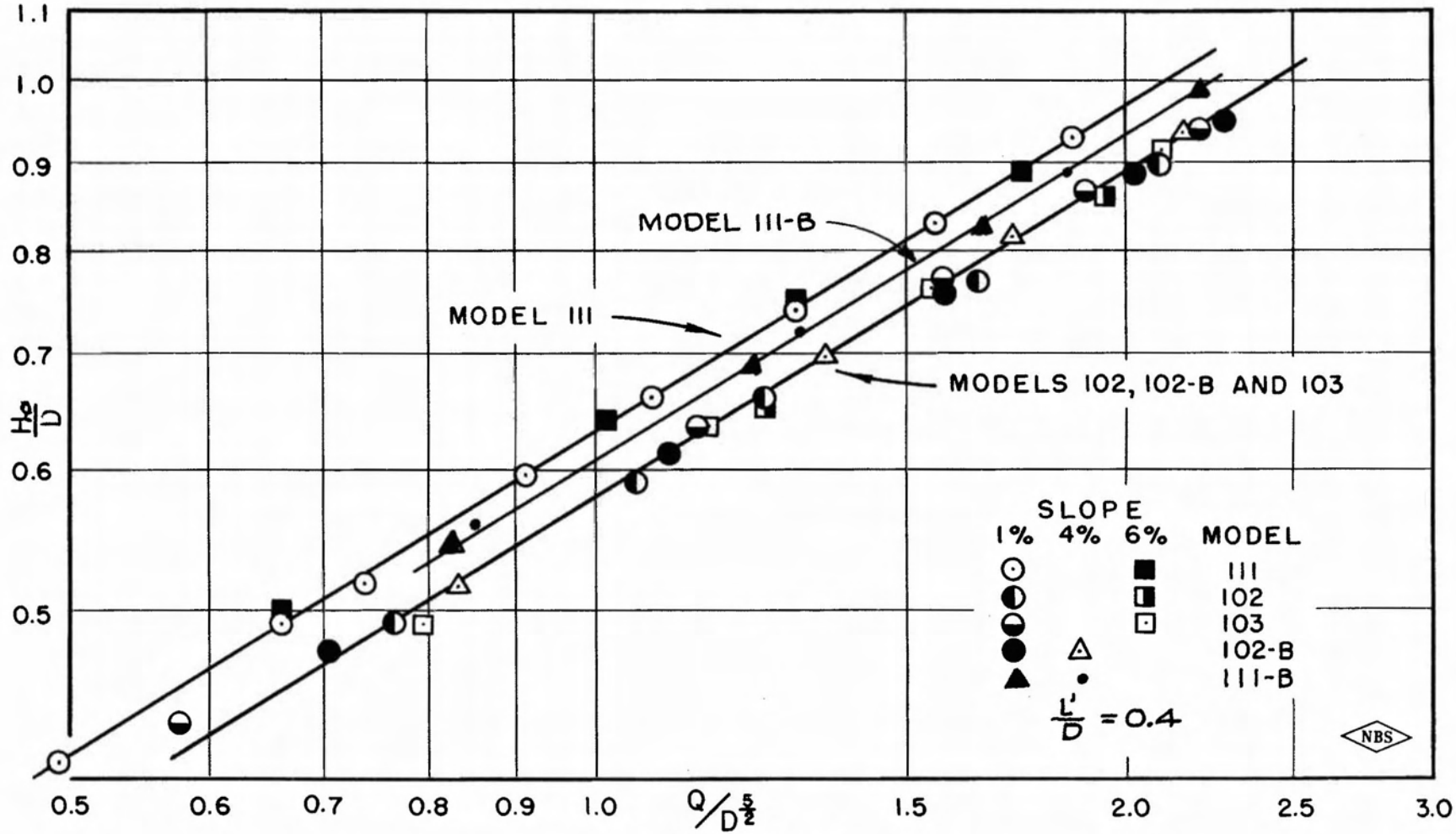

FIGURE 12
NON-SUBMERGED ENTRANCE – ENTRANCE CONTROL
MODELS 102, 102-B, 103, 111 & 111-B

FIGURE 13
SQUARE EDGE FLUSH WITH EMBANKMENT SLOPE
NON-SUBMERGED ENTRANCE - ENTRANCE CONTROL

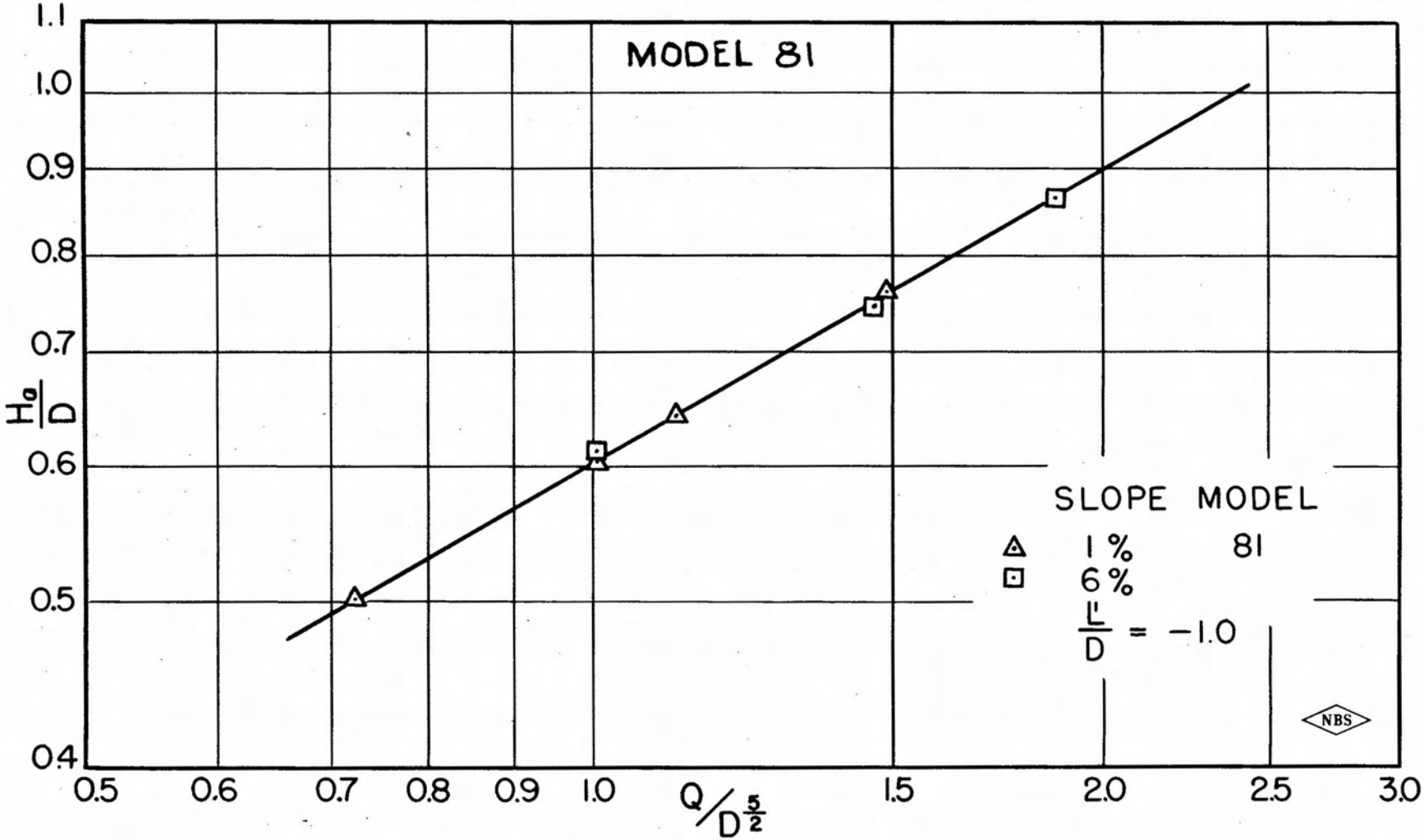

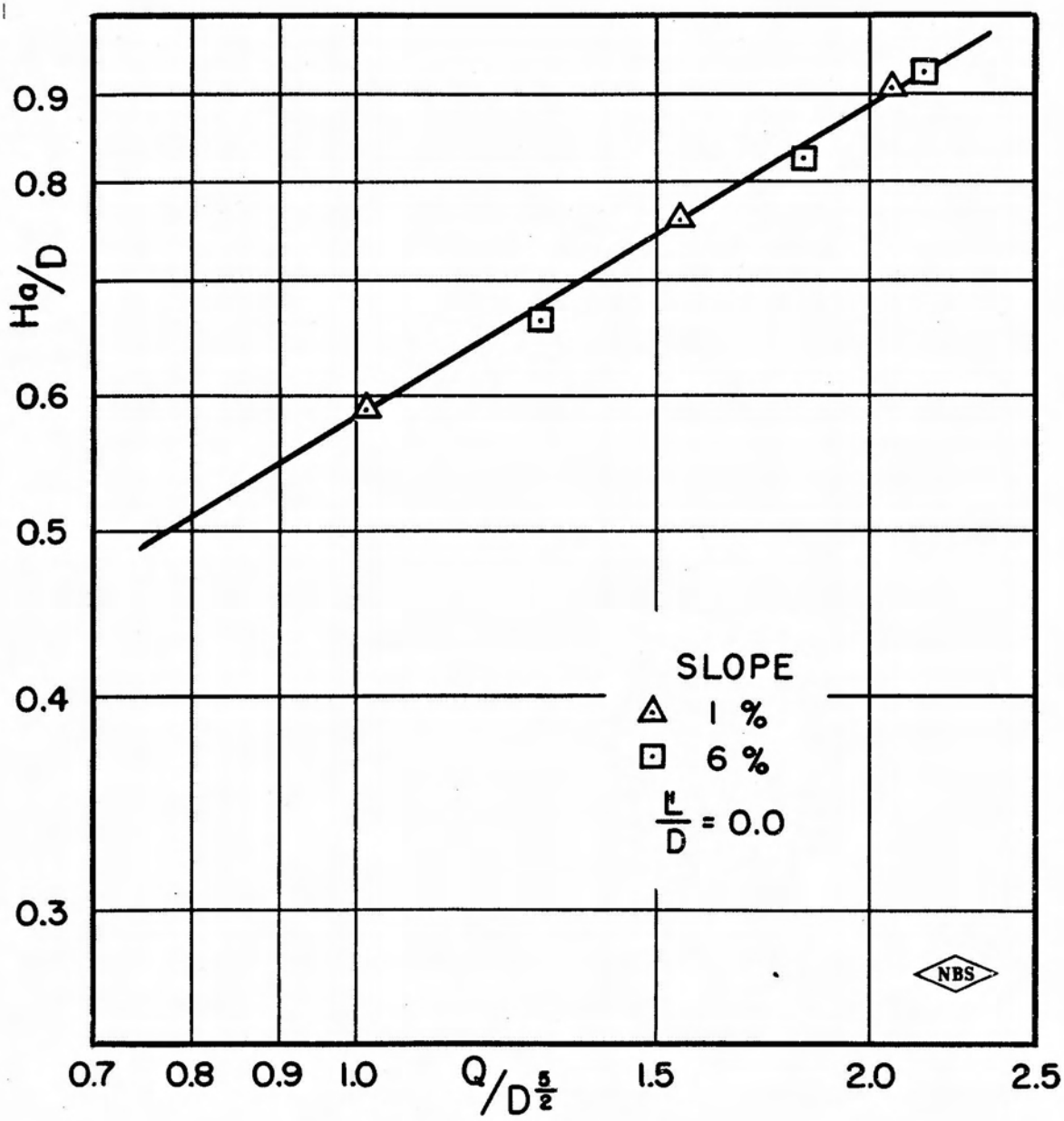

FIGURE 14
NON-SUBMERGED ENTRANCE-ENTRANCE CONTROL
MODEL 61

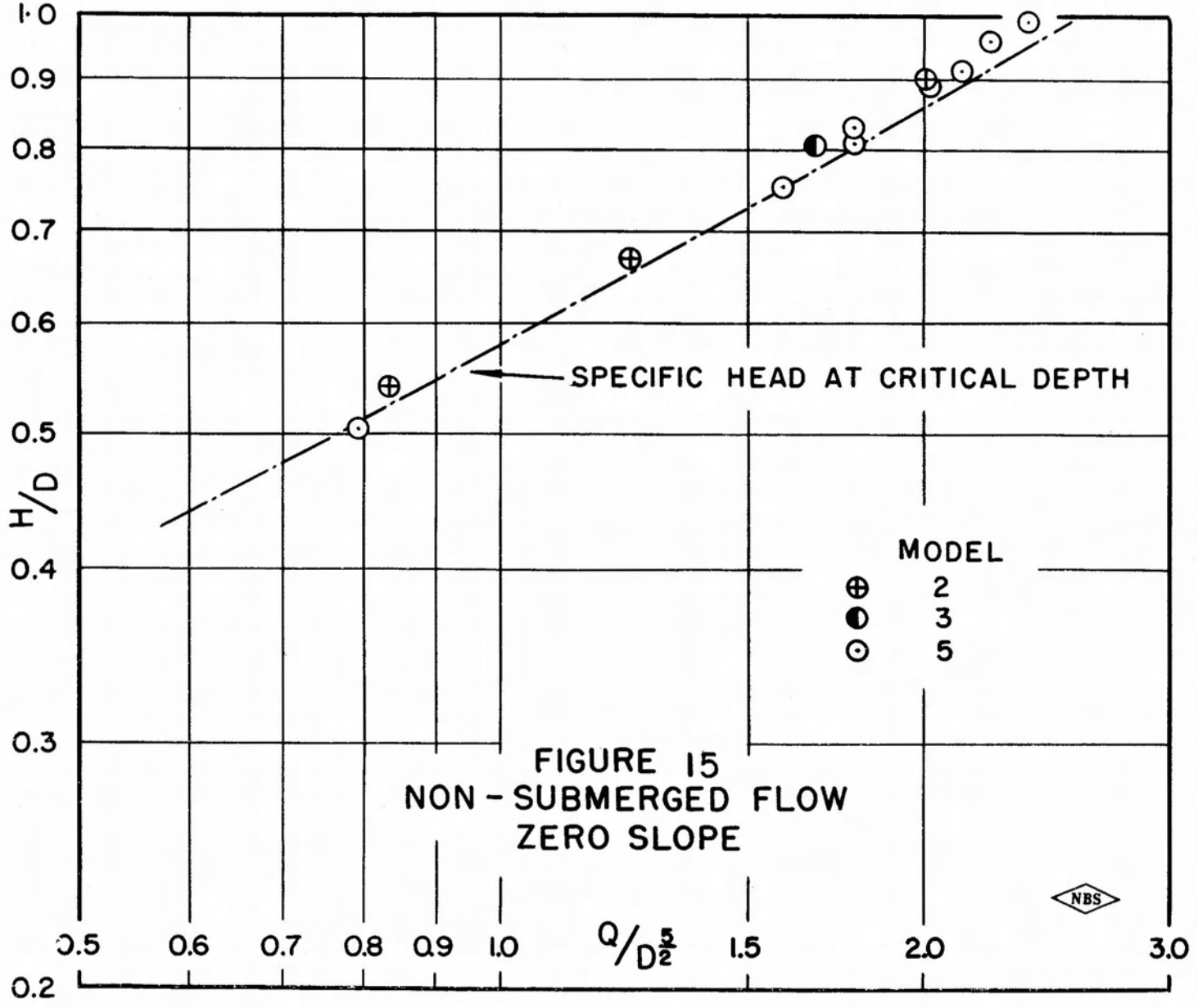

FIGURE 15
NON-SUBMERGED FLOW
ZERO SLOPE

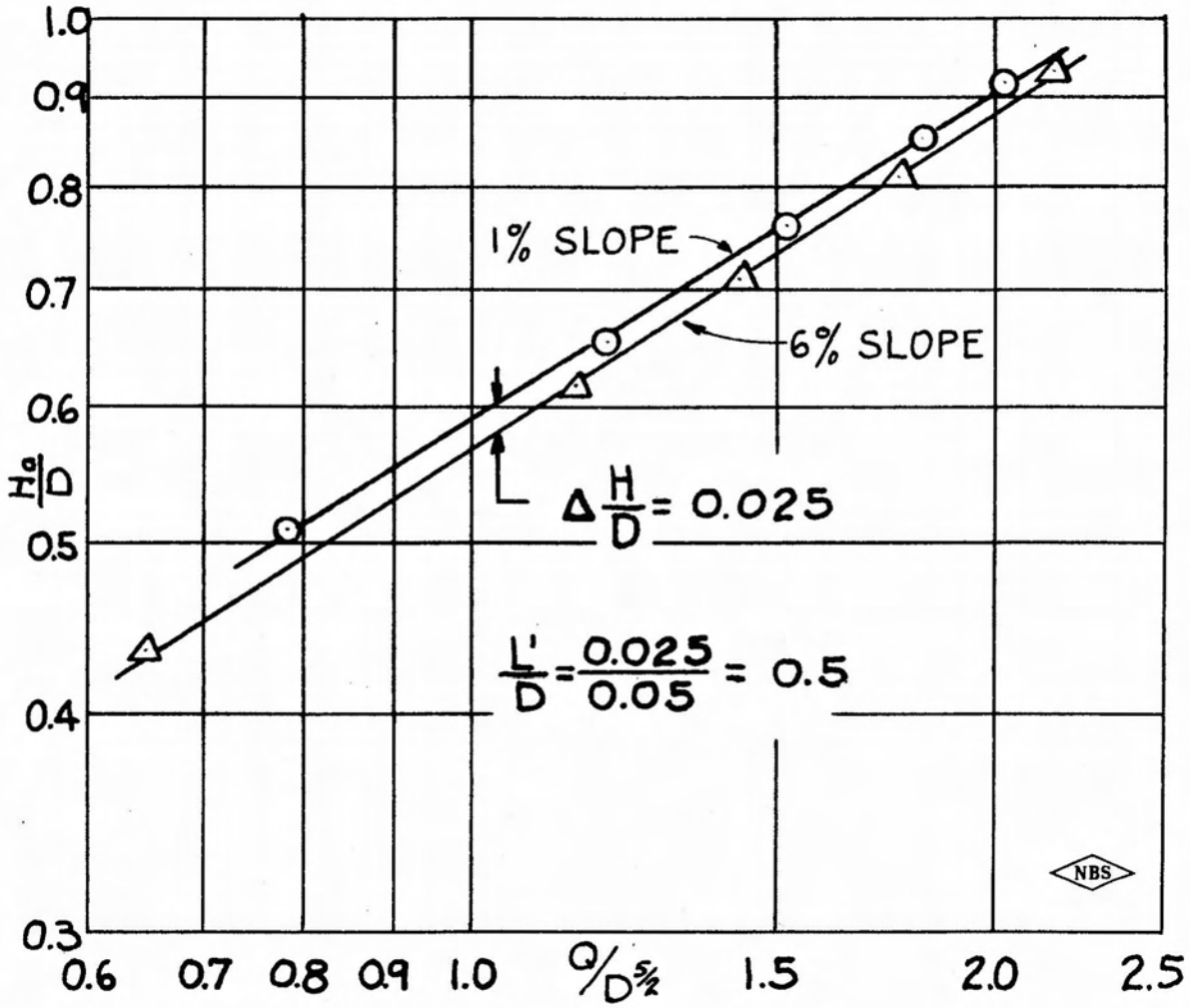

FIGURE 16

DETERMINATION OF $\frac{L'}{D}$

MODEL 1

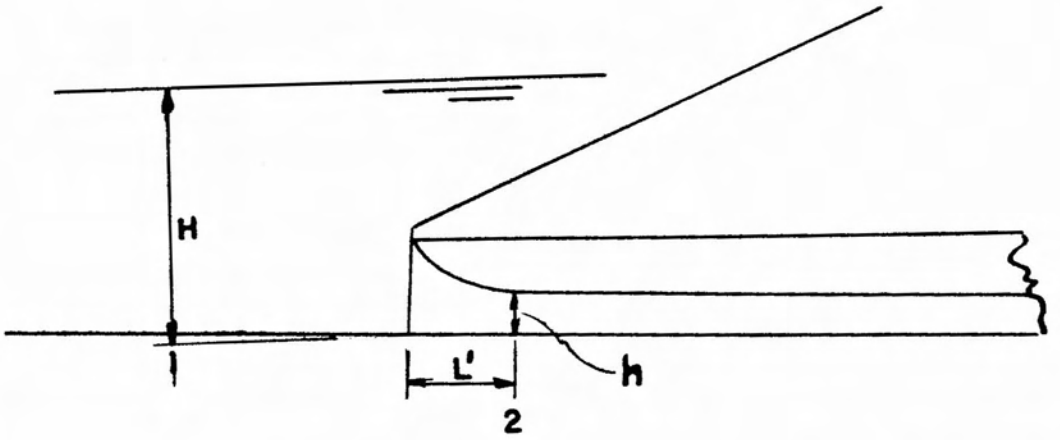

FIGURE 17– SUBMERGED ENTRANCE ENTRANCE CONTROL

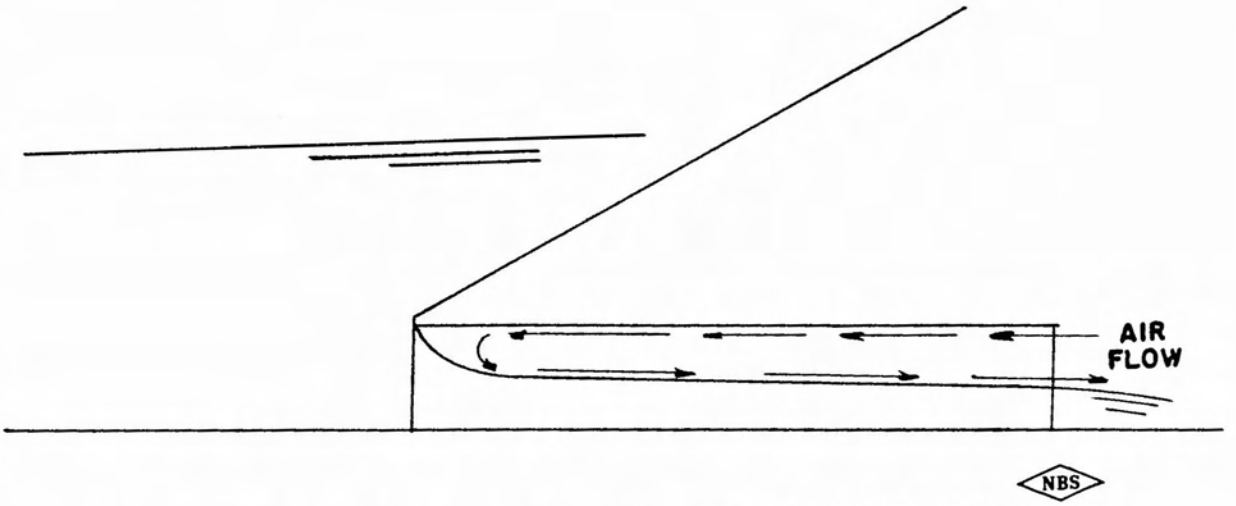

FIGURE 18–AIR FLOW INTO CULVERT FROM OUTLET

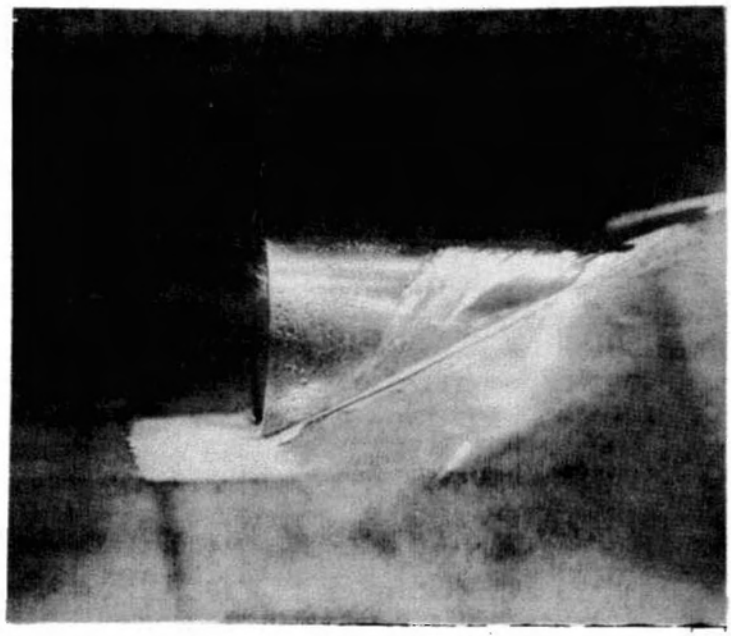

(a) SIDE VIEW

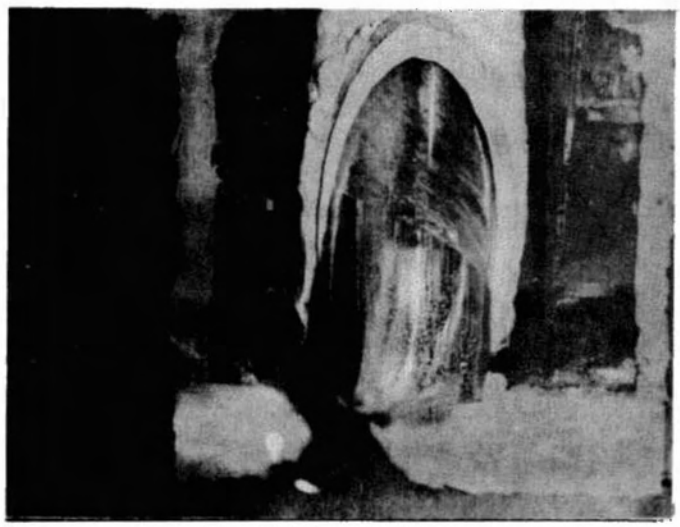

(b) TOP VIEW

FIGURE 19

FLOW CONDITIONS AT INLET MODEL III

$\frac{H}{D}$= 3.0, S = 6%, $\frac{L}{D}$ = 12.0

FIGURE 20 – SPIRAL MOTION IN CULVERT INLET

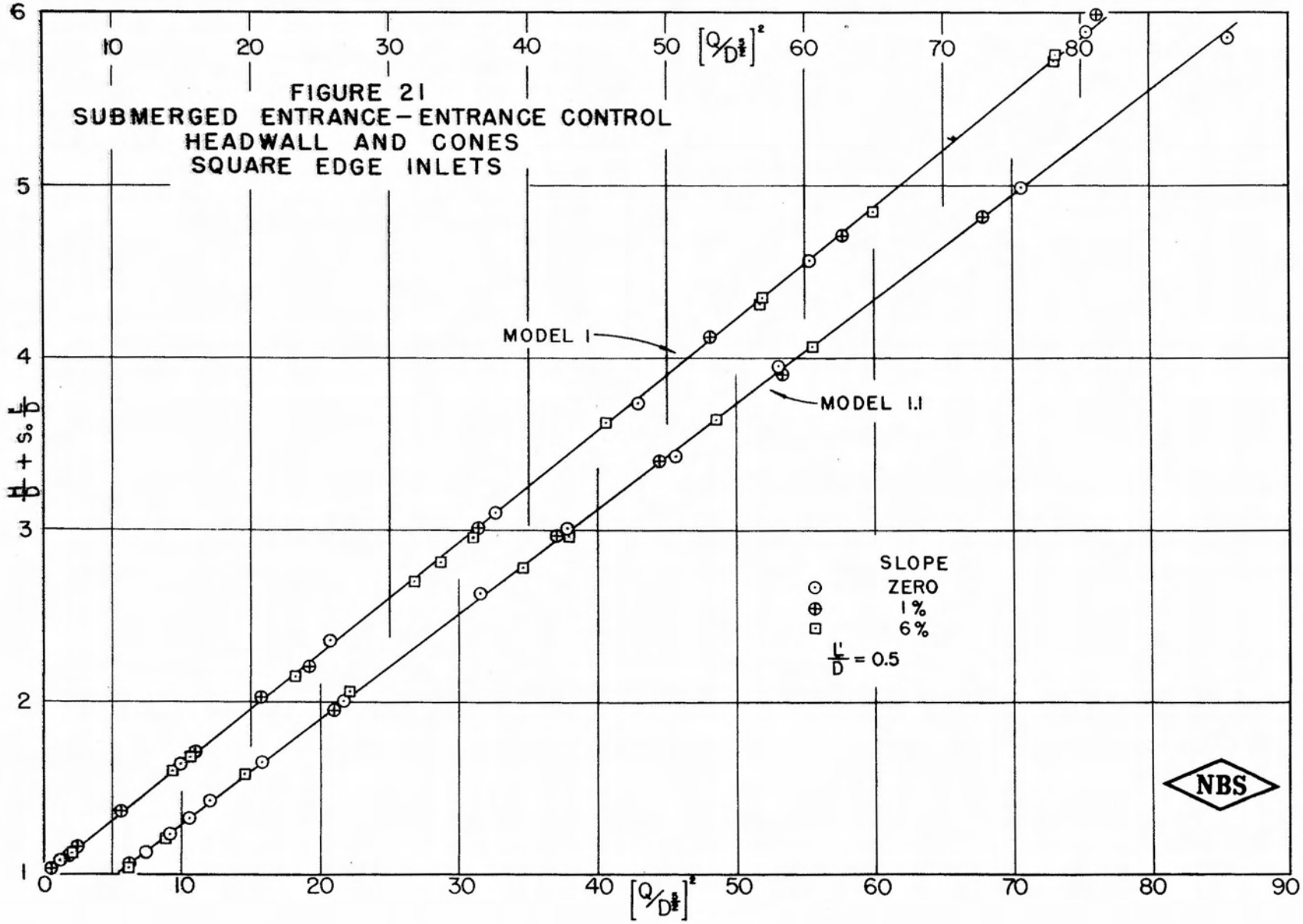
FIGURE 21
SUBMERGED ENTRANCE – ENTRANCE CONTROL
HEADWALL AND CONES
SQUARE EDGE INLETS
$\left[Q/D^{\frac{5}{2}}\right]^2$
$\frac{H}{D} + S_o\frac{L}{D}$
MODEL 1
MODEL 1.1
SLOPE
ZERO
1%
6%
$\frac{L'}{D} = 0.5$
NBS

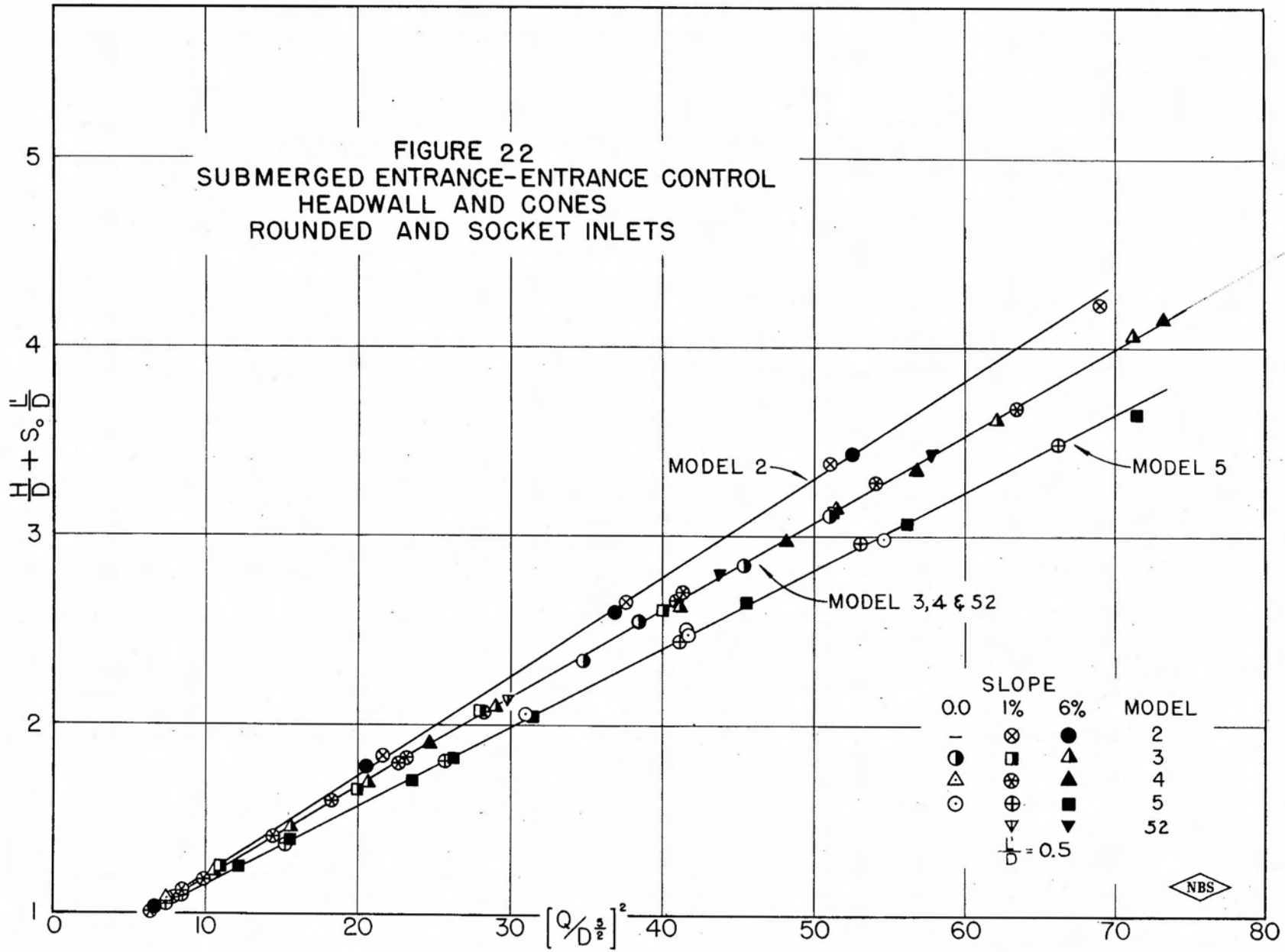
FIGURE 22
SUBMERGED ENTRANCE-ENTRANCE CONTROL
HEADWALL AND CONES
ROUNDED AND SOCKET INLETS
H/D + S_o L/D
[Q/D^5/2]^2
MODEL 2
MODEL 5
MODEL 3,4 & 52
SLOPE
0.0
1%
6%
MODEL
2
3
4
5
52
L/D = 0.5
NBS

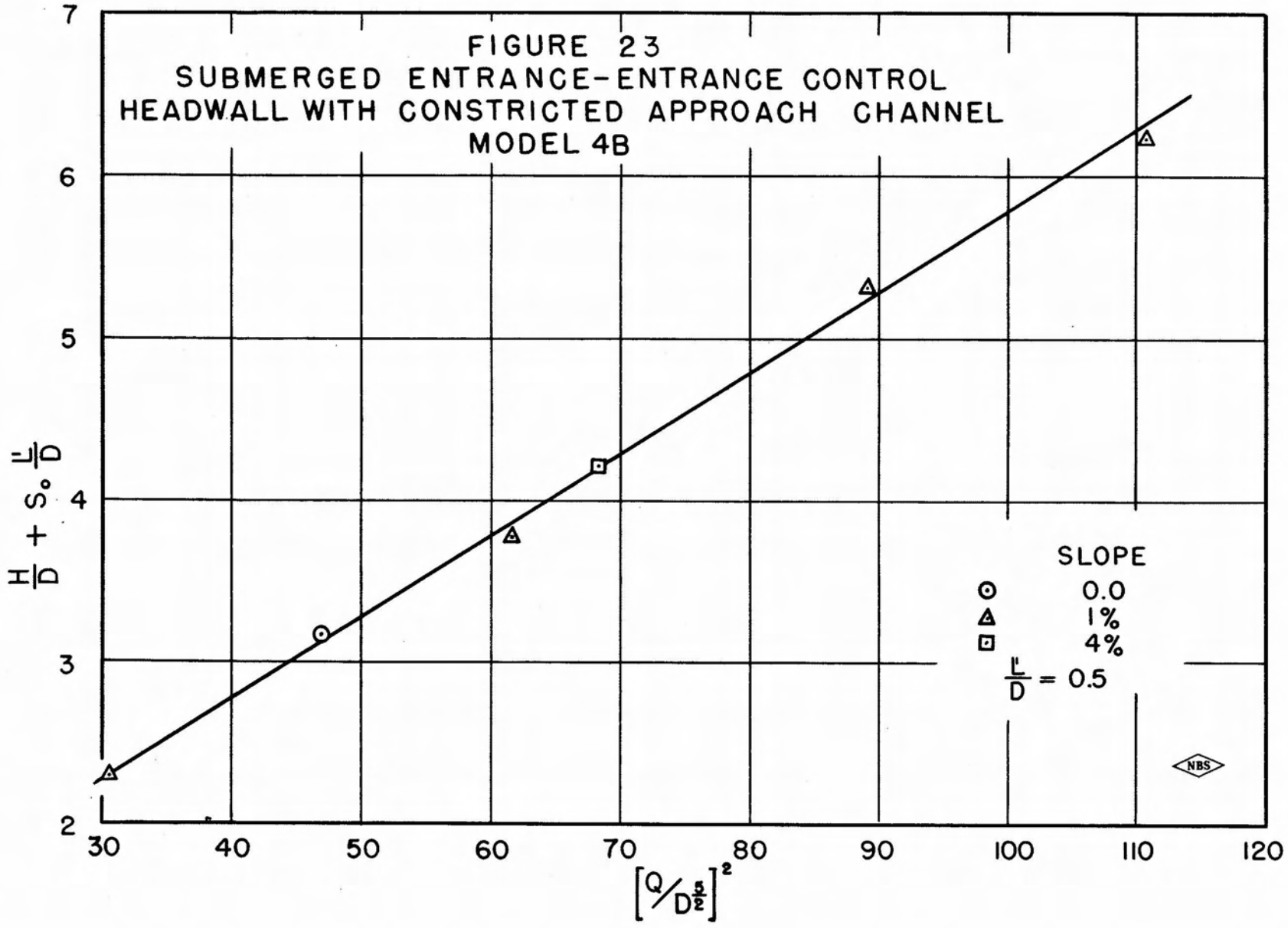
FIGURE 23
SUBMERGED ENTRANCE-ENTRANCE CONTROL
HEADWALL WITH CONSTRICTED APPROACH CHANNEL
MODEL 4B
$\frac{H}{D} + S_o \frac{L}{D}$
$\left[\frac{Q}{D^{\frac{5}{2}}}\right]^2$
SLOPE
0.0
1%
4%
$\frac{L}{D} = 0.5$
NBS
2
3
4
5
6
7
30
40
50
60
70
80
90
100
110
120

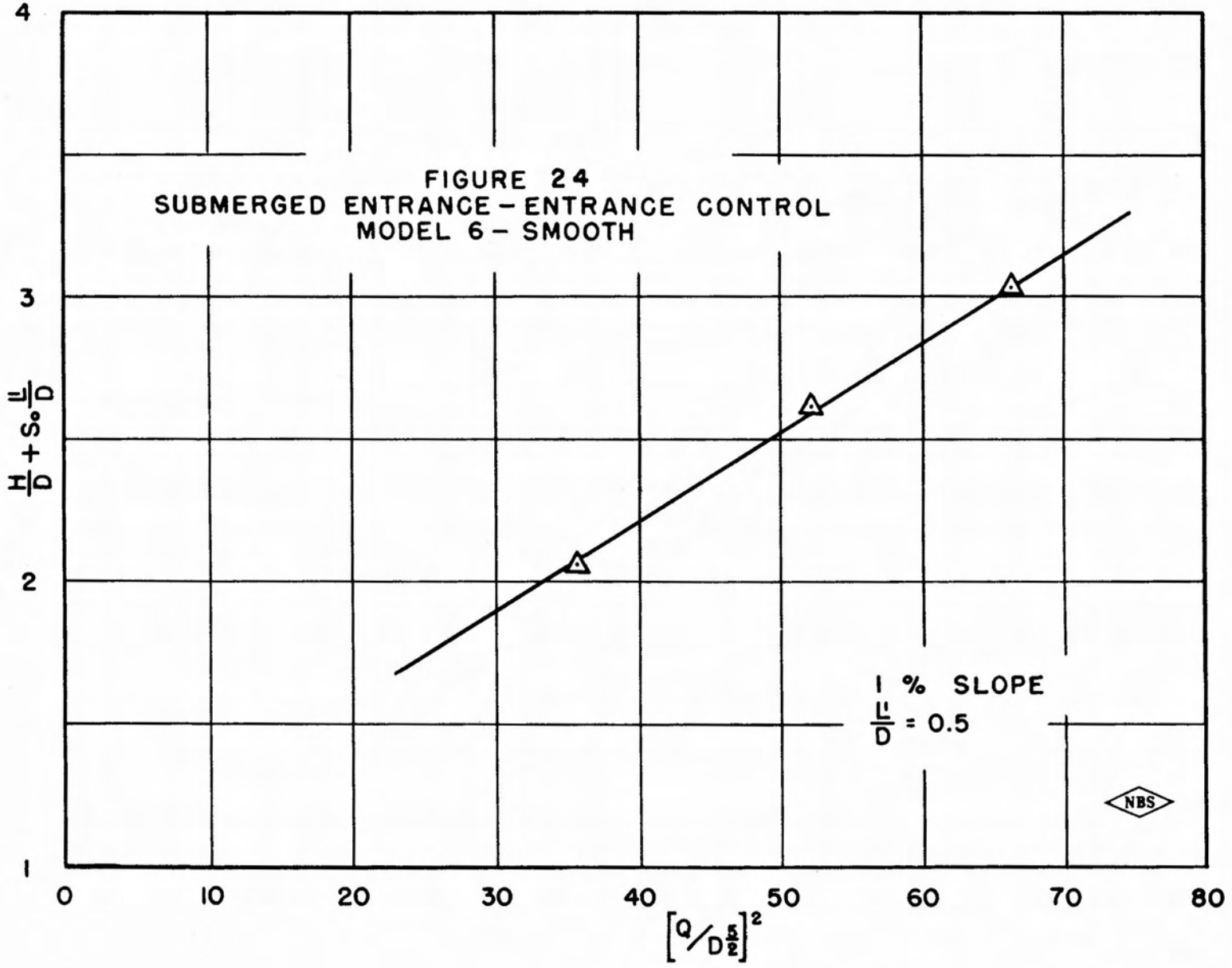
FIGURE 24
SUBMERGED ENTRANCE – ENTRANCE CONTROL
MODEL 6 – SMOOTH
4
3
2
1
H/D + S₀ l/D
0
10
20
30
40
50
60
70
80
[Q/D^(5/2)]²
1 % SLOPE
l/D = 0.5
NBS

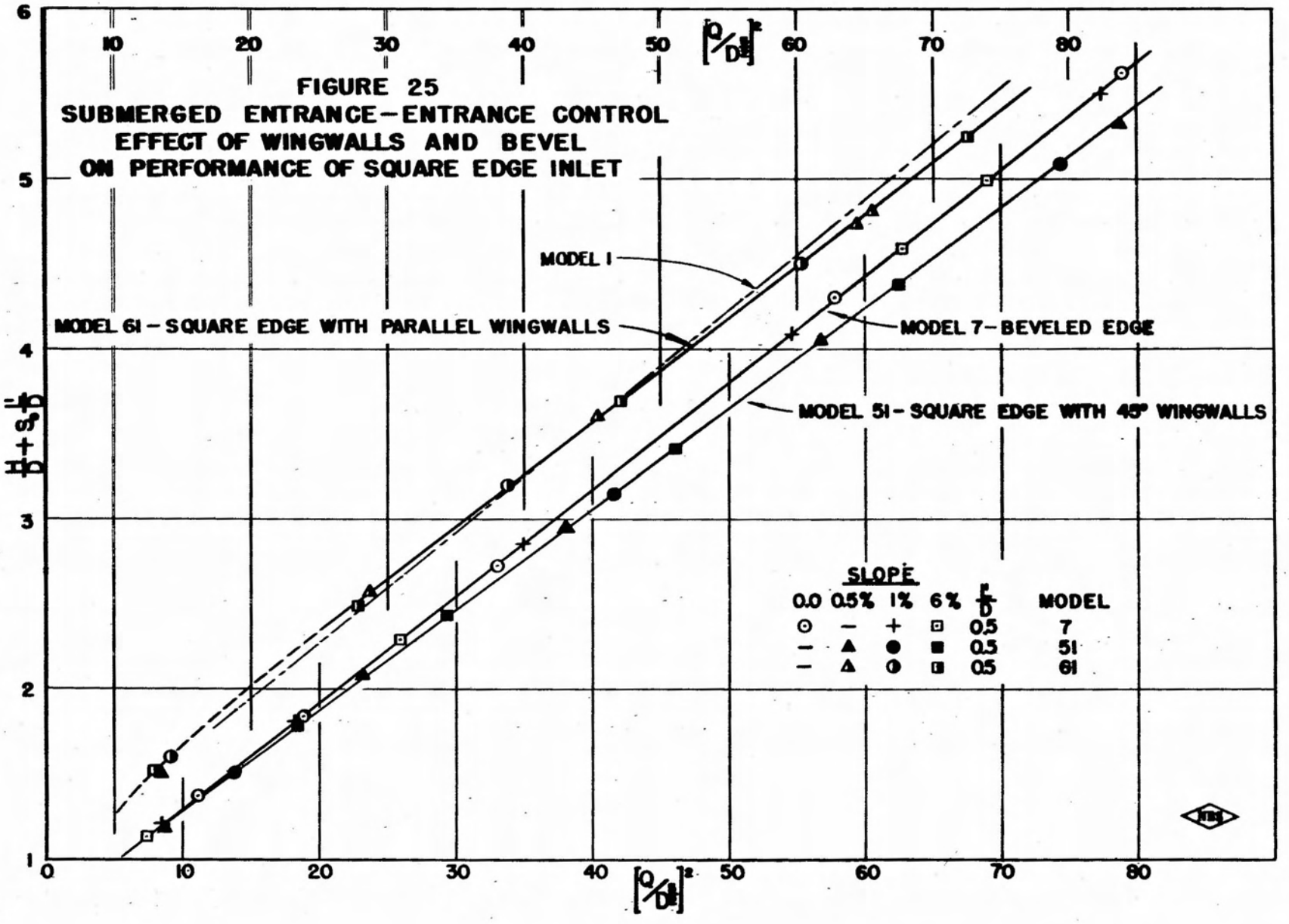
FIGURE 25
SUBMERGED ENTRANCE-ENTRANCE CONTROL
EFFECT OF WINGWALLS AND BEVEL
ON PERFORMANCE OF SQUARE EDGE INLET
MODEL 1
MODEL 61 - SQUARE EDGE WITH PARALLEL WINGWALLS
MODEL 7 - BEVELED EDGE
MODEL 51 - SQUARE EDGE WITH 45° WINGWALLS
SLOPE
0.0 0.5% 1% 6% S/D MODEL
0.5 7
0.5 51
0.5 61
[Q/D^2.5]^2
H/D + S/D

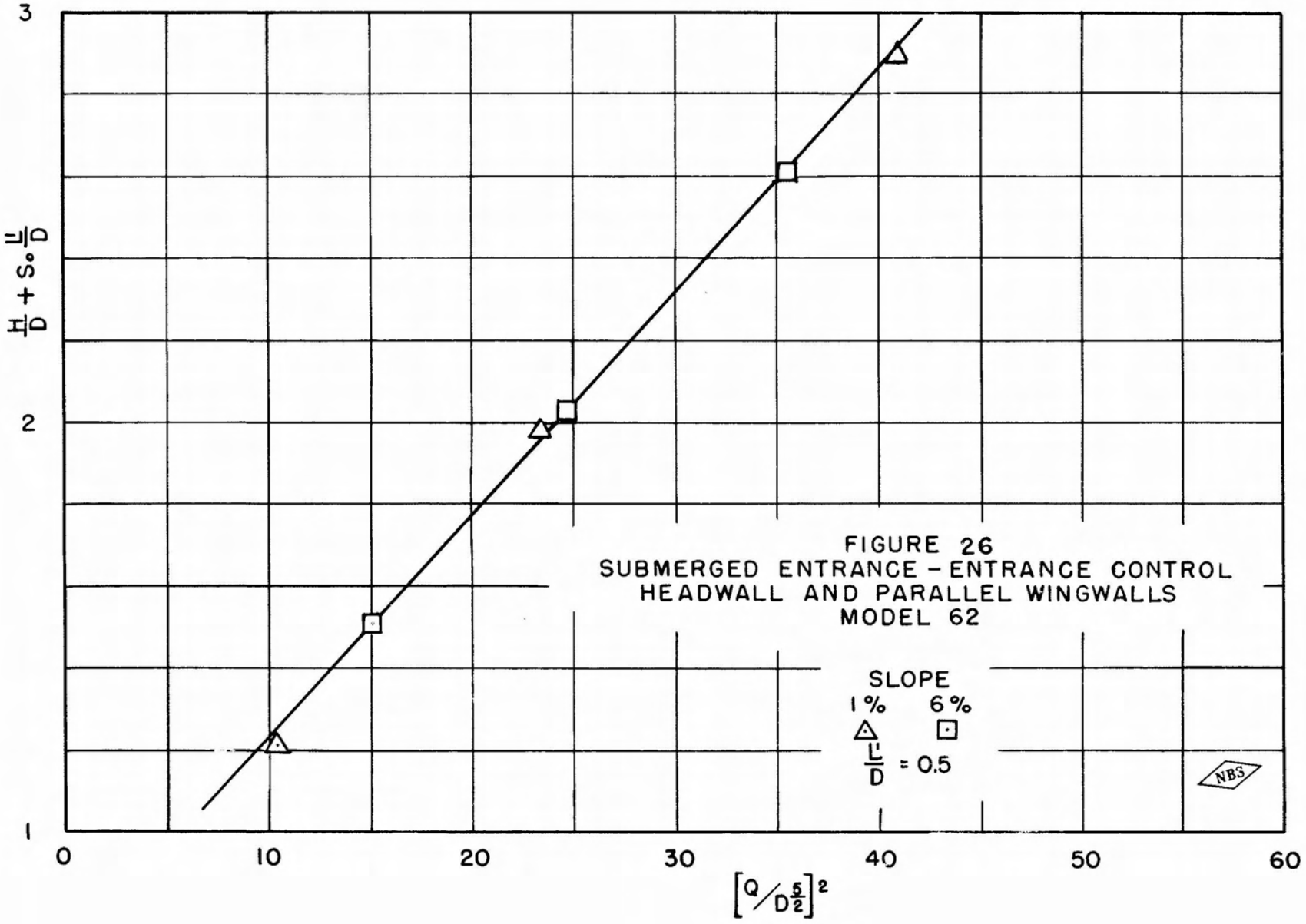

FIGURE 26
SUBMERGED ENTRANCE - ENTRANCE CONTROL
HEADWALL AND PARALLEL WINGWALLS
MODEL 62

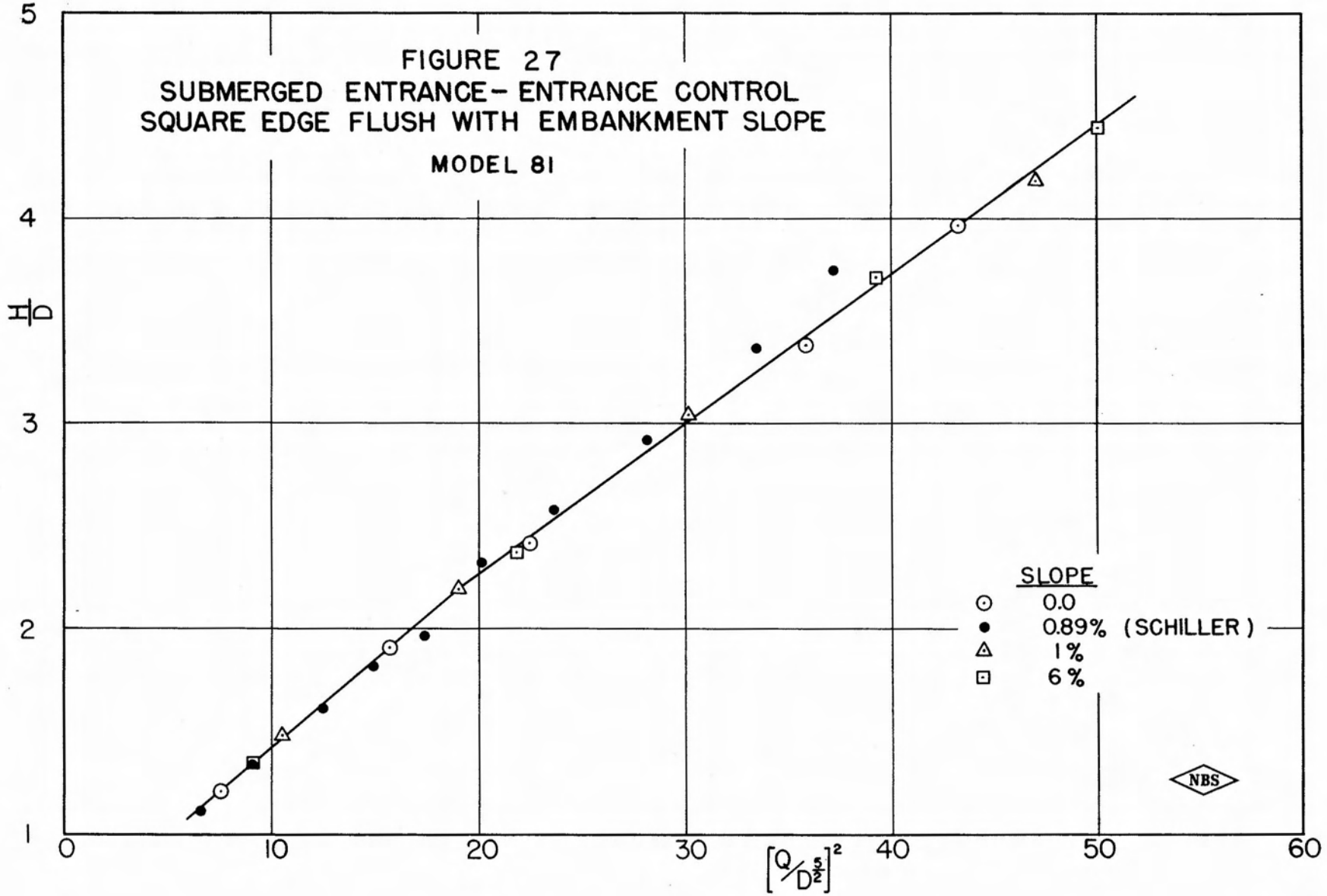
FIGURE 27
SUBMERGED ENTRANCE- ENTRANCE CONTROL
SQUARE EDGE FLUSH WITH EMBANKMENT SLOPE
MODEL 81
H/D
5
4
3
2
1
0
10
20
30
40
50
60
$[Q/D^{\frac{5}{2}}]^2$
SLOPE
0.0
0.89% (SCHILLER)
1%
6%
NBS

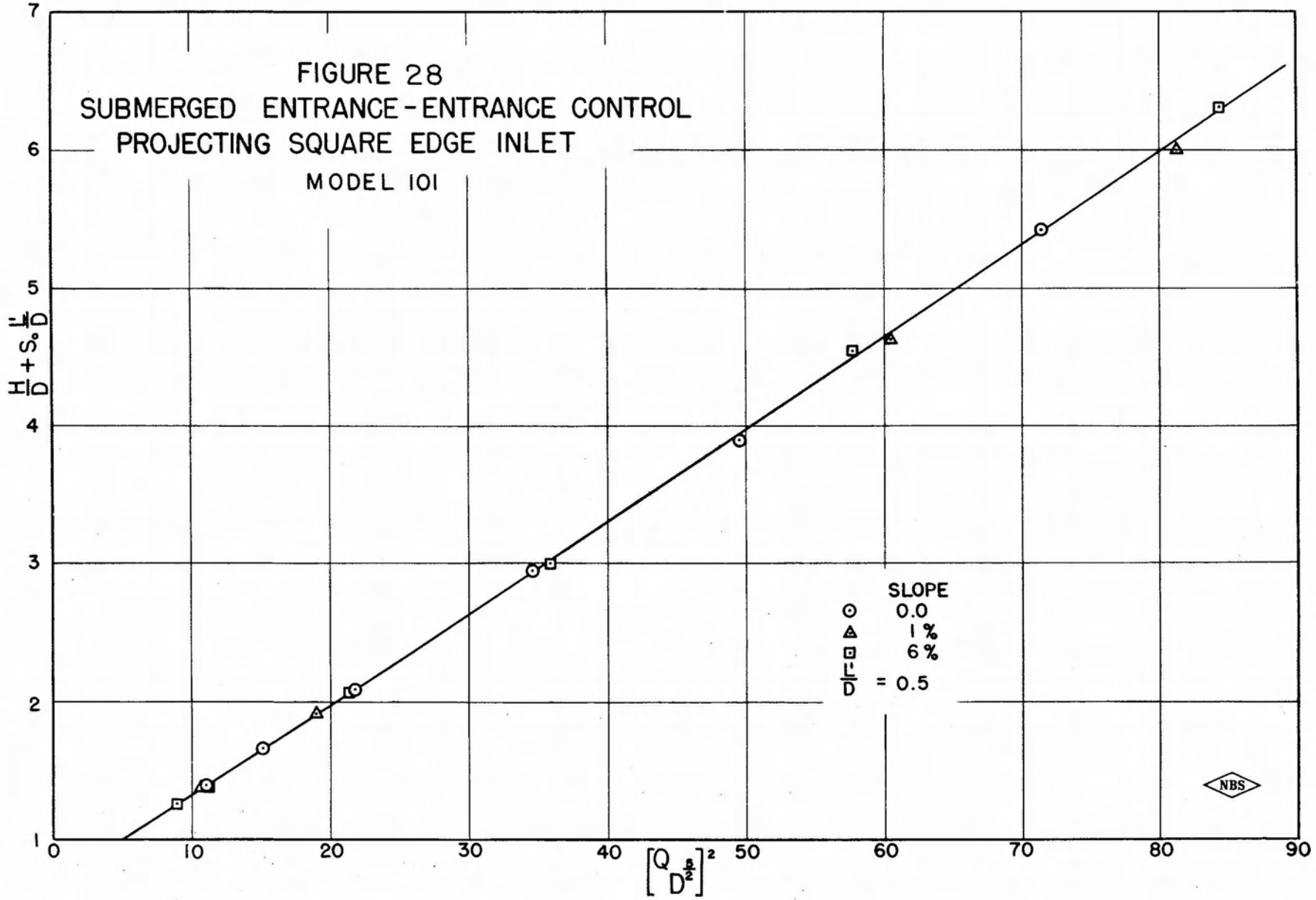
FIGURE 28
SUBMERGED ENTRANCE - ENTRANCE CONTROL
PROJECTING SQUARE EDGE INLET
MODEL 101
$\frac{H}{D} + S_o \frac{L}{D}$
$\left[\frac{Q}{D^{\frac{5}{2}}}\right]^2$
SLOPE
0.0
1%
6%
$\frac{L}{D}$ = 0.5
NBS
1
2
3
4
5
6
7
0
10
20
30
40
50
60
70
80
90

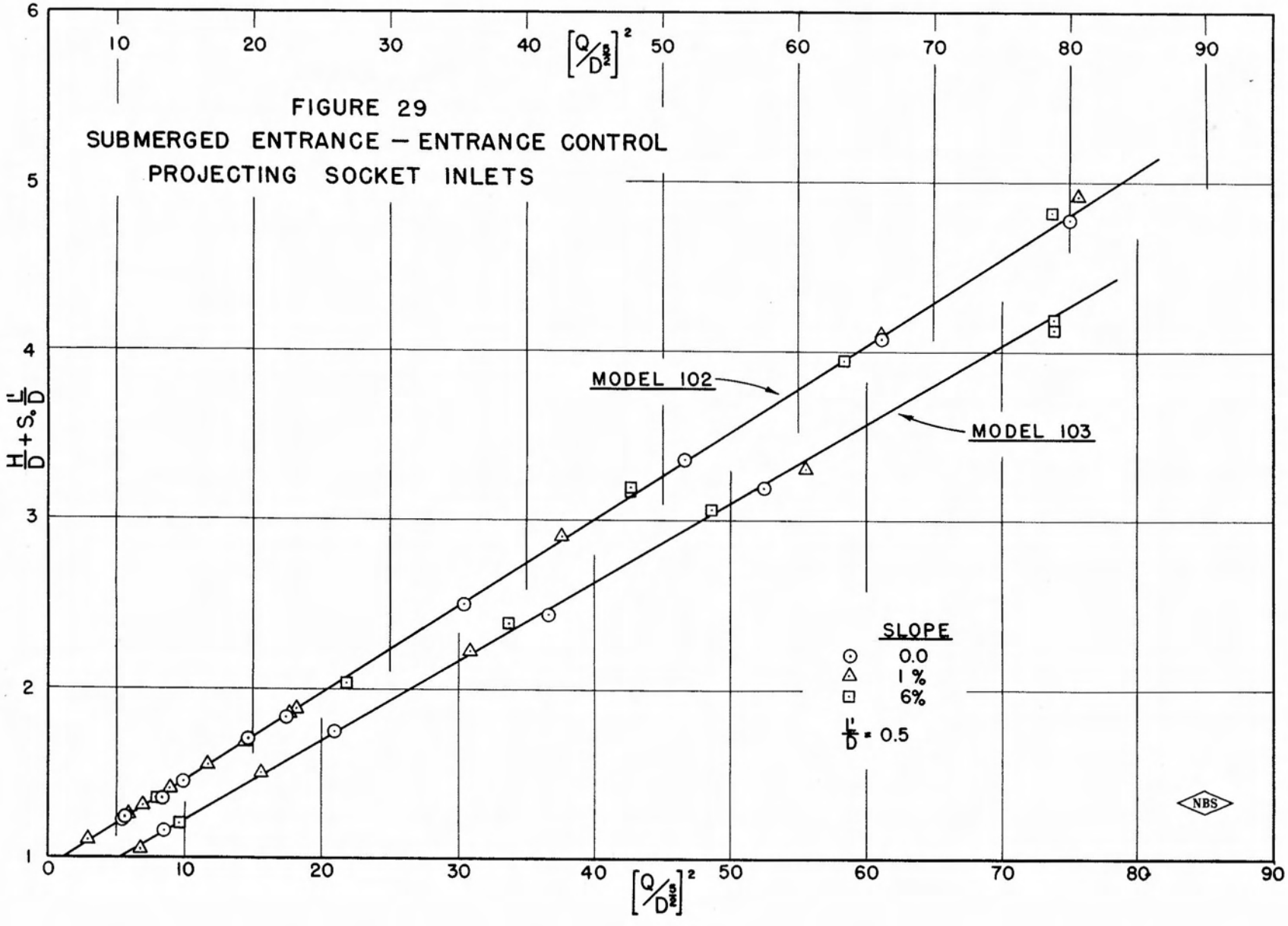
FIGURE 29
SUBMERGED ENTRANCE — ENTRANCE CONTROL
PROJECTING SOCKET INLETS
$\left[\frac{Q}{D^{2.5}}\right]^2$
$\frac{H}{D}+S_o\frac{L}{D}$
MODEL 102
MODEL 103
SLOPE
0.0
1 %
6%
$\frac{L}{D}$ = 0.5
NBS

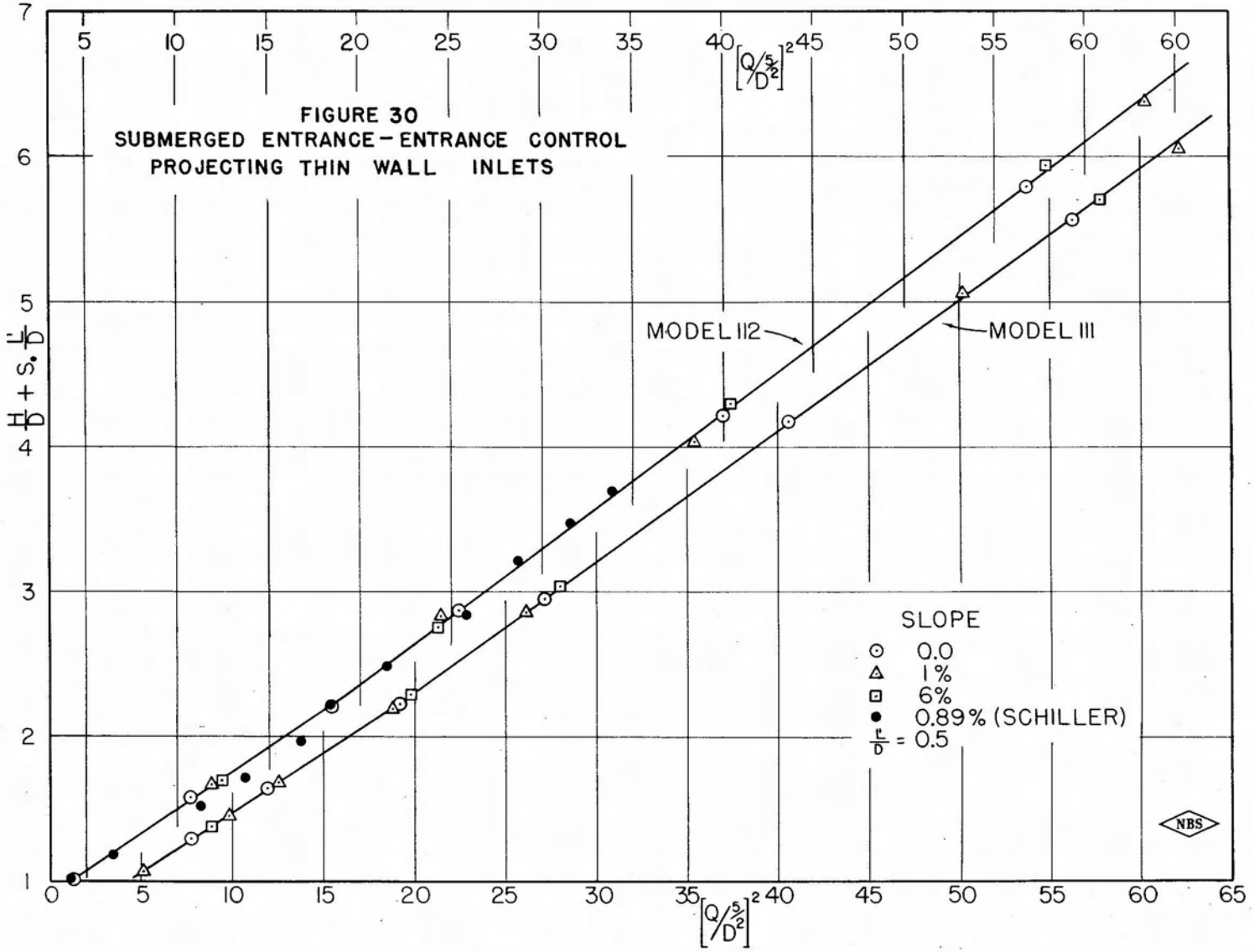
FIGURE 30
SUBMERGED ENTRANCE – ENTRANCE CONTROL
PROJECTING THIN WALL INLETS
MODEL 112
MODEL 111
SLOPE
0.0
1%
6%
0.89% (SCHILLER)
r/D = 0.5
NBS
H/D + S·L/D
[Q/D^2.5]^2

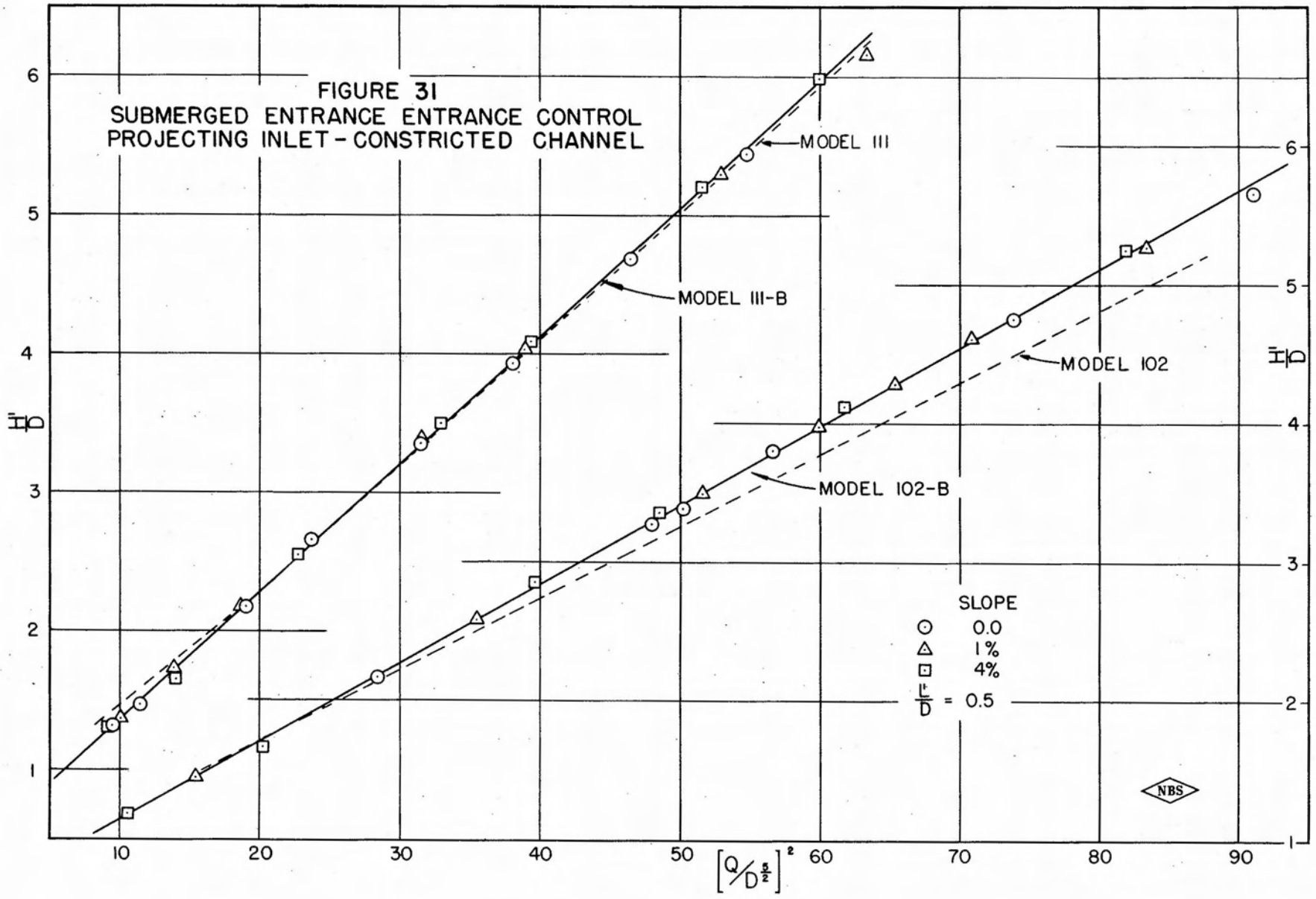
FIGURE 31
SUBMERGED ENTRANCE ENTRANCE CONTROL
PROJECTING INLET - CONSTRICTED CHANNEL
MODEL 111
MODEL 111-B
MODEL 102
MODEL 102-B
SLOPE
0.0
1%
4%
L/D = 0.5
H/D
[Q/D^5/2]^2
NBS

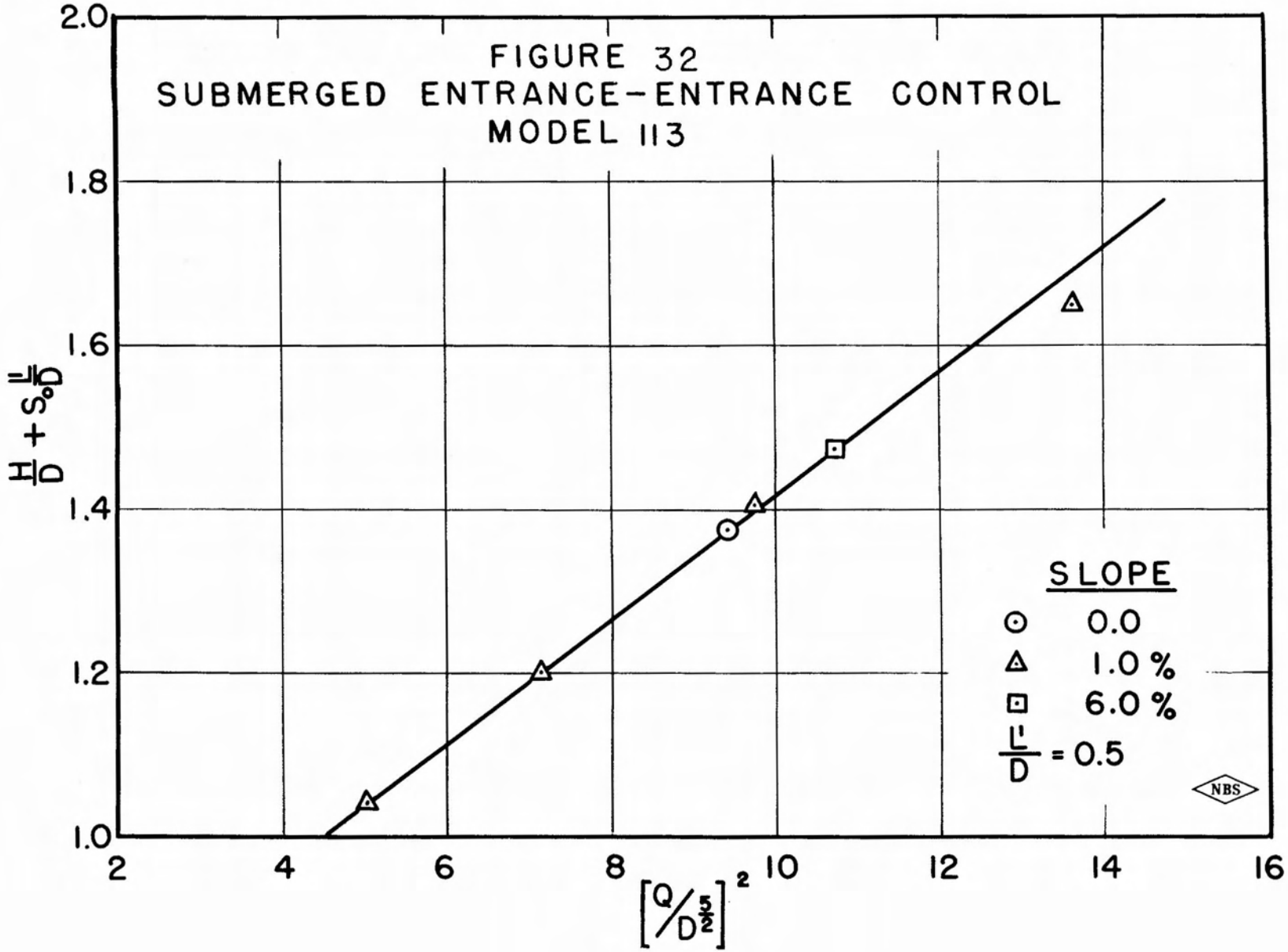
FIGURE 32
SUBMERGED ENTRANCE-ENTRANCE CONTROL
MODEL 113
2.0
1.8
1.6
1.4
1.2
1.0
H/D + S₀L/D
2
4
6
8
10
12
14
16
[Q/D^5/2]^2
SLOPE
0.0
1.0 %
6.0 %
L'/D = 0.5
NBS

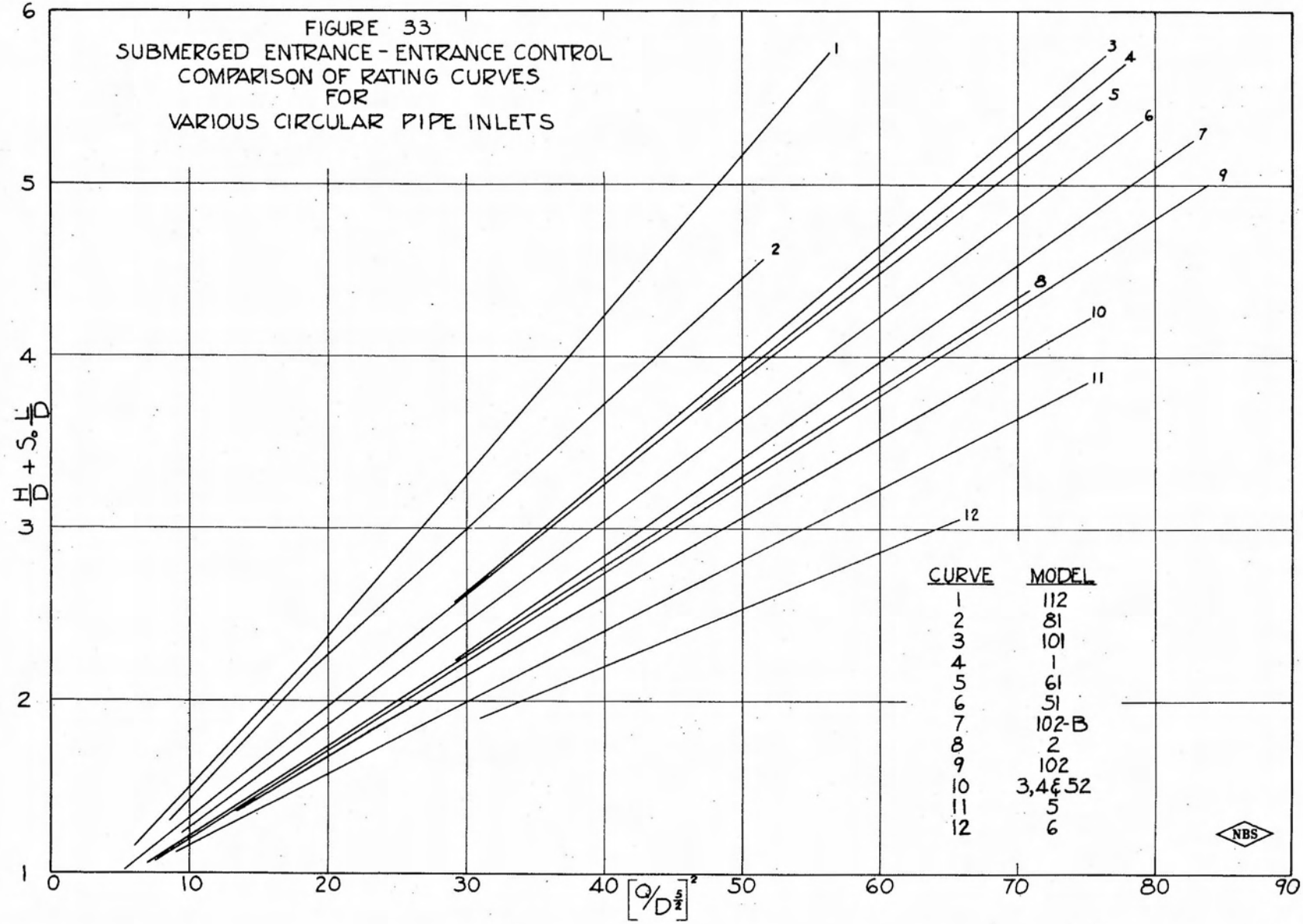
FIGURE 33
SUBMERGED ENTRANCE - ENTRANCE CONTROL
COMPARISON OF RATING CURVES
FOR
VARIOUS CIRCULAR PIPE INLETS
$\frac{H}{D} + S_o \frac{L}{D}$
$\left[\frac{Q}{D^{\frac{5}{2}}}\right]^2$
0
10
20
30
40
50
60
70
80
90
1
2
3
4
5
6
CURVE MODEL
1 112
2 81
3 101
4 1
5 61
6 51
7 102-B
8 2
9 102
10 3,4&52
11 5
12 6
NBS

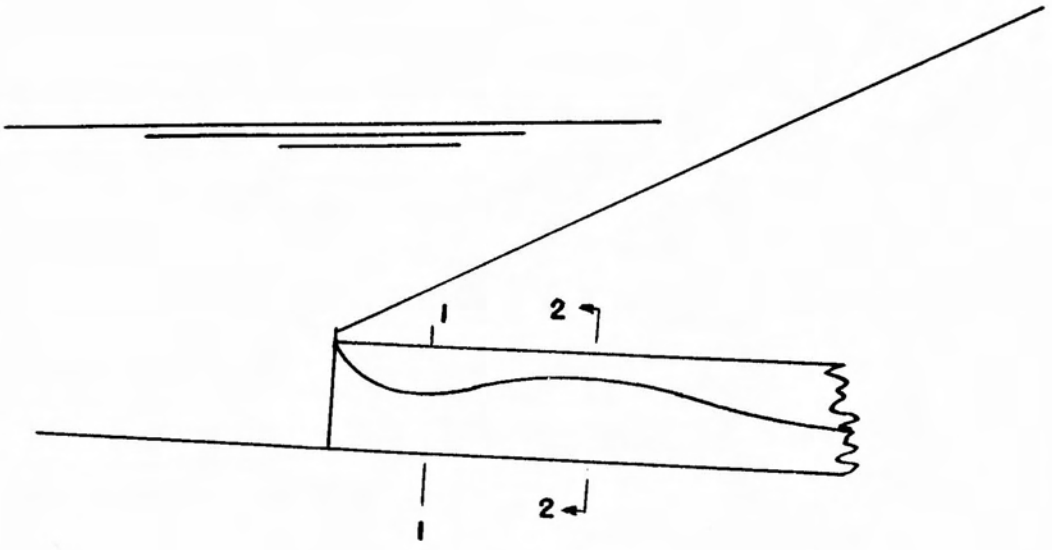

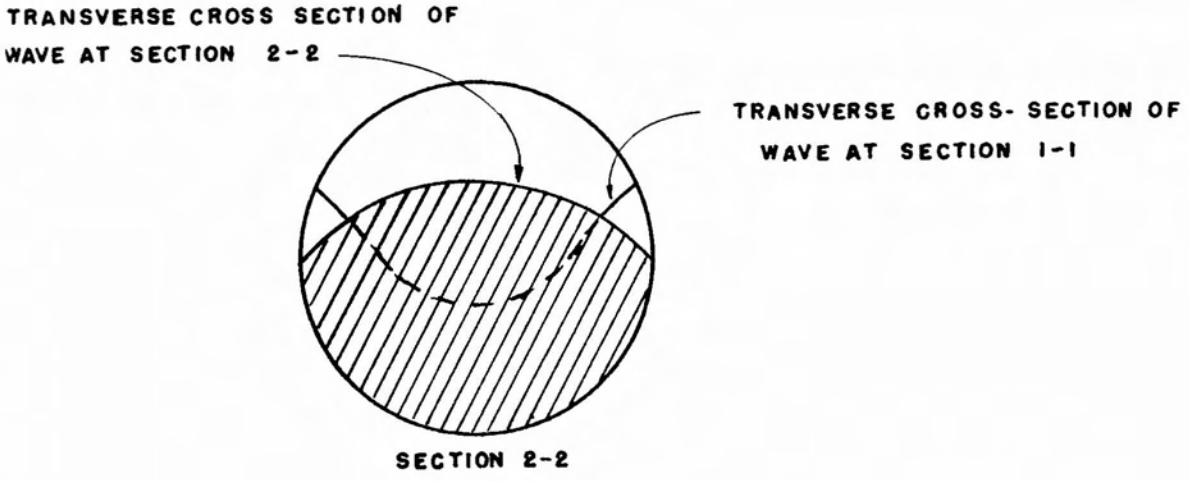

NBS

FIGURE 34

SURFACE WAVES TYPICAL OF SLUICE TYPE FLOW

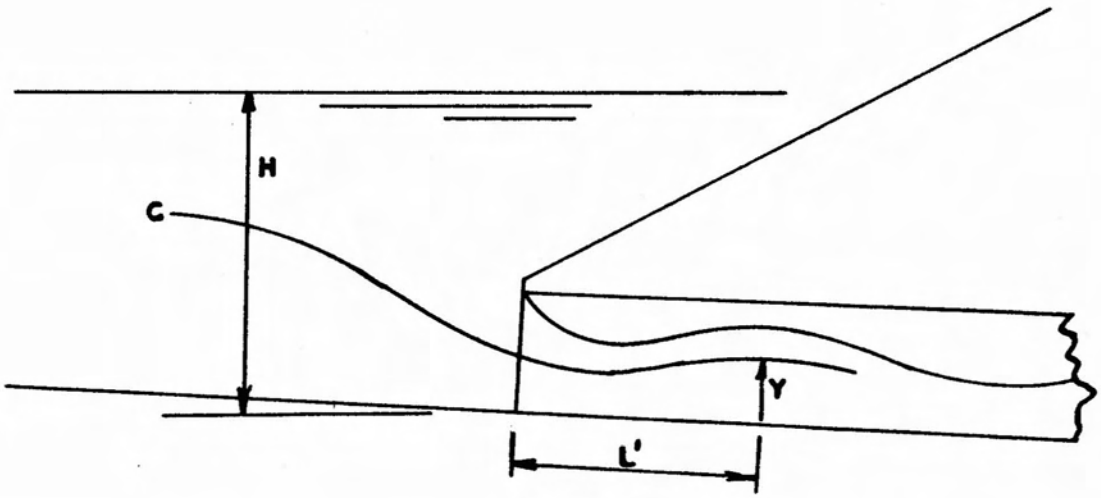

FIGURE 35 SLUICE TYPE FLOW

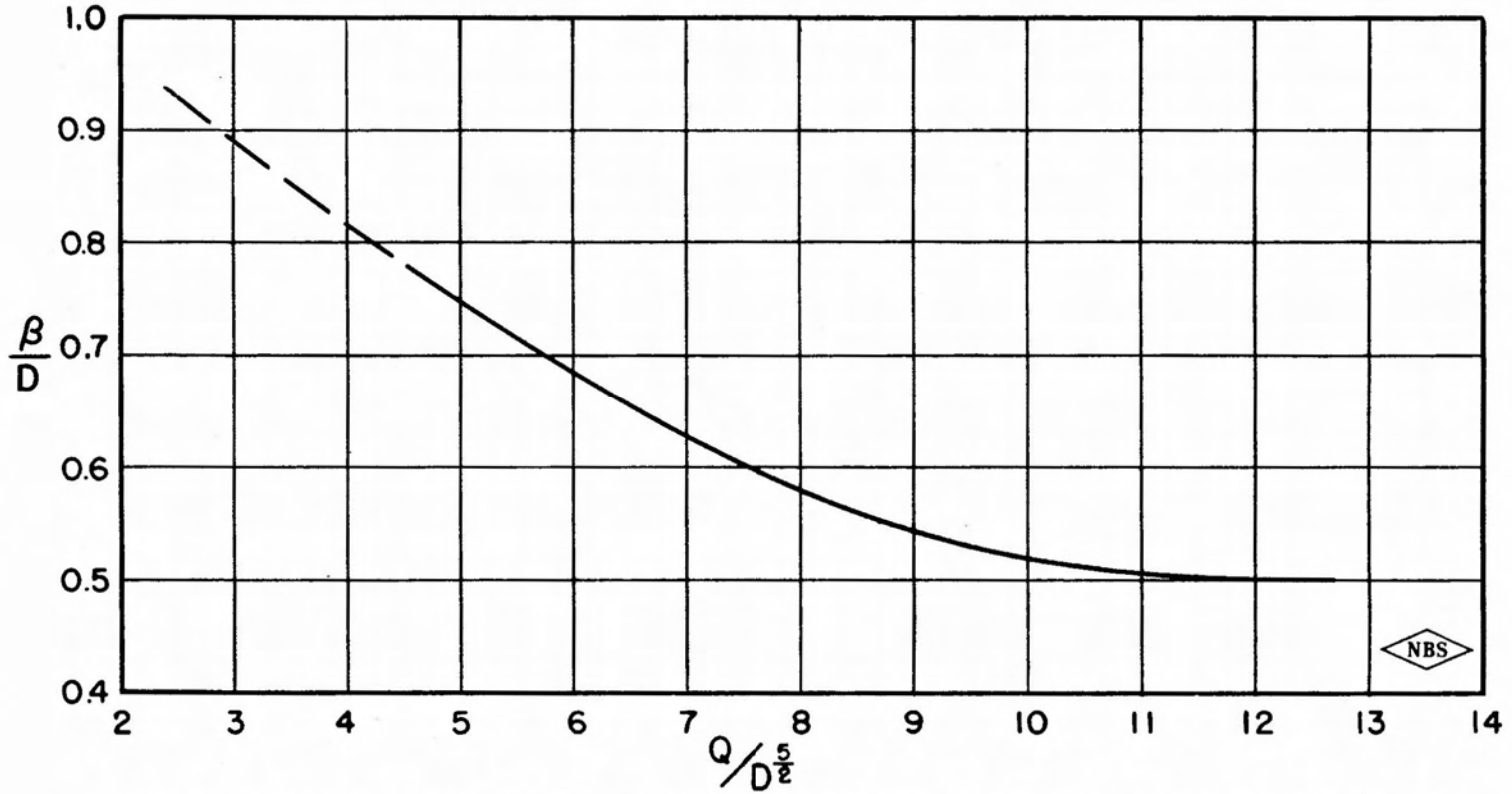

FIGURE 36. LI'S DATA ON EFFECTIVE POSITION OF PRESSURE LINE AT OUTLET OF CIRCULAR PIPE – SUPPORTED JET

FIGURE 37
FULL CONDUIT FLOW – SQUARE, ROUNDED AND SHARP EDGE INLETS

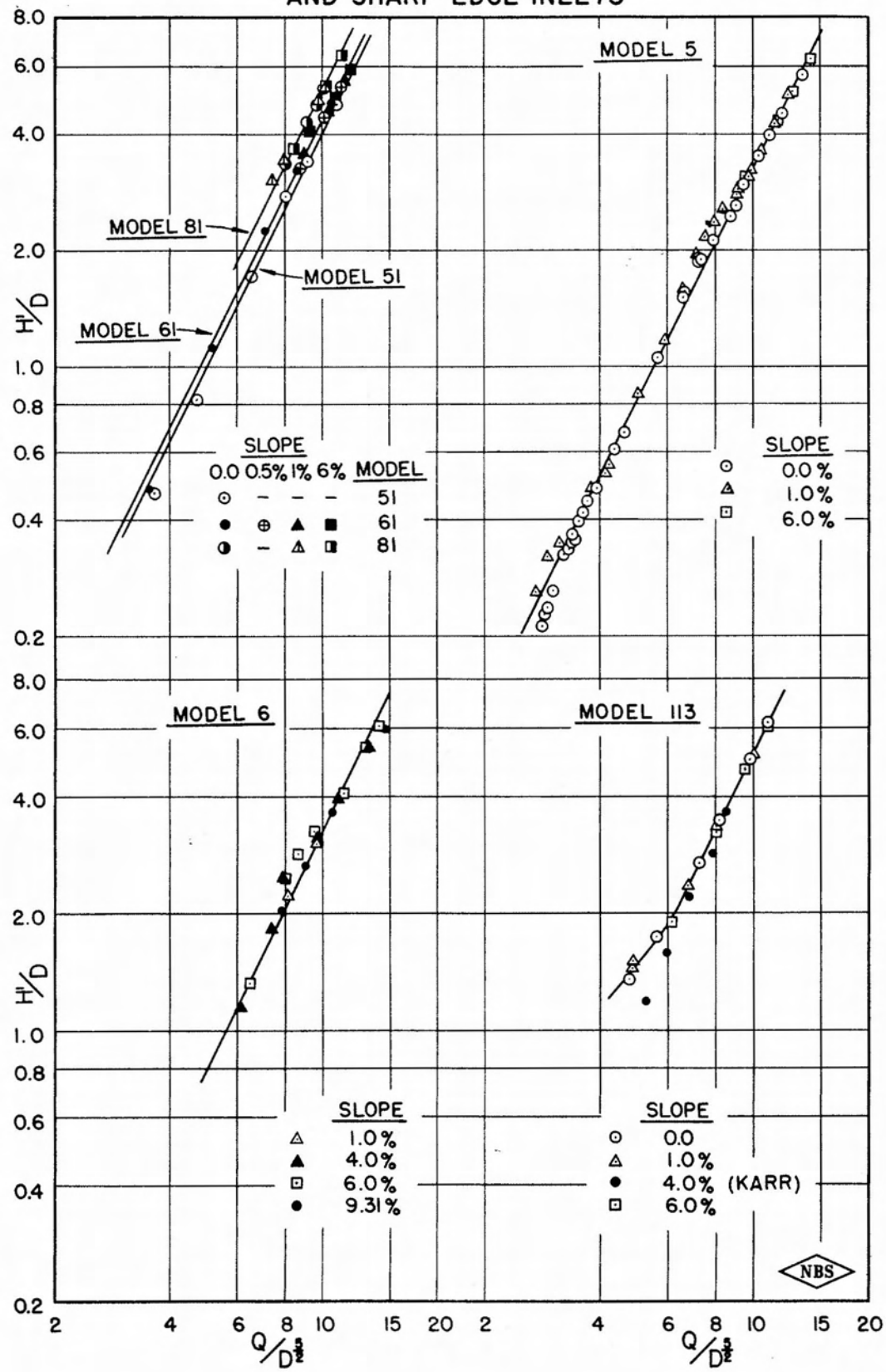

FIGURE 38
FULL CONDUIT FLOW – SOCKET INLETS

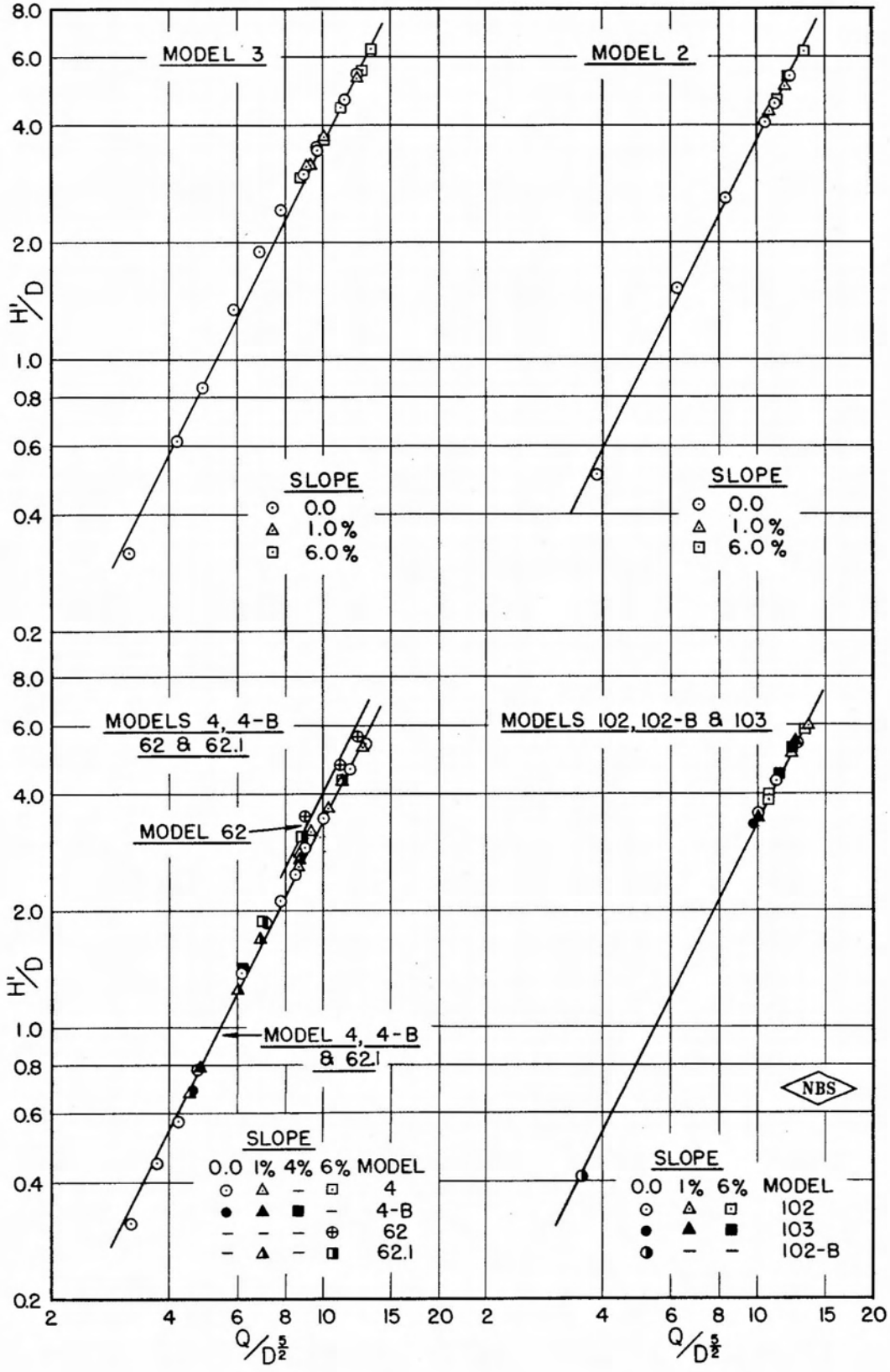

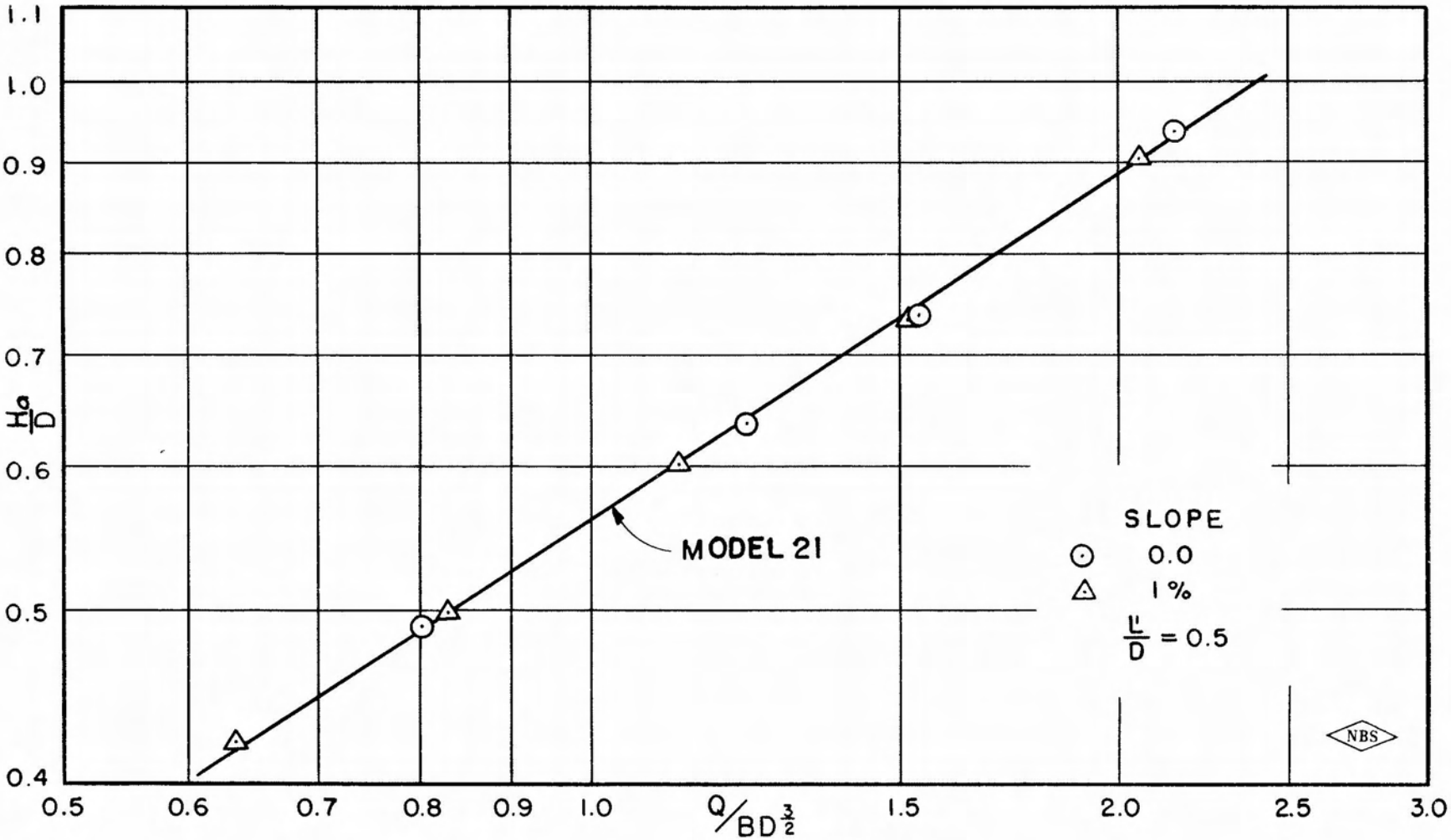

FIGURE 39

NON-SUBMERGED ENTRANCE - ENTRANCE CONTROL
HEAD WALLS & CONES
PIPE ARCH SECTION - SQUARE EDGE

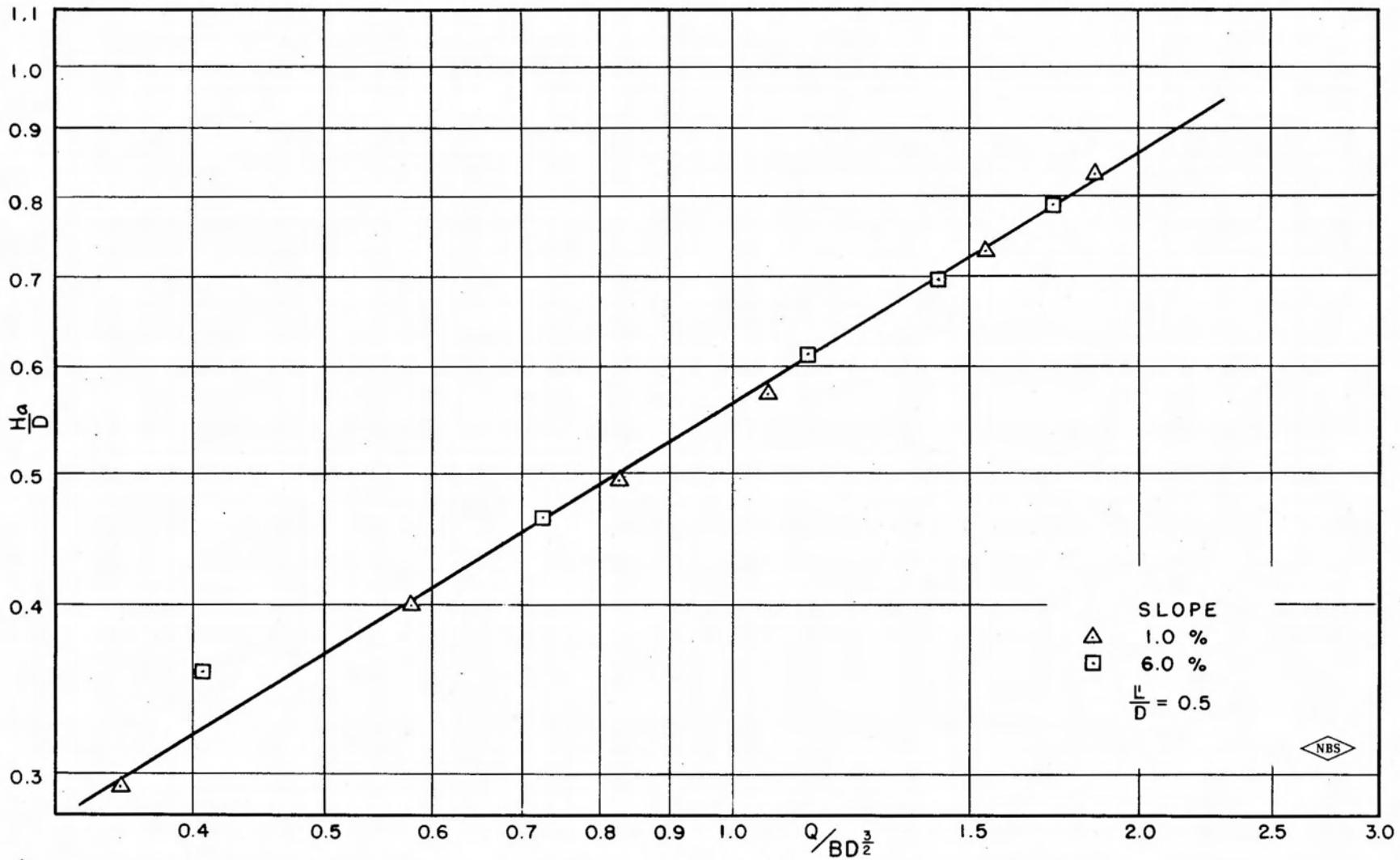

FIGURE 40
NON-SUBMERGED ENTRANCE-ENTRANCE CONTROL
PIPE ARCH MODEL 22

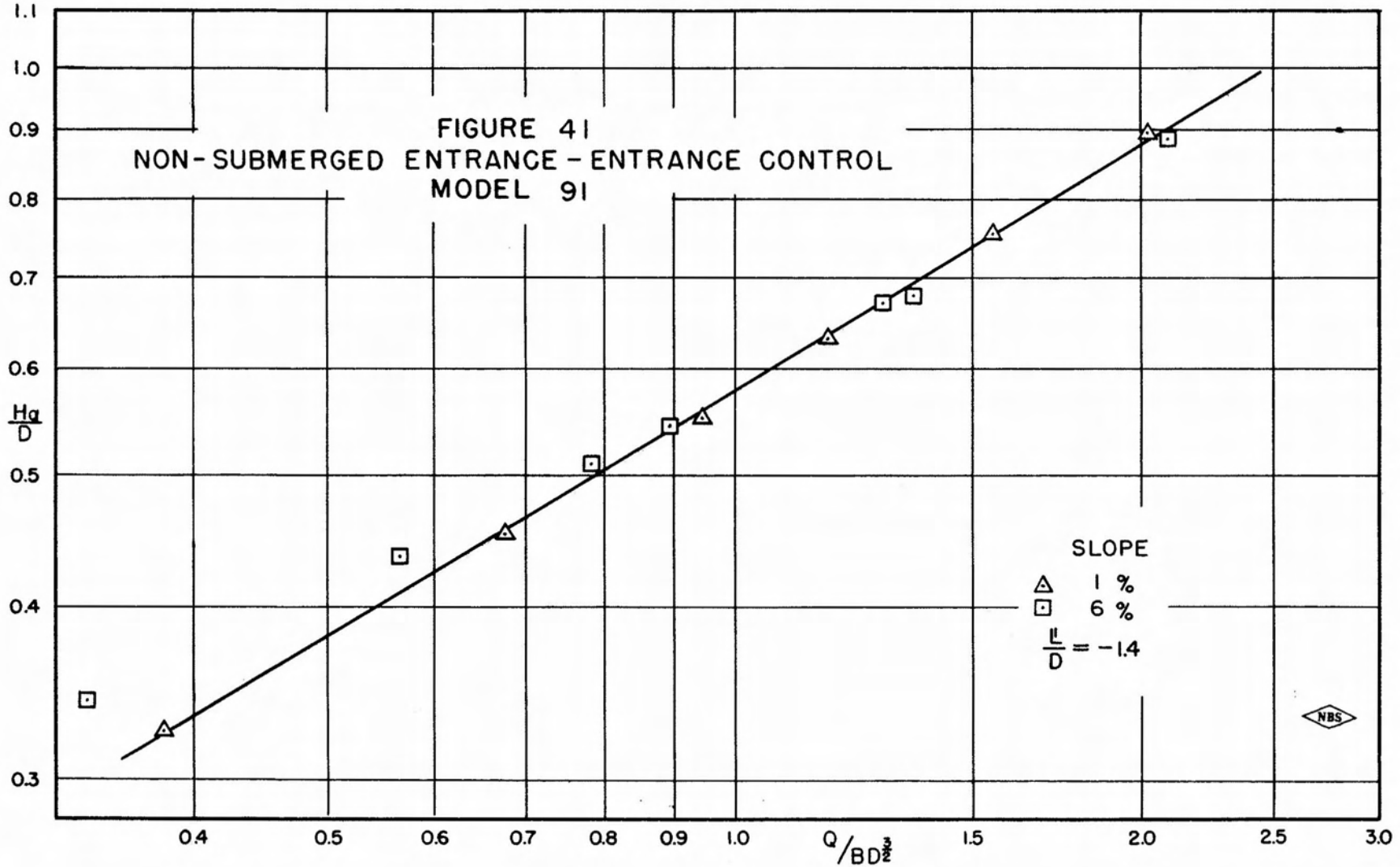
FIGURE 41
NON-SUBMERGED ENTRANCE - ENTRANCE CONTROL
MODEL 91
1.1
1.0
0.9
0.8
0.7
0.6
Hq/D
0.5
0.4
0.3
0.4
0.5
0.6
0.7
0.8
0.9
1.0
Q/BD^3/2
1.5
2.0
2.5
3.0
SLOPE
1 %
6 %
ll/D = -1.4
NBS

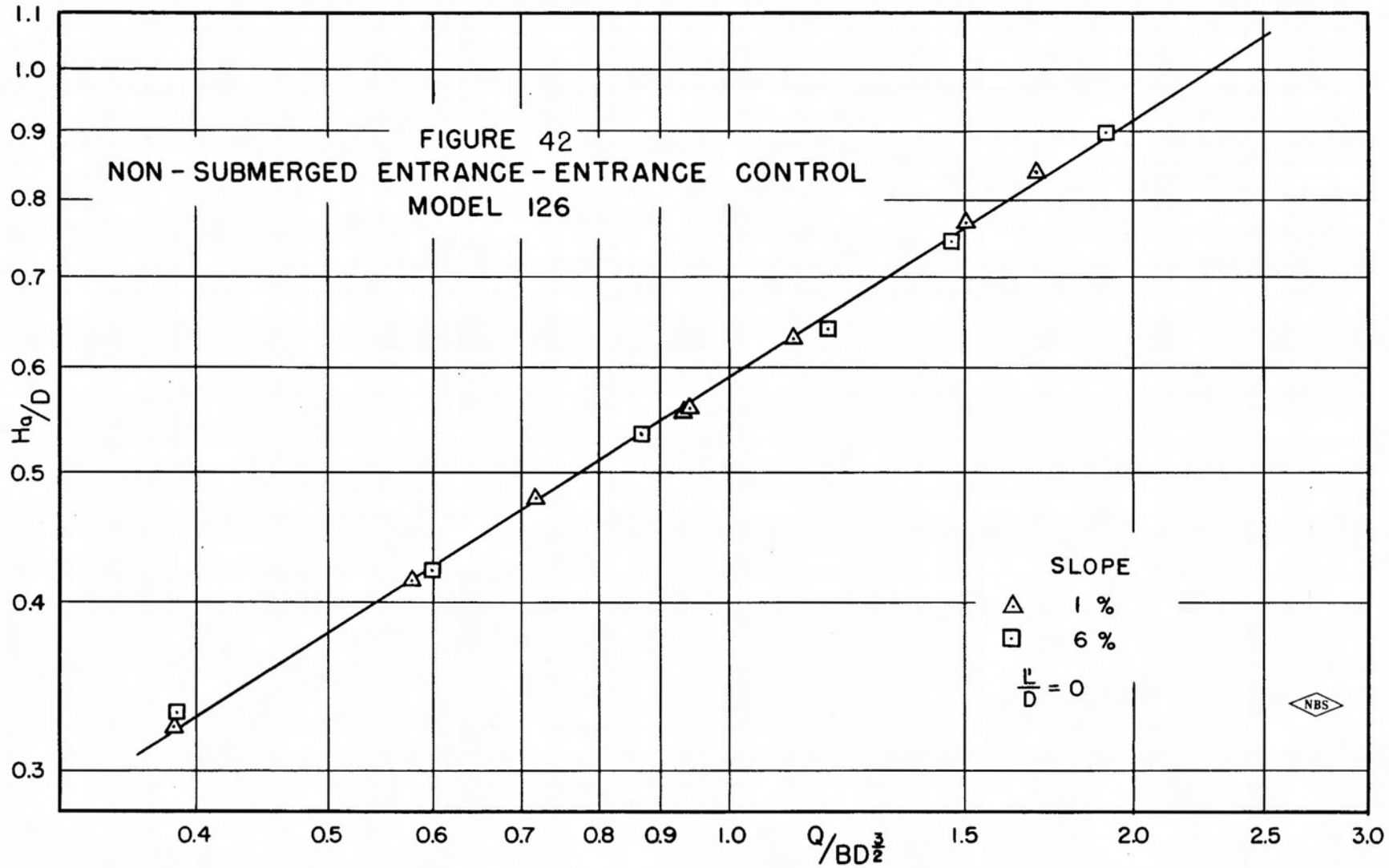
FIGURE 42
NON - SUBMERGED ENTRANCE - ENTRANCE CONTROL
MODEL 126
SLOPE
1 %
6 %
l'/D = 0
NBS
Ha/D
Q/BD^3/2
1.1
1.0
0.9
0.8
0.7
0.6
0.5
0.4
0.3
0.4
0.5
0.6
0.7
0.8
0.9
1.0
1.5
2.0
2.5
3.0

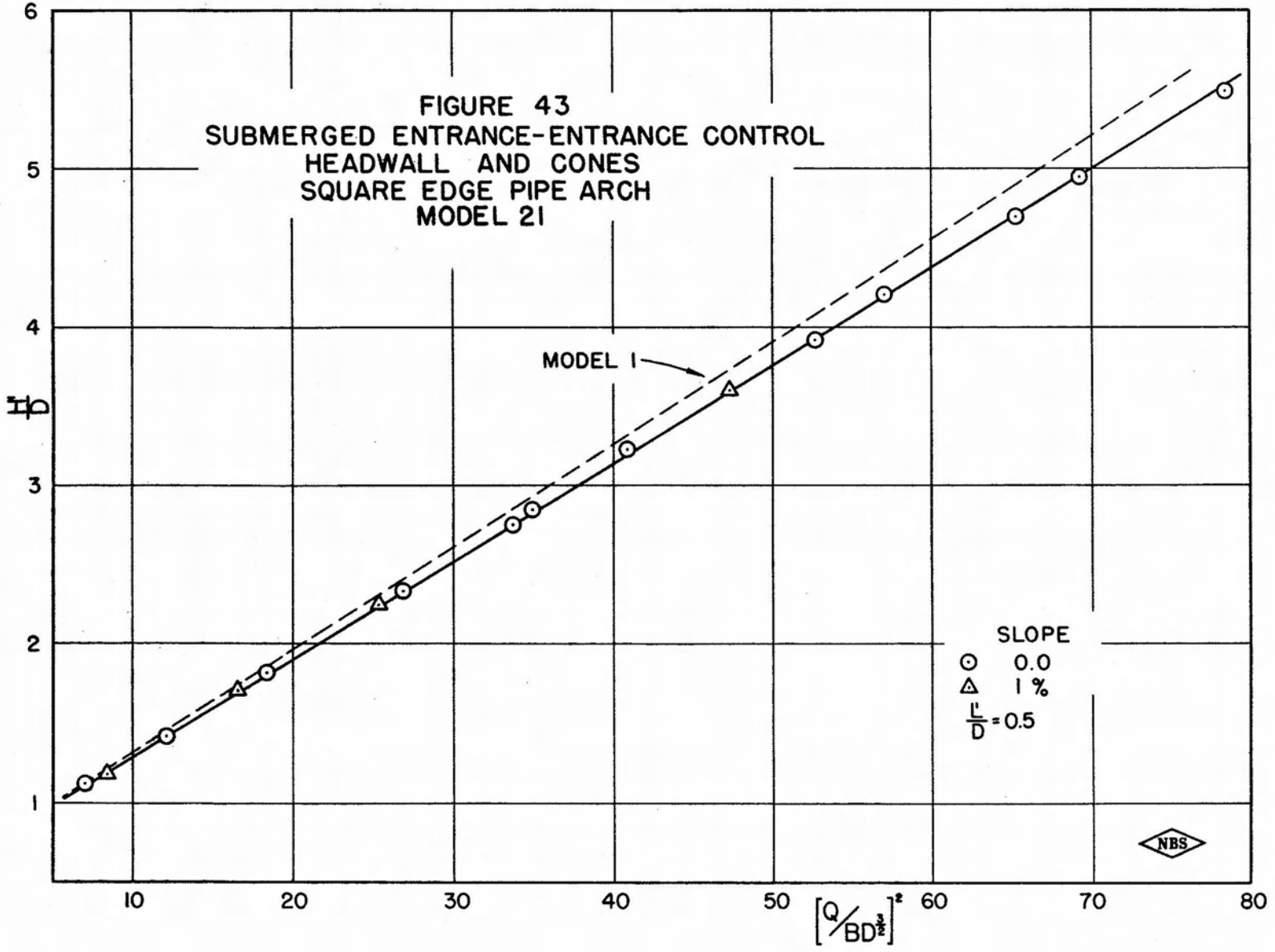
FIGURE 43
SUBMERGED ENTRANCE-ENTRANCE CONTROL
HEADWALL AND CONES
SQUARE EDGE PIPE ARCH
MODEL 21
MODEL 1
SLOPE
0.0
1 %
L'/D = 0.5
NBS
H/D
[Q/BD^3/2]^2
1
2
3
4
5
6
10
20
30
40
50
60
70
80

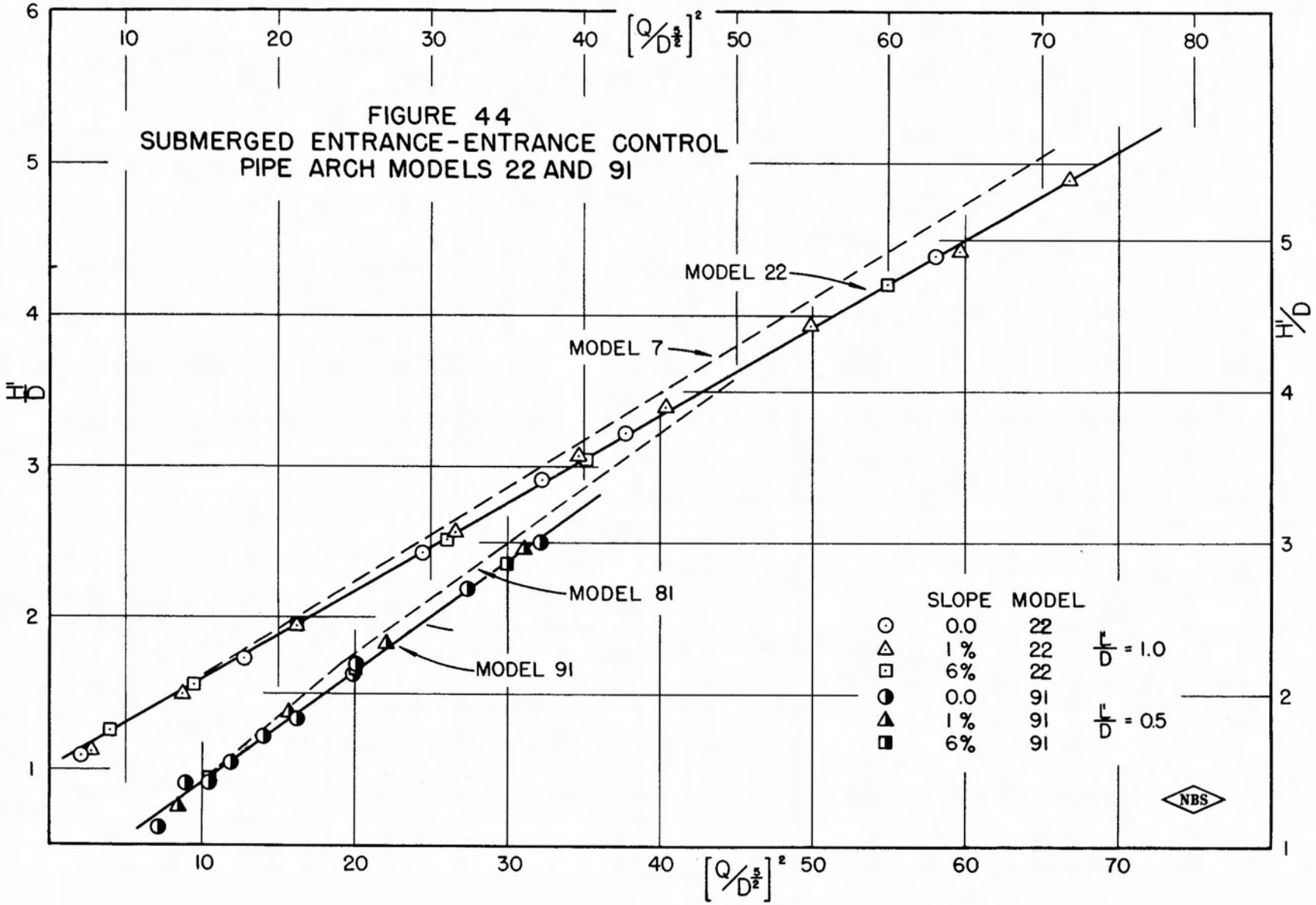
FIGURE 44
SUBMERGED ENTRANCE-ENTRANCE CONTROL
PIPE ARCH MODELS 22 AND 91
$\left[Q/D^{\frac{5}{2}}\right]^2$
H'/D
MODEL 22
MODEL 7
MODEL 81
MODEL 91
SLOPE MODEL
0.0 22
1 % 22
6% 22
0.0 91
1 % 91
6% 91
$\frac{r}{D}$ = 1.0
$\frac{r}{D}$ = 0.5
NBS

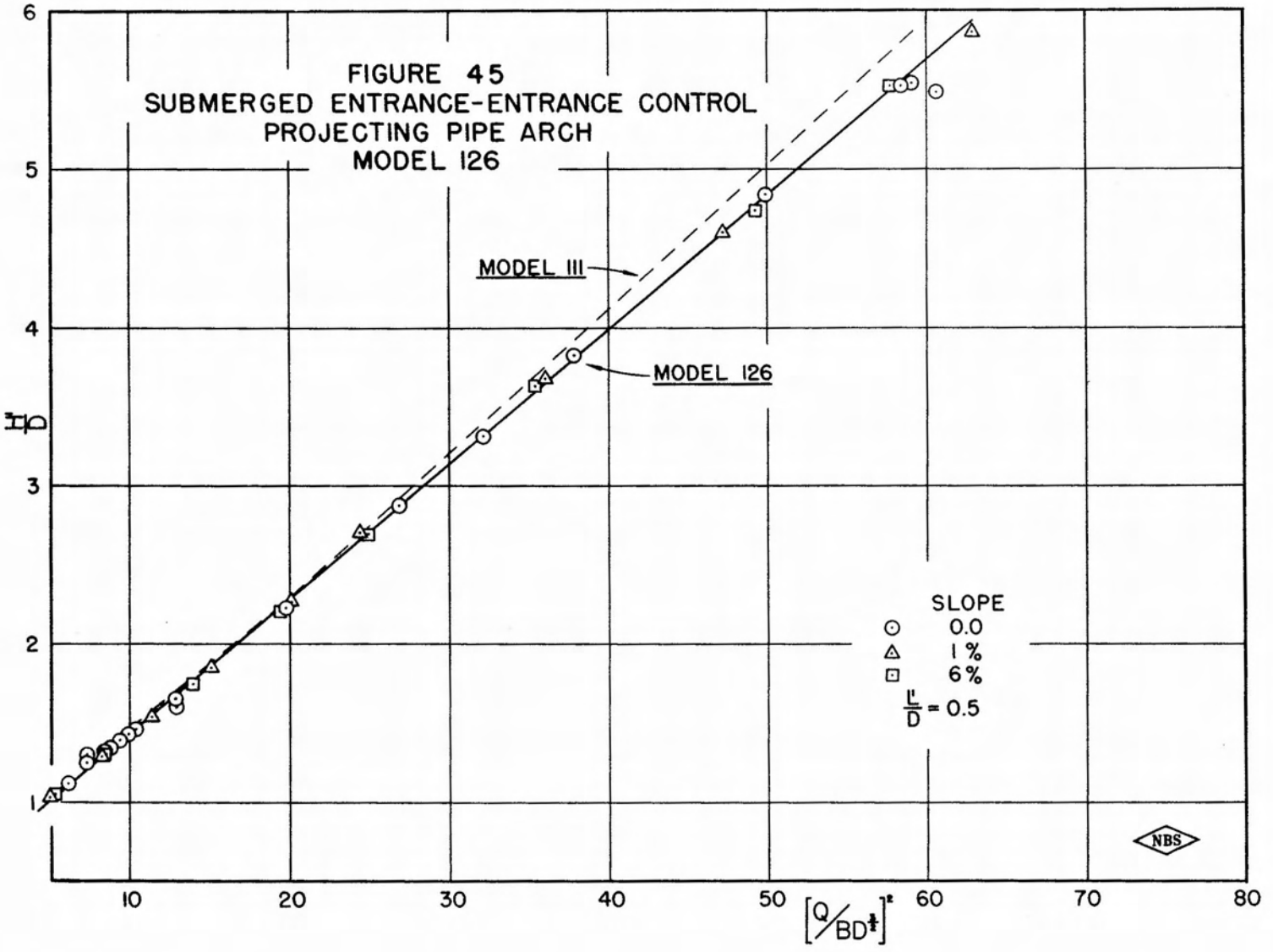
FIGURE 45
SUBMERGED ENTRANCE-ENTRANCE CONTROL
PROJECTING PIPE ARCH
MODEL 126
MODEL III
MODEL 126
SLOPE
0.0
1%
6%
l'/D = 0.5
NBS
HD
[Q/BD^½]²
1
2
3
4
5
6
10
20
30
40
50
60
70
80

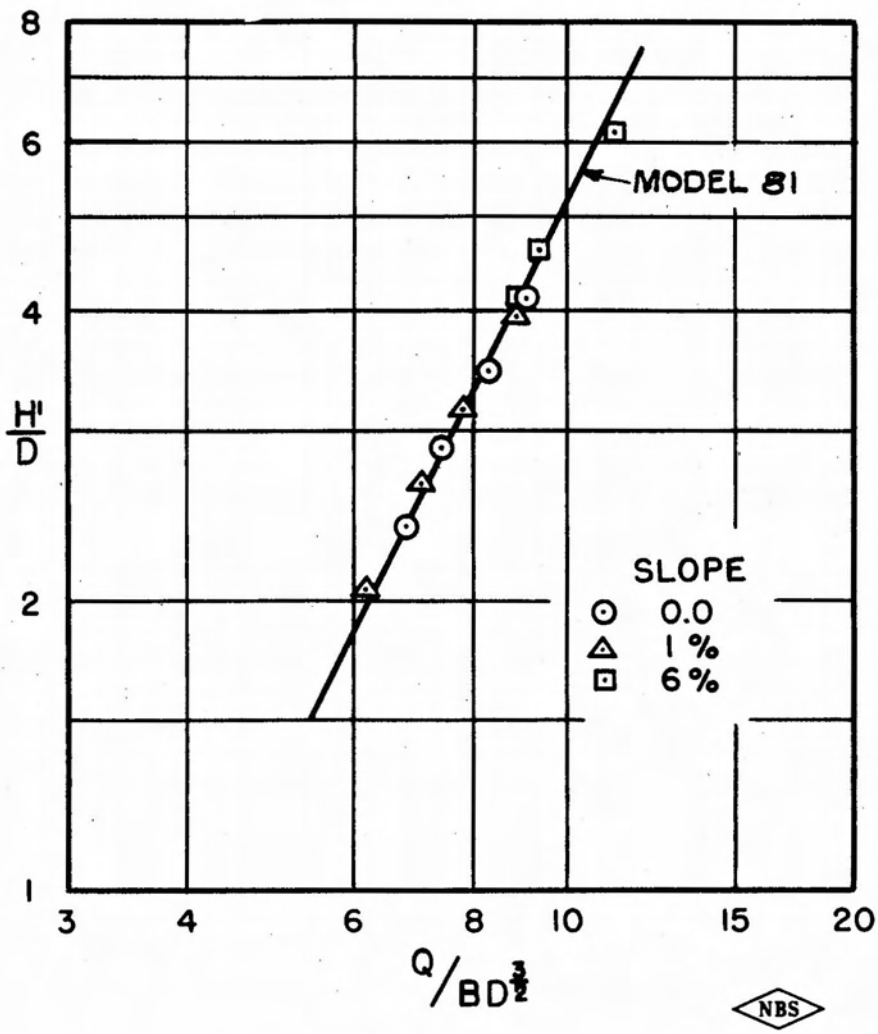

FIGURE 46
FULL CONDUIT FLOW
MODEL 91

FIGURE 47
REGIME OF FLOW IN MODEL CULVERTS

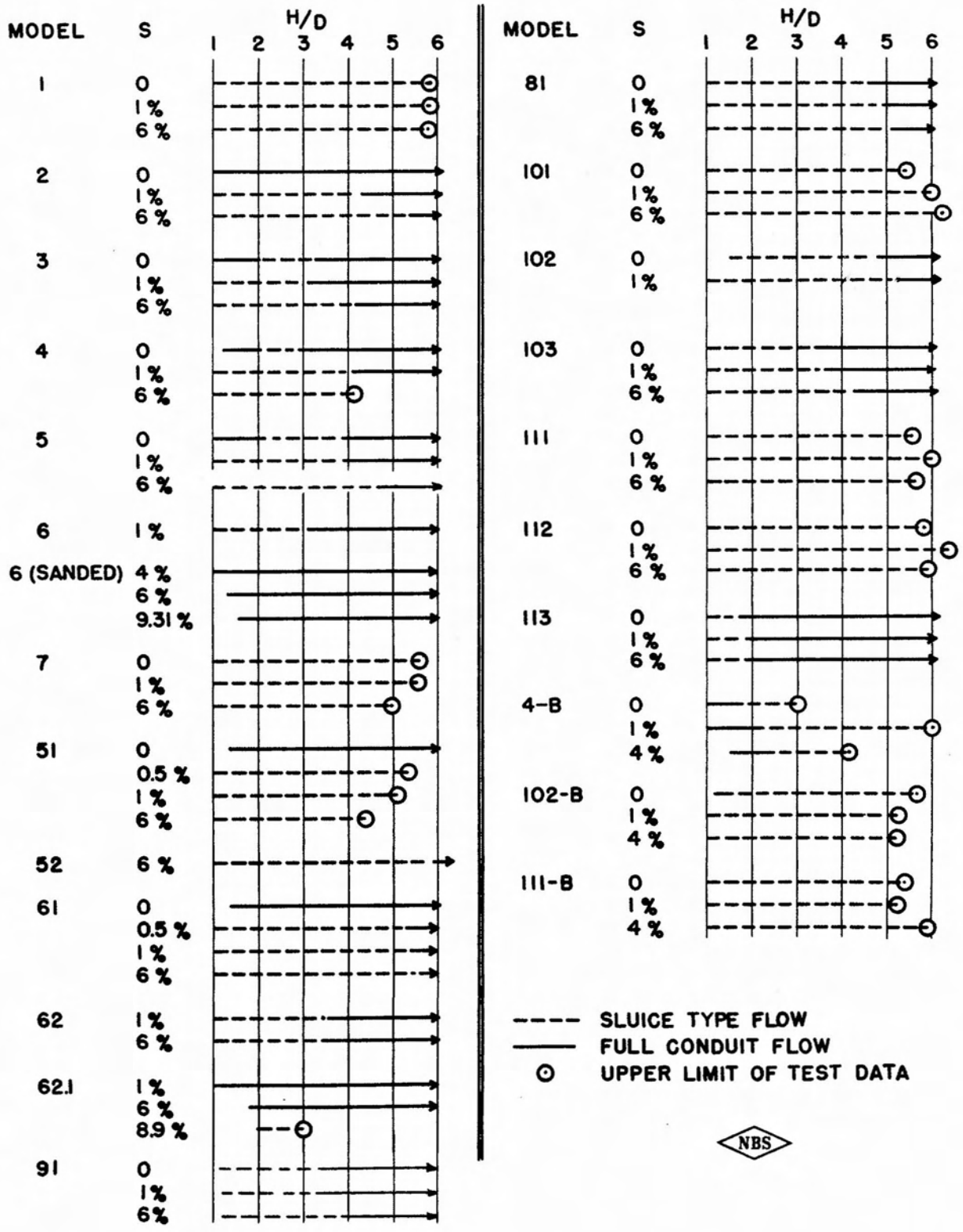

FIGURE 48
AIR PRESSURE IN MODEL CULVERT

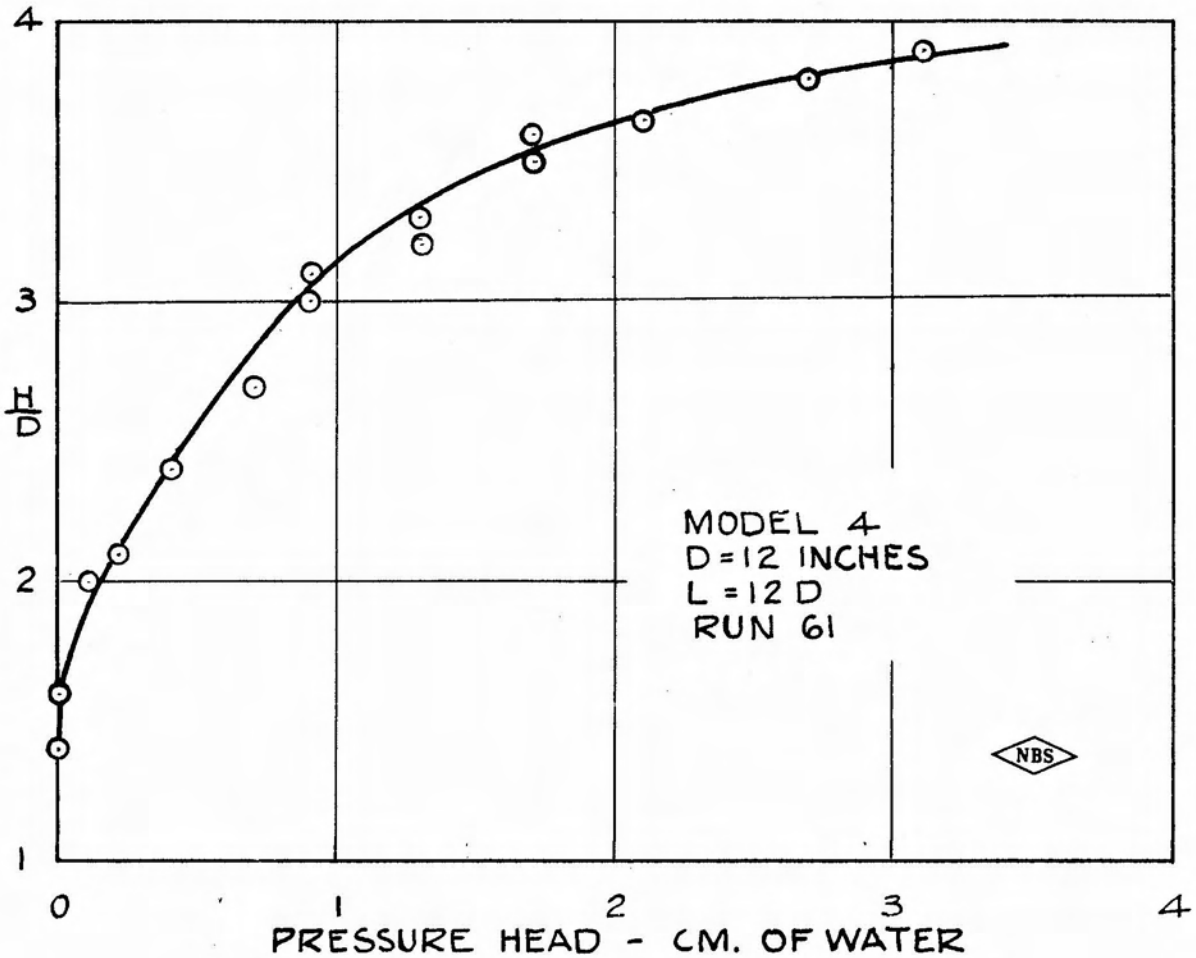

APPENDIX A

The experimental data for the various model inlets tested have been plotted in figures 49 to 70 to an arithmetic scale for values of H/D below 2.0.

List of Figures

Head-Discharge Curves for Entrance Control Flow, Headwater less than 2.0D

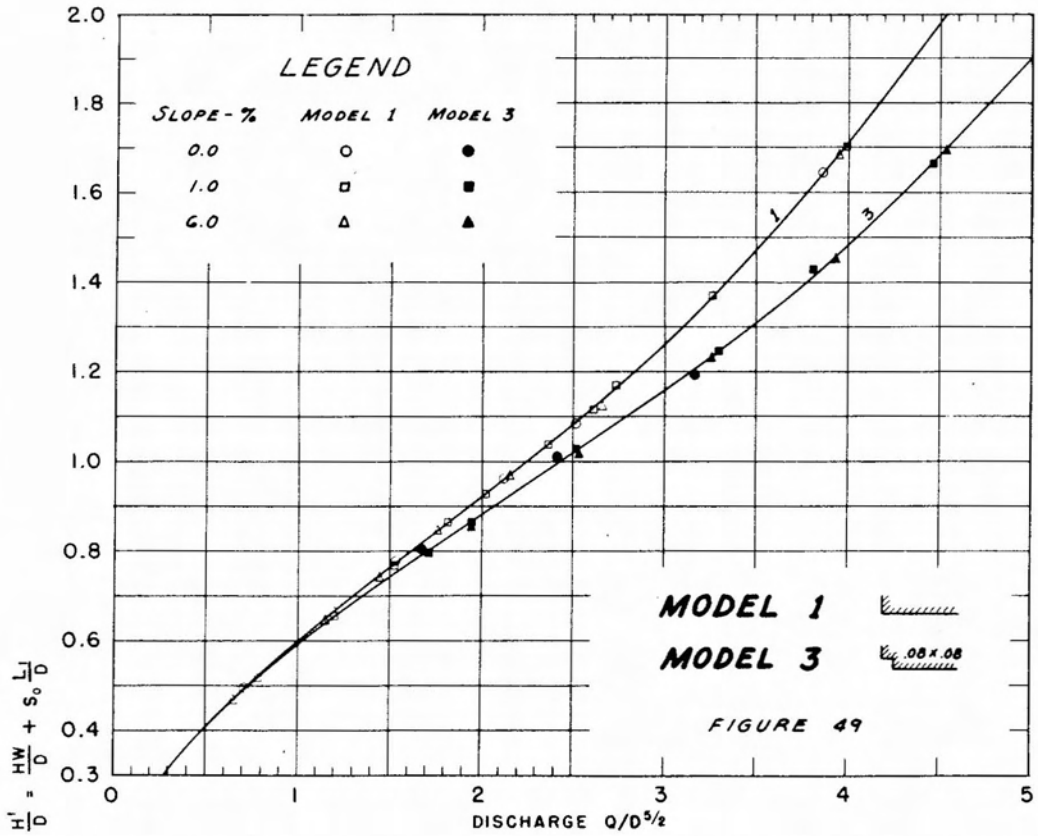

FIGURE 49

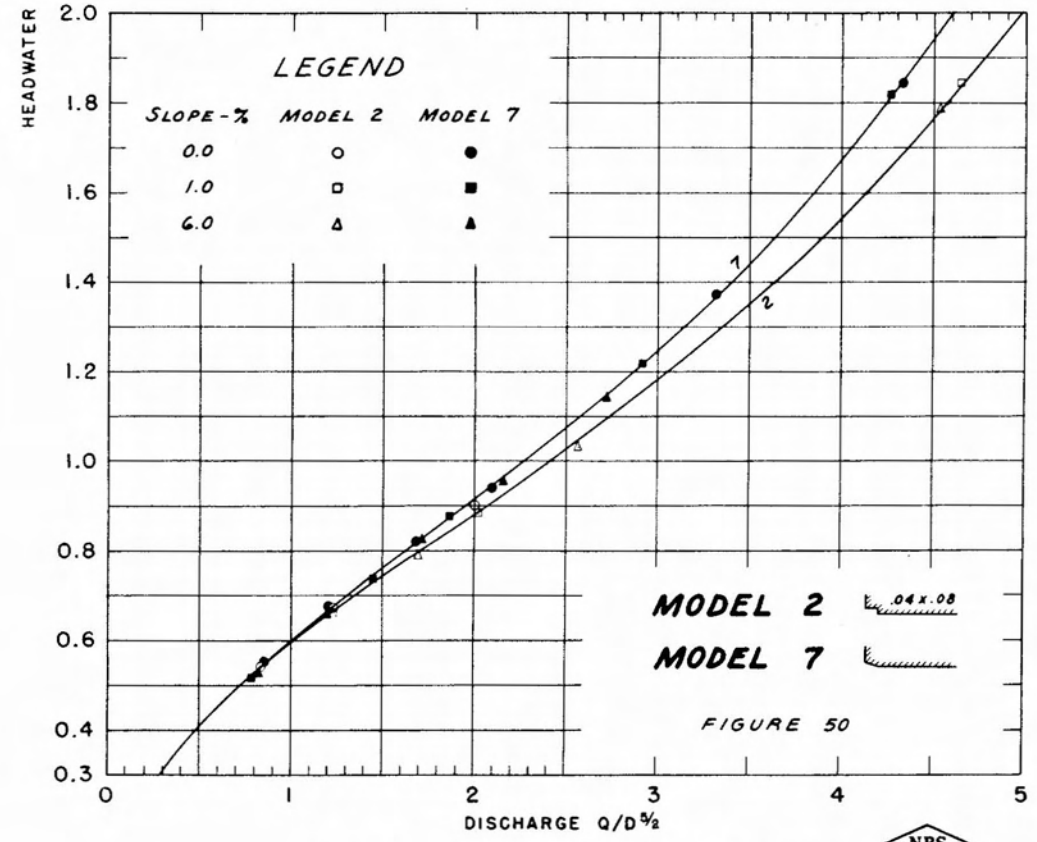

FIGURE 50

NBS

TYPE I CULVERTS $H'/D < 2$

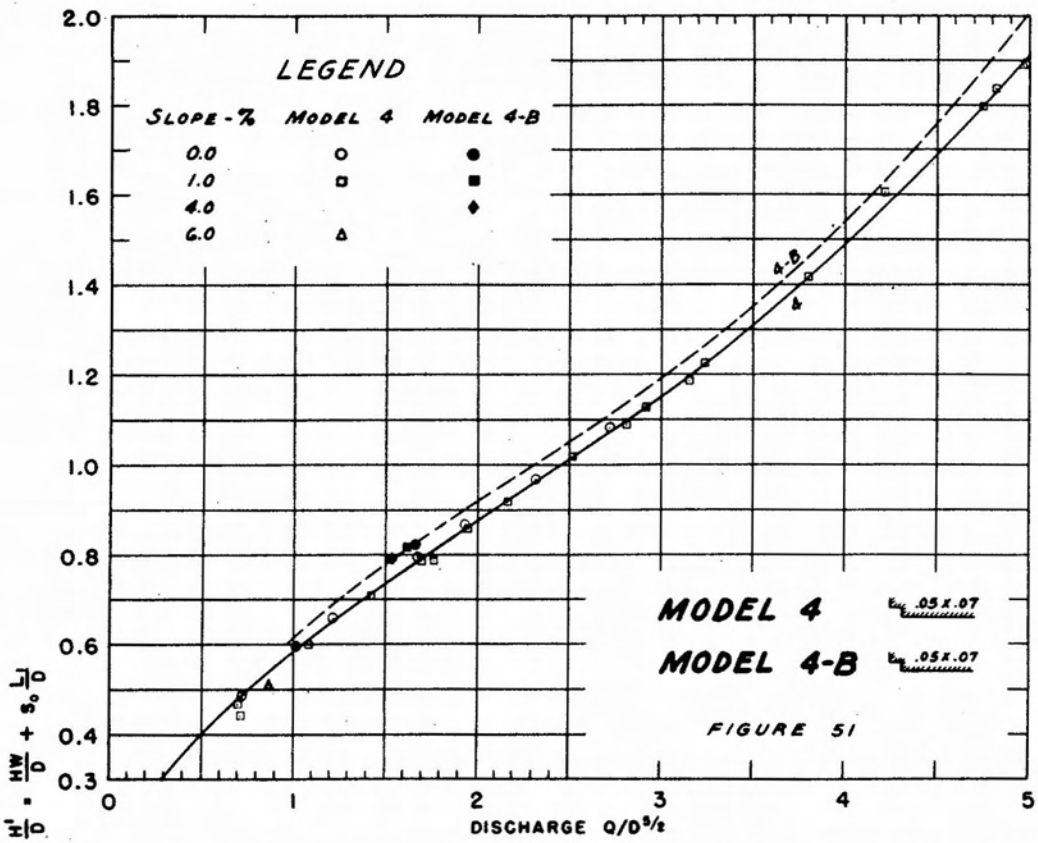

FIGURE 51

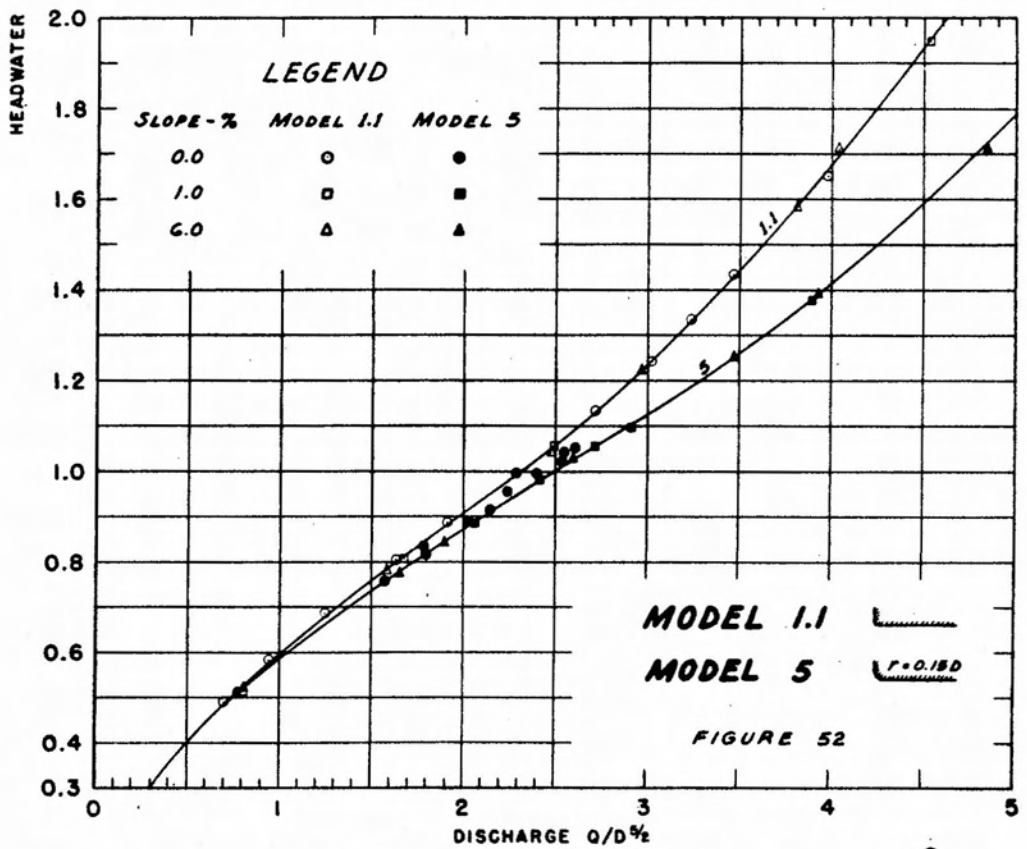

FIGURE 52

TYPE I CULVERTS $H'/D < 2$

NBS

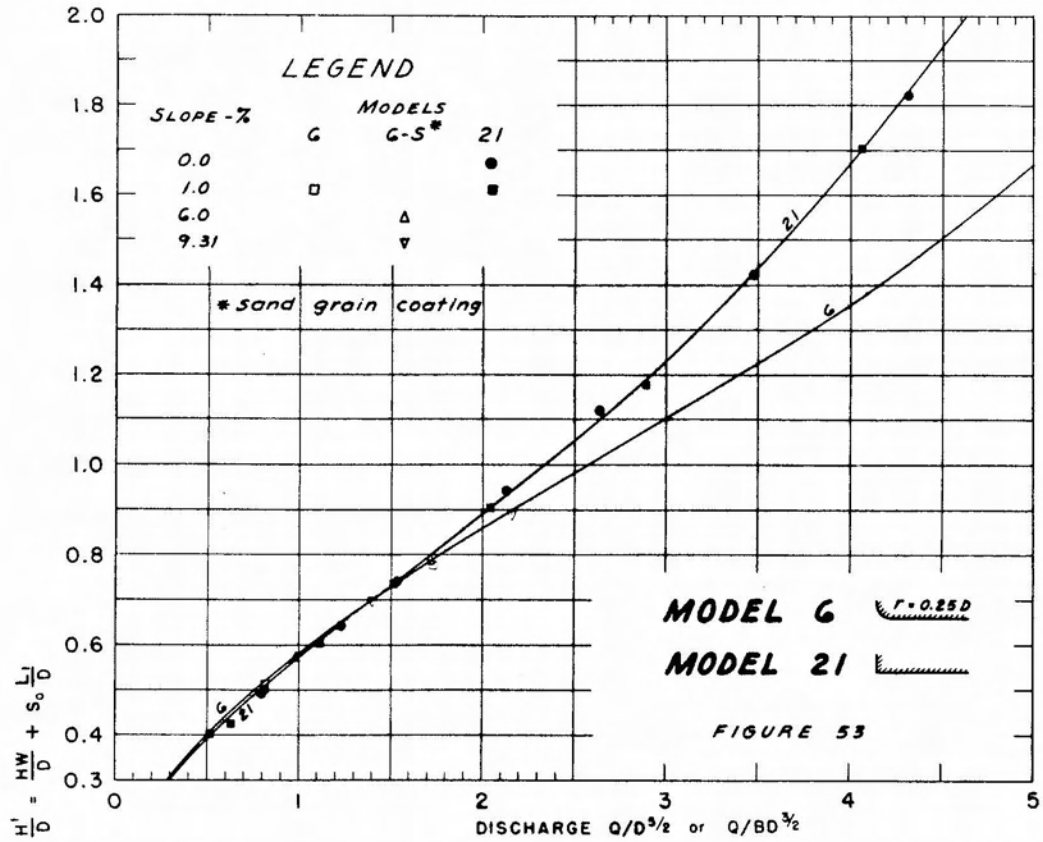

FIGURE 53

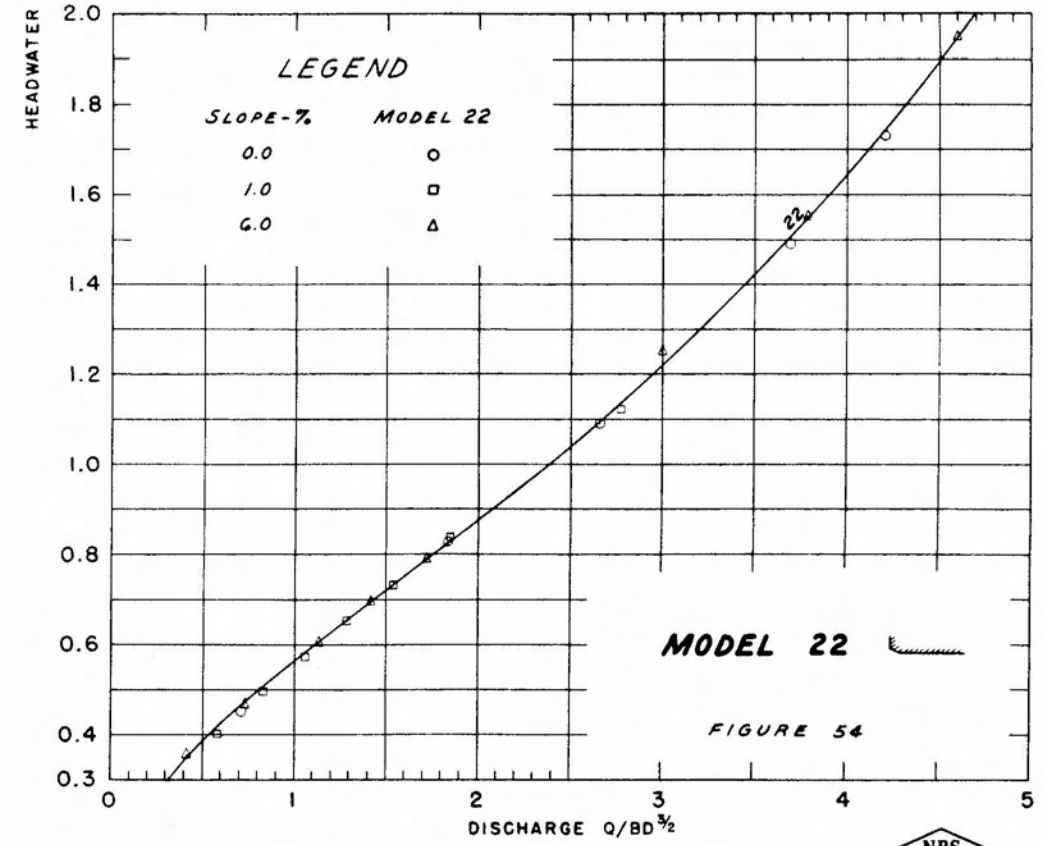

FIGURE 54

NBS

TYPE I CULVERTS $H'/D < 2$

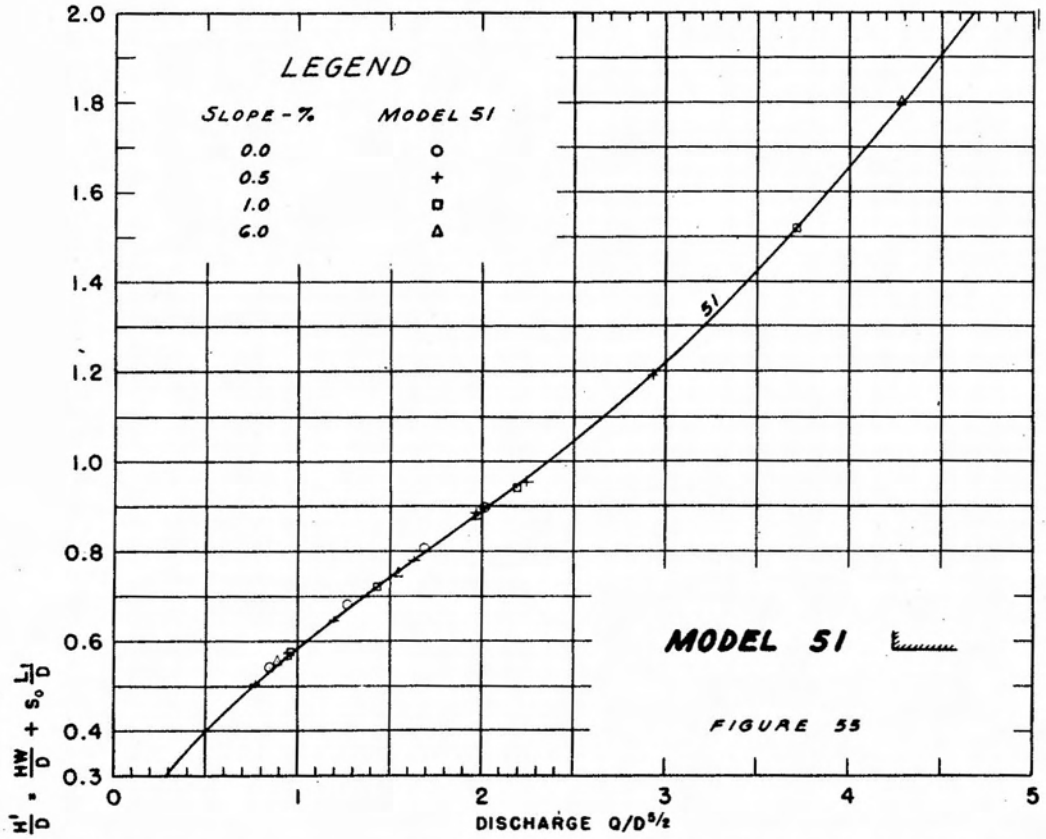

FIGURE 55

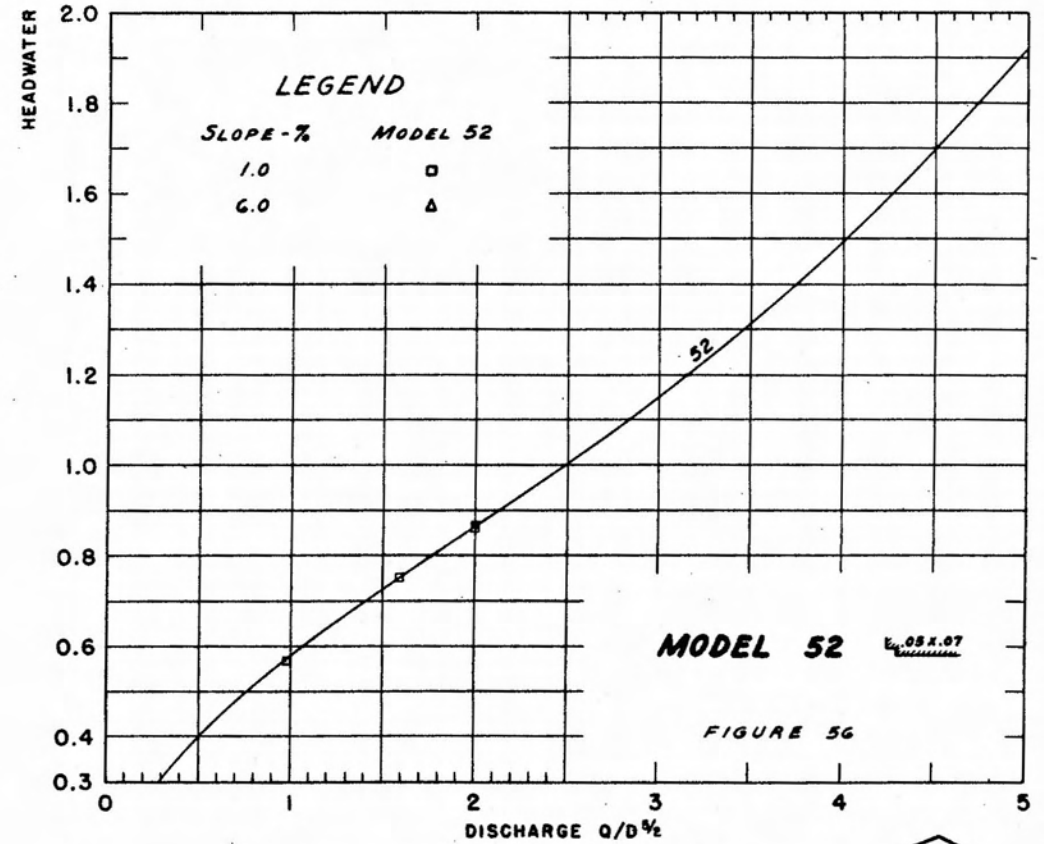

FIGURE 56

NBS

TYPE 2 CULVERTS $H'/D < 2$

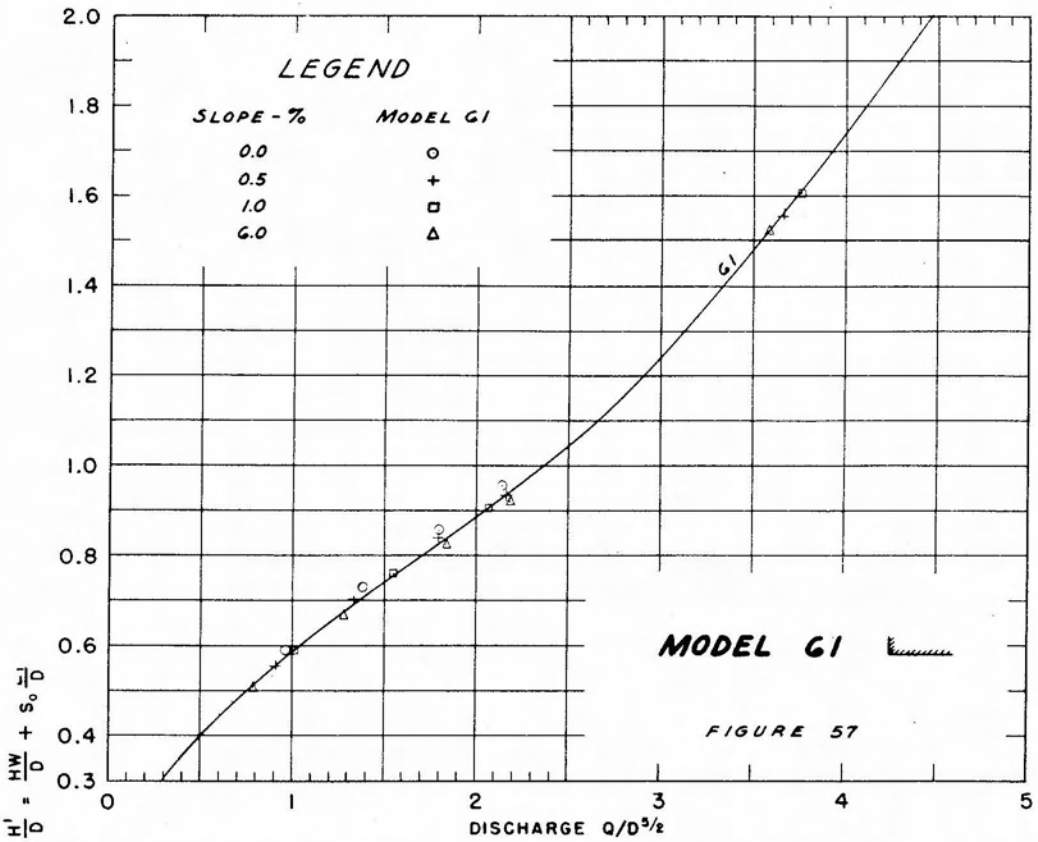

FIGURE 57

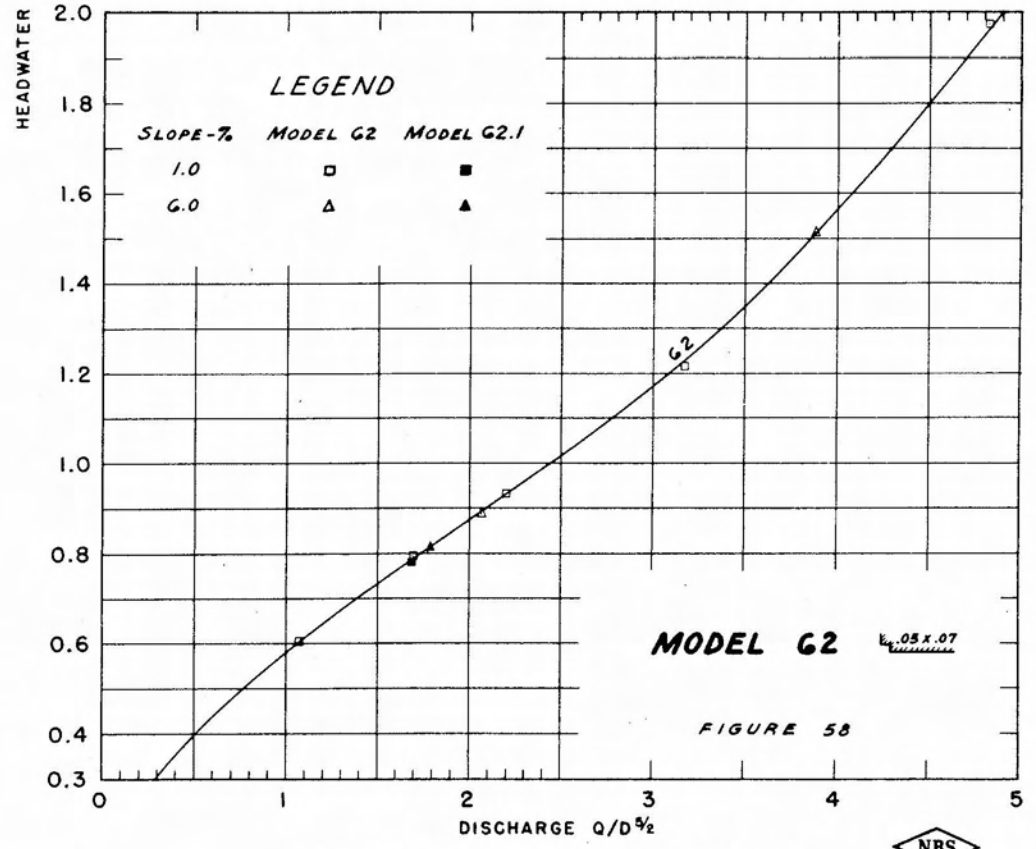

FIGURE 58

NBS

TYPE 2 CULVERTS $H'/D < 2$

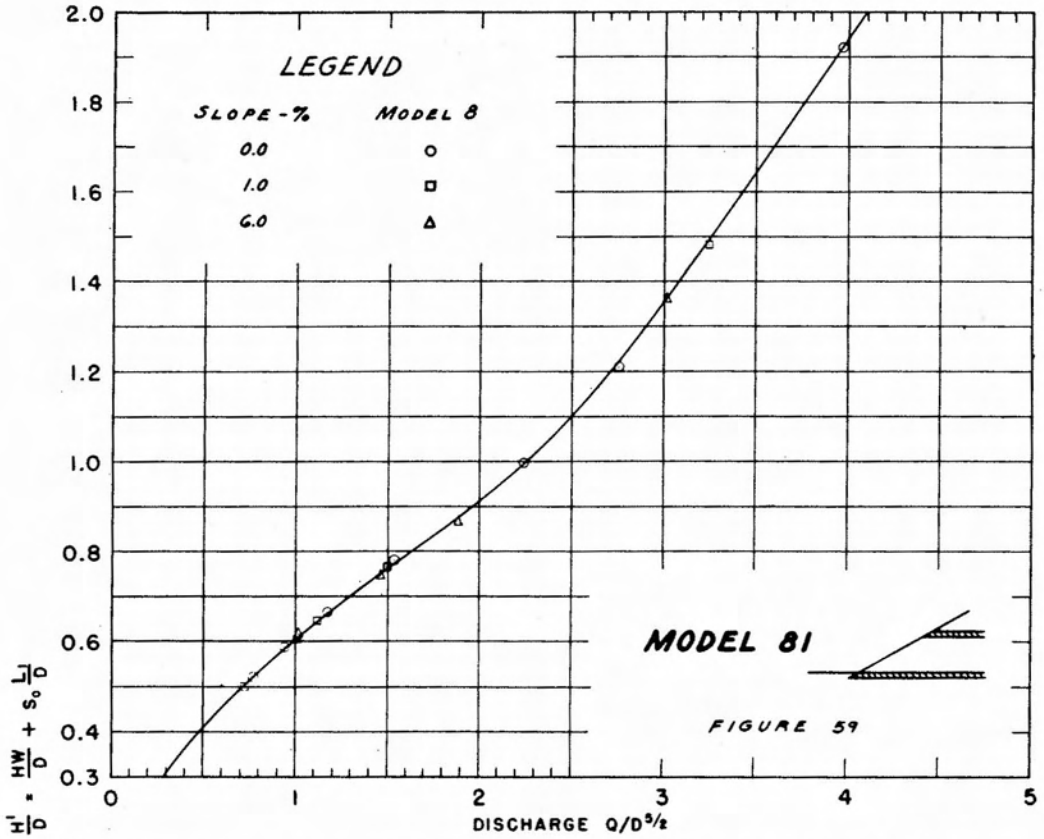

FIGURE 59

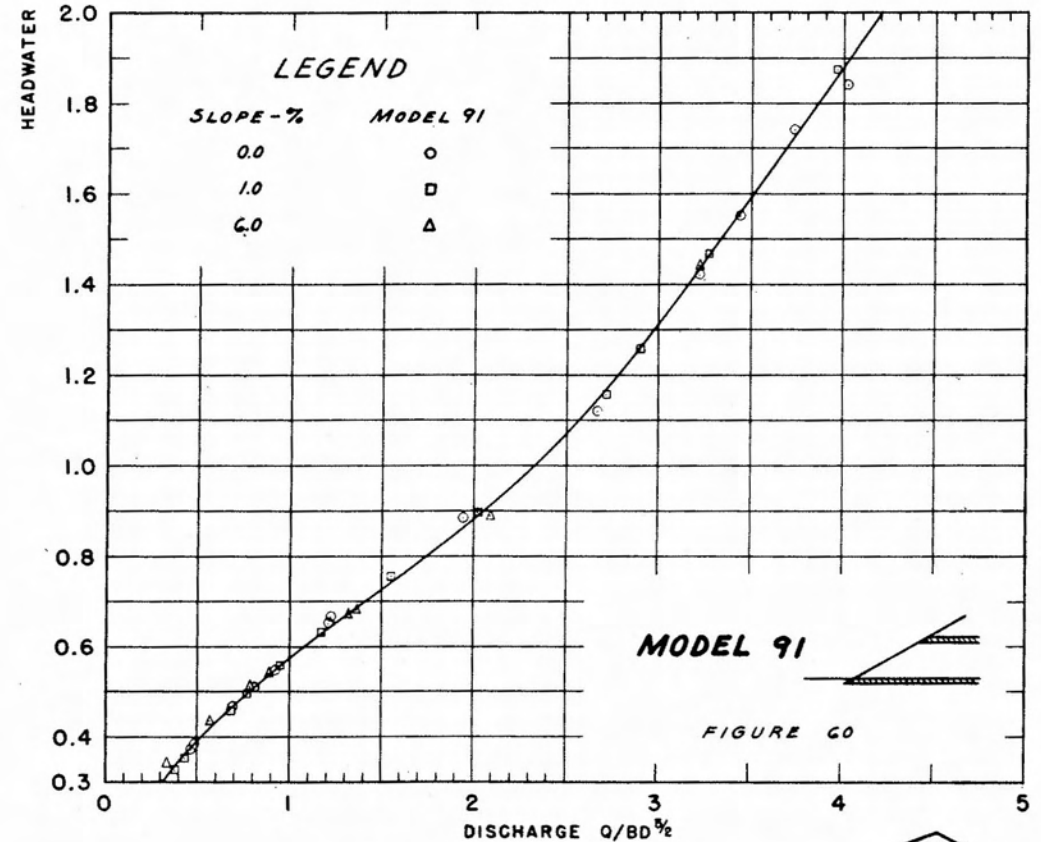

FIGURE 60

NBS

TYPE 3 CULVERTS $H'/D < 2$

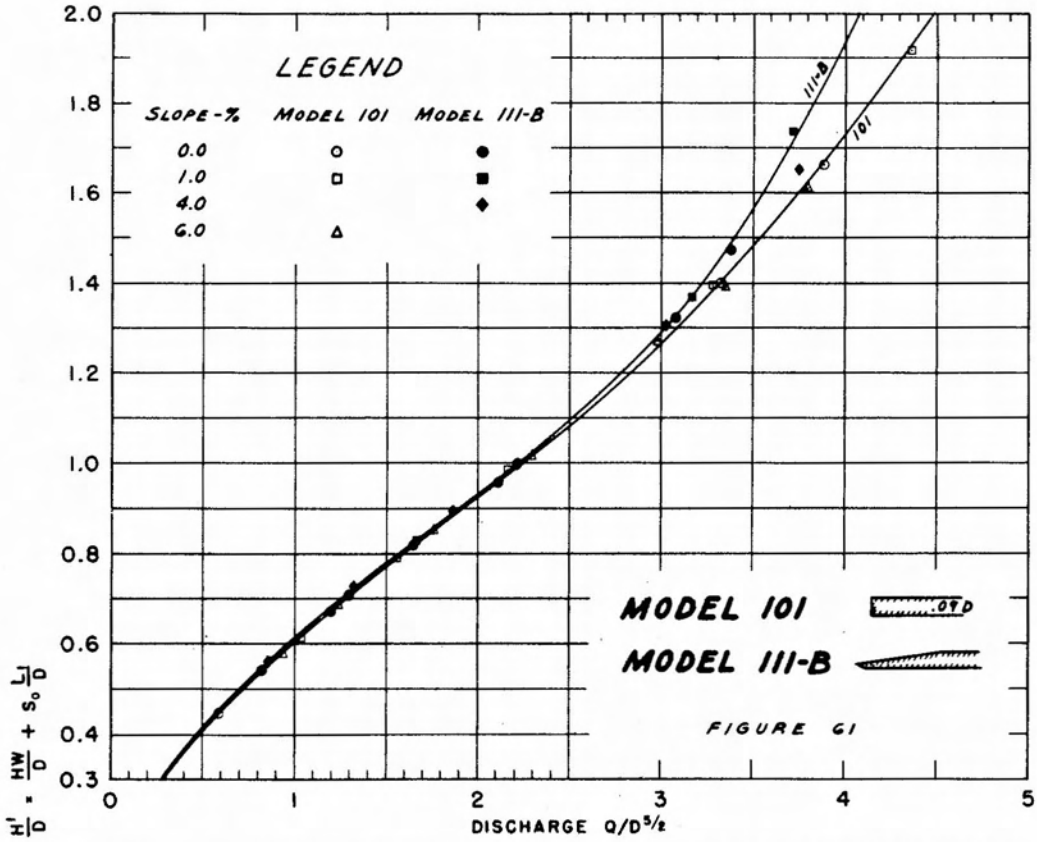

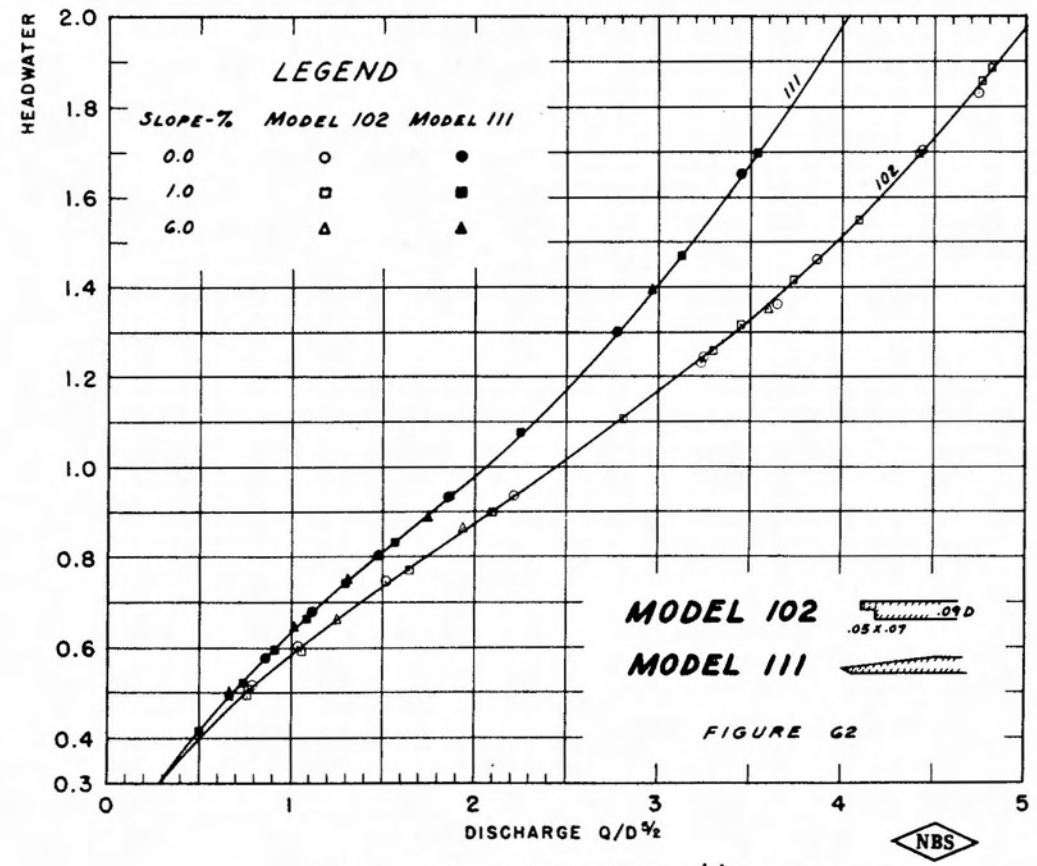

TYPE 4 CULVERTS $H'/D < 2$

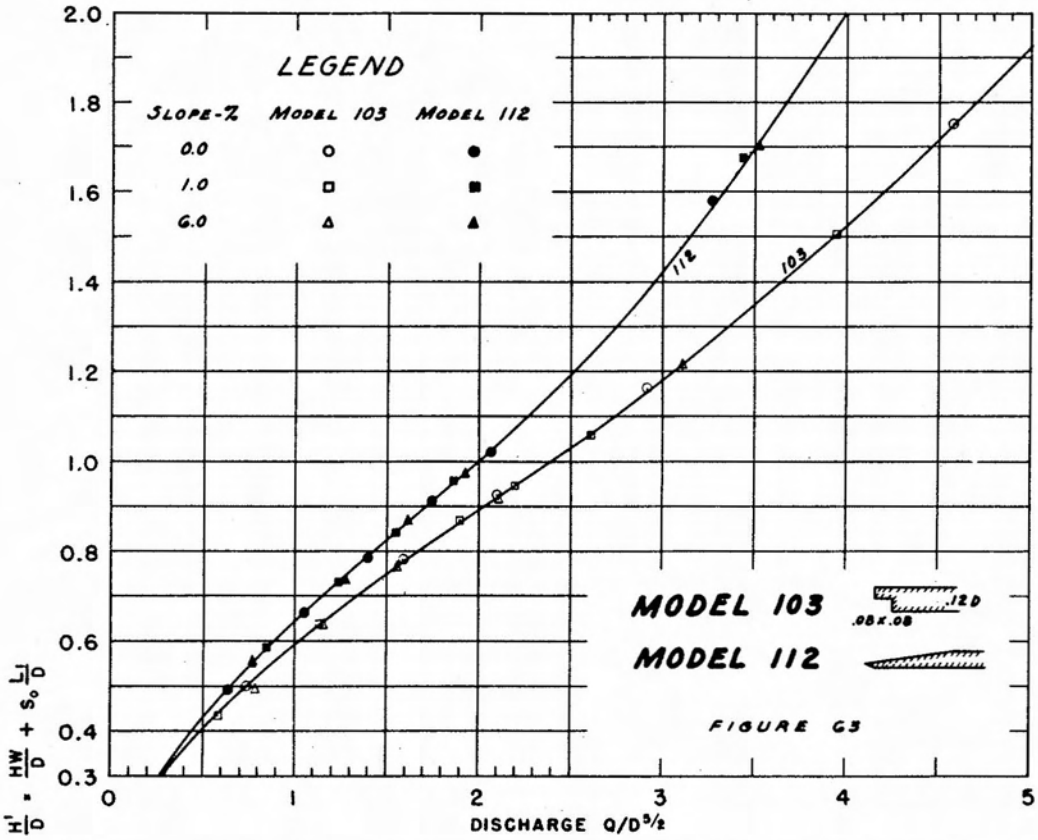

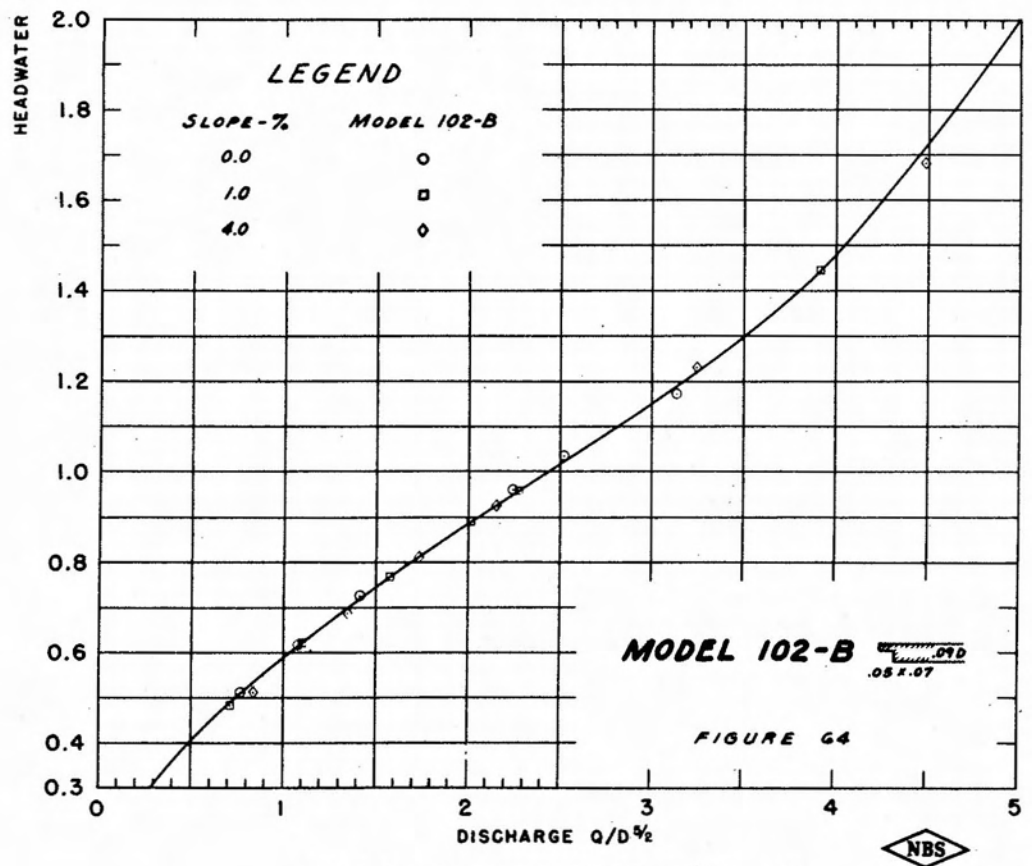

TYPE 4 CULVERTS $H'/D < 2$

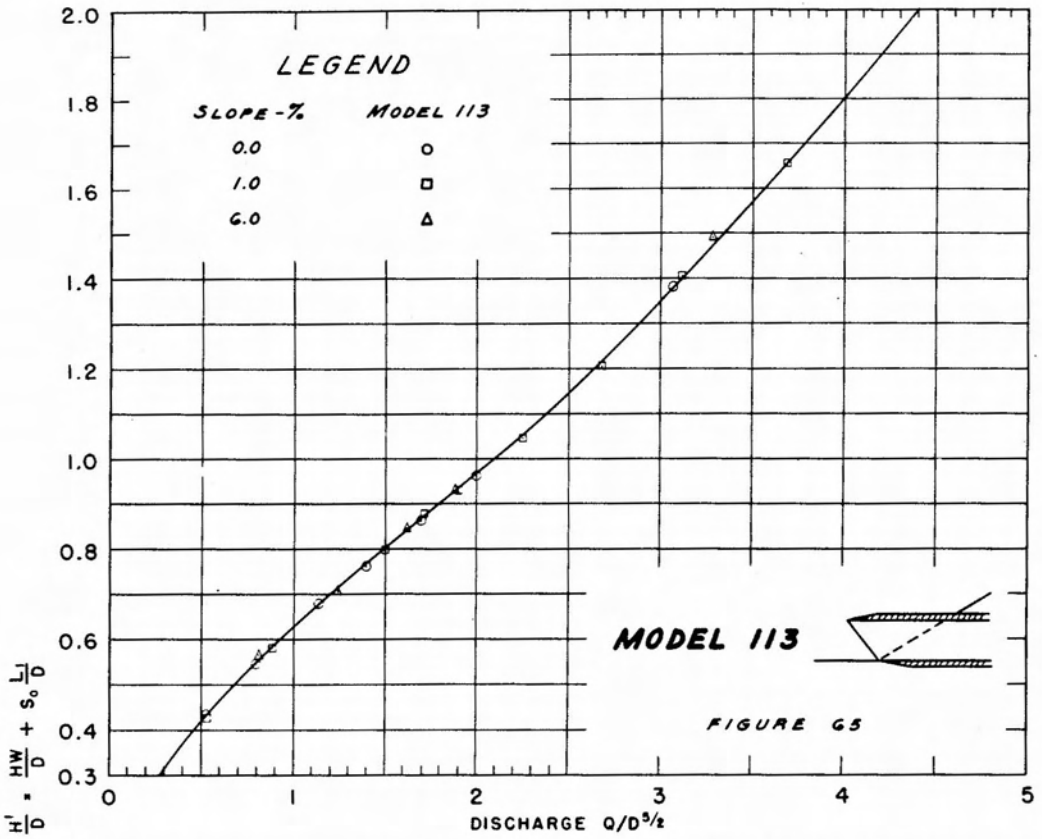

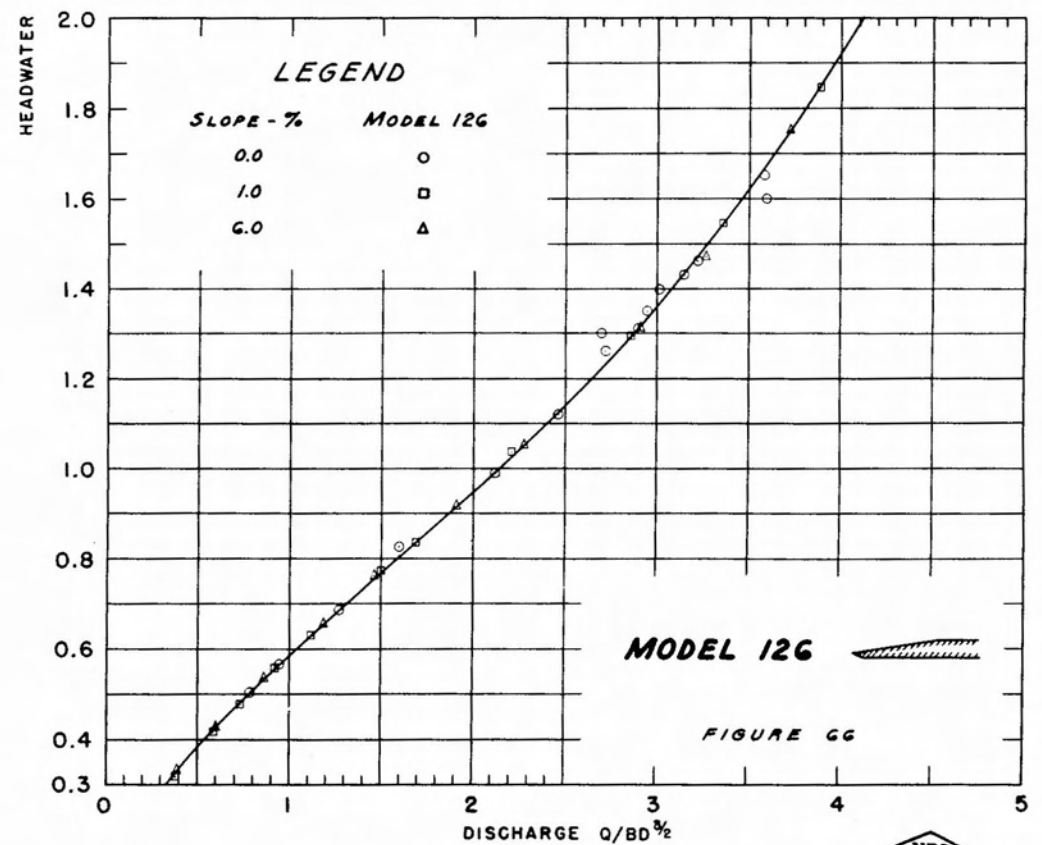

TYPE 4 CULVERTS $H'/D < 2$

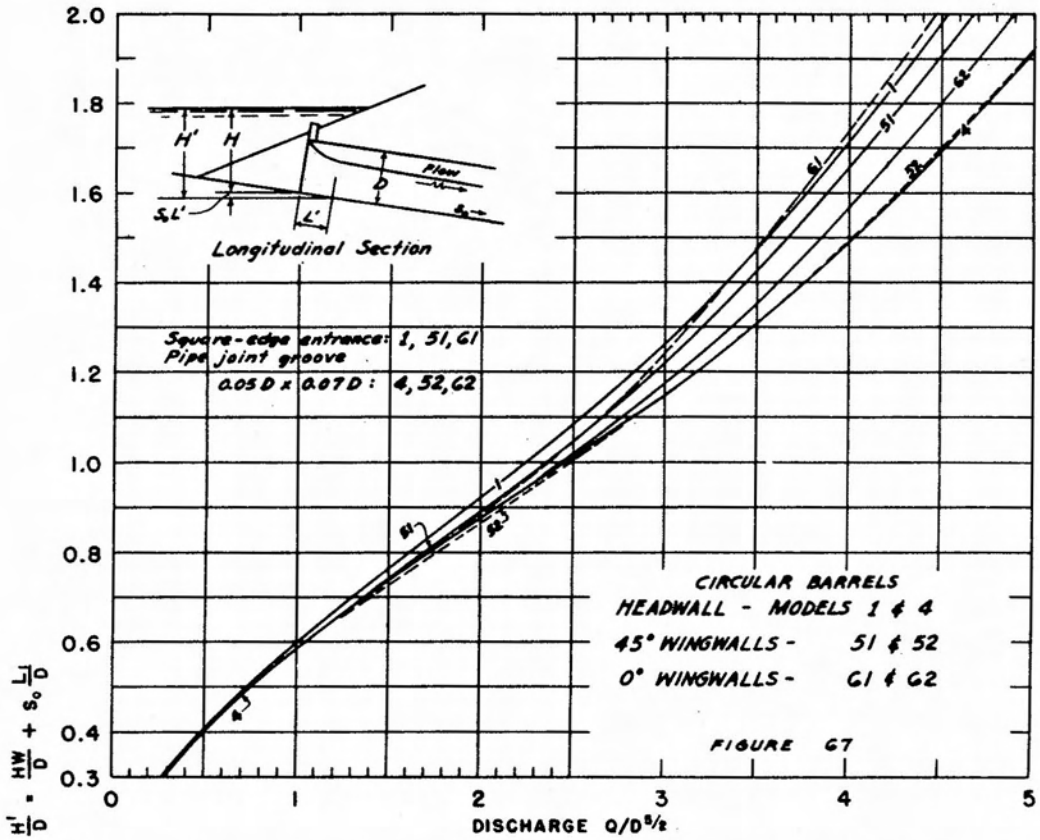

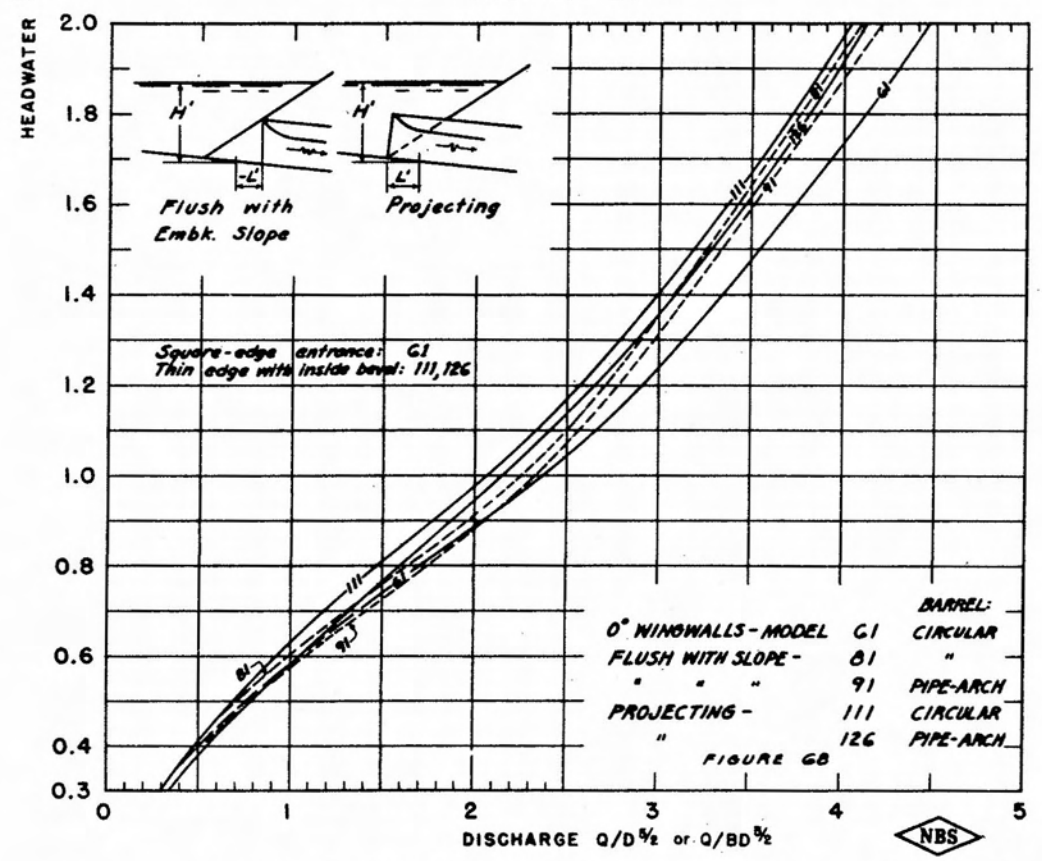

COMPARATIVE HEAD-DISCHARGE CURVES

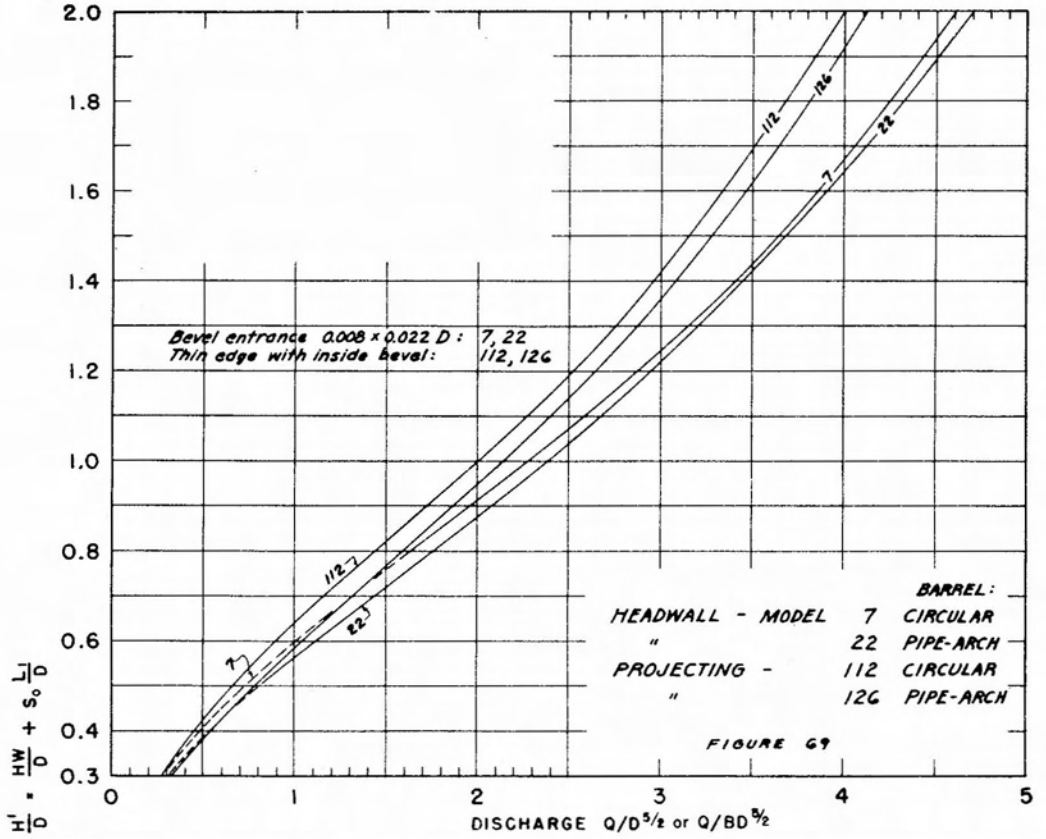

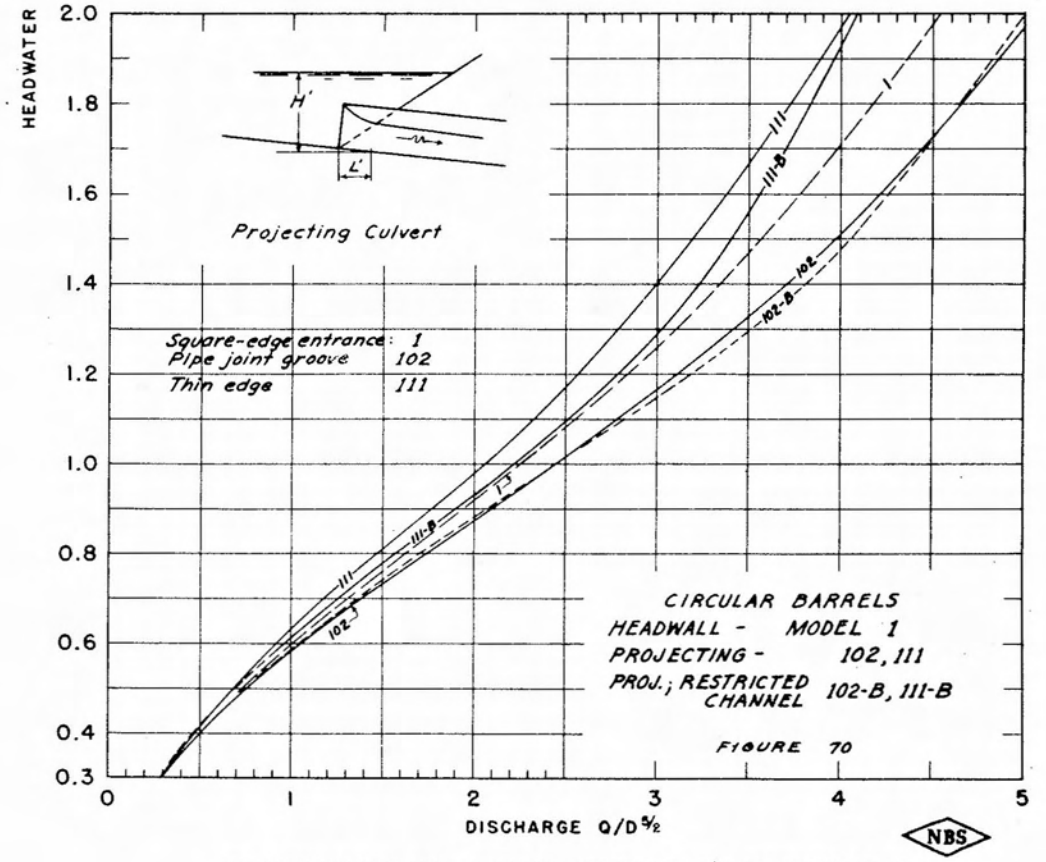

COMPARATIVE HEAD-DISCHARGE CURVES

APPENDIX B

In tables 7 to 33 are given the experimental observations reported herein. Under remarks part full flow and full flow are indicated by P.F. and F.F., respectively.

Table 7

Experimental Observations Model 1

Temperature 21° C

$Q/D^{5/2}$	H/D	S	Remarks	$Q/D^{5/2}$	H/D	S	Remarks
.782	.510	1%		6.14	3.10	0.0	P.F.-intermittent vortex
1.20	.654			6.92	3.74		" " "
1.52	.761			7.77	4.56		P.F.-vortex
1.82	.854			8.97	5.89		" -no vortex
2.02	.918			.650	.435	6%	
2.73	1.16		P.F.	1.148	.615		
3.99	1.70		"	1.43	.710		
4.92	2.20		" -vortex	1.77	.814		
6.03	3.00		" "	2.16	.933		
7.29	4.12		"	2.66	1.09		P.F.
2.61	1.11		"	3.95	1.65		"
2.37	1.03		"	4.81	2.12		" -small vortex
3.26	1.36		"	5.64	2.67		" -intermittent vortex
4.58	2.02		" -vortex	6.75	3.59		" " "
7.92	4.70		" "	8.06	4.82		" " "
9.02	5.98		" -no vortex	8.84	5.72		" " "
.712	.496	0.0		3.80	1.57		" " "
1.22	.680			6.00	2.92		" " "
1.53	.774			7.54	4.29		" -no vortex
2.13	.960			3.80	1.58		P.F.
2.51	1.08		P.F.	5.80	2.78		" -intermittent vortex
3.86	1.64		"	7.54	4.32		" " "
5.07	2.36		" -intermittent vortex	8.84	5.69		" -no vortex

Table 8

Experimental Observations Model 1.1

Temperature 15° C

$Q/D^{5/2}$	H/D	S	Remarks	$Q/D^{5/2}$	H/D	S	Remarks
.702	.488	0.0		6.08	2.96	1%	P.F.-no vortex
.944	.580			6.66	3.39		" -vortex
1.25	.684			7.30	3.90		" "
1.64	.806			8.24	4.81		" -no vortex
1.91	.886			9.22	5.84		" -intermittent vortex
2.29	.995			.804	.512	↓	
2.72	1.13		Jump 6 Diameters downstream of ent.	.804	.489	6%	
3.02	1.24		P.F.	1.59	.750		
3.24	1.33		"	2.48	1.01		P.F.
3.47	1.43		"	2.97	1.19		"
3.98	1.65		"	3.81	1.55		"
4.65	2.01		" -small vortex	4.70	2.03		" -strong vortex
5.62	2.64		" -no vortex	5.88	2.75		" -vortex
6.15	3.01		"	6.16	2.93		" -strong vortex
6.75	3.43		" -vortex	6.96	3.61		" -vortex
7.29	3.96		" -intermittent vortex	7.46	4.04		" -no vortex
8.40	4.99		" -no vortex	4.04	1.68		"
9.26	5.86		"	5.93	2.82		" -intermittent vortex
9.22	5.84	↓	"	7.54	4.22		" " "
1.68	.802	1%		9.05	5.82		" -no vortex
.806	.511			8.43	5.07	↓	" -vortex
2.49	1.05		P.F.	5.62	2.68	1%	" -no vortex (Temp. 22° C)
4.53	1.94	↓	" -vortex	7.04	3.76		" -vortex (Temp. 22° D)
				7.92	4.60	↓	" -vortex (Temp. 22° C)

Table 9

Experimental Observations Model 2

Temperature 16° C

$Q/D^{5/2}$	H/D	S	Remarks	$Q/D^{5/2}$	H/D	S	Remarks
.831	.540	0.0		8.31	4.23	1%	P.F.-vortex
2.00	.899			4.65	1.84		" -intermittent vortex
6.24	2.19		F.F.-vortex	10.85	4.72		F.F. " "
8.35	3.16		" "	11.92	5.43		" -no vortex
10.56	4.60		" "	1.70	.783	↓	
11.23	5.07		" -no vortex	1.70	.758	6%	
12.18	5.87		" "	2.57	1.00		
3.88	1.33		"	4.53	1.75		P.F.-small vortex
1.24	.672	↓		6.07	2.57		" -intermittent vortex
1.24	.655	1%		7.26	3.41		"
6.13	2.65		P.F.-vortex	11.37	4.44		F.F.-no vortex
7.15	3.38		" "	12.21	5.13		" " "
2.02	.876	↓		13.35	5.98	↓	" " "

Table 10

Experimental Observations Model 3

Temperature 12° C

$Q/D^{5/2}$	H/D	S	Remarks	$Q/D^{5/2}$	H/D	S	Remarks
1.68	.806	0.0		6.33	2.60	1%	P.F.-vortex
2.42	1.01			7.18	3.12		" "
3.17	1.19		F.F. except for 3" at outlet	9.08	3.56		F.F.-vortex
4.21	1.42		F.F.	9.29	3.59		"
4.88	1.61		"	10.11	4.12		" "
5.90	2.34		P.F.	12.29	5.69		" -no vortex
6.20	2.55		" -vortex	1.95	.856	↓	
6.74	2.85		" "	1.95	.822	6%	
7.14	3.11		" "	2.53	.986		
5.88	2.04		F.F.-vortex	3.26	1.20		P.F.
6.88	2.52		" "	3.94	1.42		"
7.82	3.02		" "	4.54	1.66		"
8.94	3.54		" "	5.39	2.06		" -vortex
9.72	3.98		" "	6.42	2.60		" "
11.46	5.19		" -no vortex	7.18	3.12		" "
12.32	5.92		" " "	7.88	3.59		" "
9.68	4.04	↓	F.F.	8.45	4.03		" -no vortex
1.71	.788	1%		11.20	4.22		F.F.-no vortex
2.51	1.02		P.F.	12.67	5.35		" "
3.30	1.24		"	13.39	6.06		" "
3.81	1.42		"	8.76	2.76		F.F.-vortex
4.46	1.65		"	9.44	3.15		" "
5.29	2.07	↓	" -vortex	10.14	3.48	↓	"

Table 11

Experimental Observations Model 4

Temperature 16° C

$Q/D^{5/2}$	H/D	S	Remarks
.702	.481	0.0	
1.01	.595		
8.70	3.27		F.F.-vortex
1.21	.658		
1.67	.794		
1.93	.866		
2.31	.967		
2.72	1.08		P.F.
3.20	1.18		F.F.-no vortex
4.24	1.37		" -small vortex
4.76	1.54		" " "
6.40	2.67		P.F.-intermittent vortex
6.17	2.05		" -vortex
7.18	2.48		F.F.-vortex
8.50	3.04		F.F.-intermittent vortex
7.78	2.71		" " "
9.02	3.43		" -vortex
10.08	3.98		" "
11.83	5.14		" "
12.85	5.88		" "
3.74	1.28	↓	" -no vortex
.700	.460	1%	
1.76	.783		
2.81	1.08		P.F.
3.15	1.18	↓	"
4.82	1.83	1%	P.F.-vortex
6.40	2.66		" "
7.36	3.28		" -no vortex
8.66	3.03		F.F.-intermittent vortex
10.38	4.07	↓	" -vortex
4.97	1.86	6%	P.F.-vortex
6.94	2.94		" -large vortex
7.54	3.32		" -intermittent vortex
8.56	4.12		" " "
.875	.478	↓	

Temperature 22.6° C

$Q/D^{5/2}$	H/D	S	Remarks
.710	.437	1%	
1.08	.595		
1.42	.700		
1.70	.782		
1.95	.854		
2.17	.910		
2.92	1.12		P.F.
3.80	1.41		"
4.75	1.79		" -intermittent vortex
5.31	2.07		" " "
4.22	1.60		" " "
2.52	1.01		" -no vortex
6.44	2.70		" " "
8.73	3.23		F.F.
3.23	1.22		P.F.-no vortex
7.96	3.68	↓	P.F.-intermittent vortex

Table 12

Experimental Observations Model 4 - Sanded

Temperature 15.1° C

$Q/D^{5/2}$	H/D	S	Remarks	$Q/D^{5/2}$	H/D	S	Remarks
9.35	3.61	1%	F.F.-vortex	6.62	2.76	6%	P.F.
12.68	5.64	↓	" "	8.31	3.97	↓	"
5.28	2.05		P.F.-vortex				
7.57	3.42	↓	" "				

Table 13

Experimental Observations Model 4-B

Temperature 14.9° C

$Q/D^{5/2}$	H/D	S	$v_o^2/2gD$	Remarks	$Q/D^{5/2}$	H/D	S	$v_o^2/2gD$	Remarks
1.66	.78	0.0	.04		9.44	5.31	1%		P.F.-no vortex
4.64	1.40	↓	.06	F.F.	10.53	6.23	↓		" " "
6.86	3.16	↓		P.F.-large vortex	1.54	.74	4%	.03	
1.62	.77	1%	.04		5.18	1.38	↓	.07	Flow is between that of full and slug flow
4.79	1.35	↓	.07	F.F.					
5.54	2.30	↓		P.F.-vortex	6.22	1.50	↓	.09	F.F.-no vortex
7.85	3.76	↓		" "	8.28	4.19	↓		P.F.

Table 14

Experimental Observations Model 5

Temperature 13° C

$Q/D^{5/2}$	H/D	S	Remarks	$Q/D^{5/2}$	H/D	S	Remarks
.795	.507	0		3.52	1.25	0	F.F.
1.80	.816			3.62	1.26		"
2.15	.916			3.71	1.28		"
1.58	.758			3.22	1.20		"
3.46	1.211		F.F.	3.01	1.15		"
4.64	1.45		" -vortex	2.92	1.13		"
5.68	1.76		" "	2.74	1.10		
6.61	2.16		" "	2.53	1.02		
7.25	2.51		" "	2.24	.958		
7.96	2.71		" "	2.02	.888		
8.59	3.00		" "	1.79	.836		
10.42	4.02		" "	5.56	2.06		P.F.
11.97	5.02		" "	6.45	2.51		"
13.52	6.18		" "	7.88	3.20		"
2.53	1.02		P.F.	9.12	3.15		F.F.
4.38	1.40		F.F.	4.98	1.58		F.F.-slight vortex
3.32	1.20		"	6.29	2.40		P.F.
2.61	1.05		P.F.	6.46	2.48		P.F.
2.82	1.11		Pipe flows full 3/4 of its length	7.40	2.99		"
3.39	1.21		F.F.	9.50	3.49		F.F.
3.92	1.30		"	11.16	4.49		"
4.36	1.40		"	5.03	1.58		" -vortex
2.40	.995			6.62	2.21		" "
2.55	1.04		P.F.	7.26	2.49		" "
2.87	1.12		Flowing full for 0.9 of length	5.79	2.17	↓	P.F.
3.23	1.19		F.F.	2.06	.876	1%	
3.31	1.20		F.F.	2.42	.972		
3.39	1.22	↓	F.F.	2.72	1.05	↓	

Table 14 (continued)

Experimental Observations Model 5

Temperature 13° C

$Q/D^{5/2}$	H/D	S	Remarks	$Q/D^{5/2}$	H/D	S	Remarks
2.92	1.09	1%	P.F.-no vortex	8.42	3.00	1%	F.F.-large vortex
3.90	1.37		P.F.-intermittent vortex	9.18	3.30		" " "
3.14	1.10		Pipe flowing full for 1/2 its length	9.78	3.51		" -intermittent vortex
4.16	1.21		F.F.	9.96	3.62		" -no vortex
5.91	1.74		F.F.-vortex	1.66	.760	↓	
7.28	2.96		P.F.-vortex	1.66	.727	6%	
6.41	2.44		" "	2.60	.987		
5.08	1.81		" "	3.48	1.22		P.F.
8.14	3.48		" "	3.93	1.36		P.F.-no vortex
9.15	3.20		F.F.-vortex	4.85	1.68		" -small vortex
10.56	4.00		" "	5.12	1.80		" " "
11.48	4.64		" "	5.62	2.01		" " "
12.50	5.45		" -large vortex	6.76	2.62		" -vortex
4.23	1.24		" -no vortex	7.50	3.04		" -occasional vortex
4.11	1.21		" " "	8.45	3.62		" "
3.79	1.20		" " "	11.69	4.10		F.F.
5.07	1.47		F.F.-vortex	12.76	4.94		F.F.-large intermittent vortex
7.18	2.45		" "	14.23	6.02		F.F.-intermittent vortex
6.63	2.12		" "	1.90	.799		
7.99	2.83		" "	9.60	2.91	↓	F.F.-intermittent vortex
7.57	2.64	↓	" "	7.40	2.51	0	F.F.-vortex

Table 15

Experimental Observations Model 6 - Smooth Lucite

Temperature 13.5° C

$Q/D^{5/2}$	H/D	S	Remarks	$Q/D^{5/2}$	H/D	S	Remarks
.816	.495	1%		8.15	3.04	1%	P.F.-vortex
1.73	.768			8.15	2.68		F.F.-vortex
5.99	2.06		P.F.-vortex	9.72	3.43	↓	" -no vortex
7.24	2.62	↓	" "				
Model 6 - Sanded Entrance - Temperature 13° C							
6.12	1.35	4%	F.F.-no vortex	9.54	3.08	6%	F.F.-strong vortex
7.40	1.96		" -vortex	11.41	3.87		" -small vortex
7.88	2.59		Pulsating flow similar to slug flow-vortex	12.92	5.16		" -vortex
				14.13	5.90	↓	" -no vortex
9.72	3.18		F.F.-vortex	1.40	.631	9.31%	
11.00	3.96		F.F.-strong intermittent vortex	2.16	.826		
13.20	5.39	↓	F.F.-no vortex	3.63	1.12		P.F.
.978	.527	6%		6.82	1.27		Slug flow
1.72	.742			7.86	1.51		F.F.-strong vortex
5.04	1.21		Slug flow	9.06	2.09		F.F.-intermittent vortex
6.48	1.26		F.F.	10.66	3.06		F.F.-vortex
8.05	2.33		F.F.-strong vortex	12.99	4.69		" "
8.62	2.69	↓	" " "	14.58	5.36	↓	" -no vortex

Table 16

Experimental Observations Model 7

Temperature 22.2° C

$Q/D^{5/2}$	H/D	S	Remarks	$Q/D^{5/2}$	H/D	S	Remarks
.859	.548	0.0		2.91	1.21	1%	P.F.
1.20	.674			4.26	1.81		" -small vortex
1.69	.814			5.90	2.85		" " "
2.10	.938			7.40	4.08		" " "
3.32	1.37		P.F.	8.80	5.49	↓	" " "
4.33	1.84		" -small vortex	.824	.492	6%	
5.74	2.72		" " "	1.20	.630		
7.60	4.30		" " "	1.72	.792		
8.89	5.62		" -no vortex	2.16	.922		
6.66	3.44	↓	" -vortex	2.72	1.11		P.F.
.792	.509	1%		5.08	2.26		" -vortex
1.45	.732			7.92	4.56		" "
1.87	.867	↓		8.31	4.96	↓	" "

Table 17

Experimental Observations Model 21

Temperature 22° C

$Q/BD^{3/2}$	H/D	S	Remarks	$Q/BD^{3/2}$	H/D	S	Remarks
.801	.490	0.0		7.55	4.21	0.0	P.F.-intermittent vortex
1.23	.639			8.86	5.47		" " "
1.54	.739			2.64	1.12	↓	P.F.
2.17	.940			.516	.397	1%	
3.48	1.42		P.F.-intermittent vortex	.629	.417		
4.32	1.82		" " "	.818	.495		
5.18	2.34		" " "	1.12	.603		
5.81	2.77		" -vortex	1.52	.732		
6.39	3.23		" "	2.05	.902		
7.26	3.92		" "	2.89	1.17		P.F.
8.08	4.70		" -small vortex	4.07	1.70		" -intermittent vortex
8.32	4.95		" " "	5.03	2.24		" " "
5.90	2.85	↓	" -vortex	6.87	3.60	↓	" " "

Table 18

Experimental Observations Model 22

Temperature 22° C

$Q/BD^{3/2}$	H/D	S	Remarks	$Q/BD^{3/2}$	H/D	S	Remarks
.339	.294	0.0		2.78	1.11	1%	P.F.
.707	.451			3.70	1.48		" -intermittent vortex
1.14	.605			4.60	1.94		" " "
1.84	.826			5.62	2.56		" -vortex
2.66	1.09		P.F.	6.29	3.06		" "
4.21	1.73		" -intermittent vortex	6.73	3.38		" "
5.42	2.43		" -intermittent vortex	7.40	3.92		P.F. -intermittent vortex
6.10	2.91		" " "	8.04	4.41		" " "
6.53	3.22		" -vortex	8.47	4.80	↓	" " "
7.94	4.39	↓	" -intermittent vortex	.407	.327	6%	
.353	.289	1%		.726	.434		
.581	.395			1.14	.576		
.828	.490			1.42	.665		
1.06	.566			1.72	.759		
1.29	.647			3.00	1.19		P.F.
1.85	.828			3.79	1.49		" -intermittent vortex
1.54	.726	↓		4.60	1.89		" " "
				5.57	2.45		" " "
				6.34	2.99		" " "
				7.74	4.14	↓	" -vortex

Table 19

Experimental Observations Model 51

Temperature 21.5° C

$Q/D^{5/2}$	H/D	S	Remarks	$Q/D^{5/2}$	H/D	S	Remarks
.848	.538	0.0		6.16	2.95	0.5%	P.F.-small vortex
1.27	.681			7.54	4.05		" -no vortex
1.69	.806			8.88	5.32		" " "
2.01	.896			.964	.568	1%	
3.67	1.31		Full flow	1.43	.716		
4.72	1.59		" "	.940	.560		
6.57	2.41		F.F.-intermittent vortex	2.19	.936		
8.08	3.35		" -vortex	3.71	1.51		P.F.
9.22	3.96		" -no vortex	6.44	3.14		P.F.-vortex
11.0	5.31		" " "	8.62	5.08		P.F.-intermittent vortex
.768	.502	0.5%		.894	.524	6%	
1.20	.646			1.55	.722		
1.64	.781			1.99	.850		
1.99	.882			4.28	1.77		
2.25	.954			5.41	2.40		P.F.-vortex
2.94	1.19		P.F.	6.78	3.39		" "
4.81	2.08		"	7.91	4.36		" -no vortex

Table 20

Experimental Observations Model 52

Temperature 22.5° C

$Q/D^{5/2}$	H/D	S	Remarks	$Q/D^{5/2}$	H/D	S	Remarks
.986	.561	1%		2.00	.826	6%	
1.59	.746			5.45	2.12		P.F.
2.00	.862			7.60	3.43		"
6.62	2.81	↓	P.F.			↓	

Table 21

Experimental Observations Model 62

Temperature 22.0° C

$Q/D^{5/2}$	H/D	S	Remarks	$Q/D^{5/2}$	H/D	S	Remarks
1.07	.597	1%		2.06	.858	6%	
1.69	.789			3.88	1.48		P.F.
2.19	.926			5.96	2.59		"
3.17	1.21		P.F.	9.02	3.30		F.F.-large vortex
4.82	1.97		P.F.	4.97	2.00		P.F.
6.40	2.88	↓	P.F.	11.09	4.55		F.F.-large vortex
				12.36	5.41	↓	" -no vortex
Model 62.1							
1.68	.774	1%		1.78	.784	6%	
4.51	1.33		F.F.	5.06	1.42		Slug flow
6.06	1.81		F.F.-no vortex	7.01	1.78		F.F.
6.89	2.20		F.F.-vortex	8.80	2.92		F.F.-large vortex
8.72	3.13		" "	11.23	4.13		" -small vortex
11.23	4.72	↓	" "			↓	

Table 22

Experimental Observations Model 61

Temperature 23° C

$Q/D^{5/2}$	H/D	S	Remarks	$Q/D^{5/2}$	H/D	S	Remarks
.958	.590	0.0		1.01	.589	1%	
1.38	.732			1.55	.760		
1.80	.857			2.06	.908		
2.14	.959			3.76	1.60		P.F.
3.55	1.33		F.F.-small vortex	6.22	3.20		P.F.-small vortex
5.20	1.86		" " "	7.77	4.50		" -no vortex
7.13	2.87		" -vortex	9.02	4.00		F.F.-vortex
8.62	3.82		" "	10.39	4.96		" "
10.71	5.37	↓	" -no vortex	11.55	5.92	↓	" -no vortex
.908	.553	0.5%		3.59	1.49	6%	P.F.
1.34	.702			5.27	2.46		" -vortex
1.80	.840			6.86	3.66		" "
2.16	.938			8.52	5.22		" "
3.66	1.55		P.F.	9.36	3.90		F.F.-vortex
5.36	2.57		" -small vortex	10.92	4.81		" "
6.74	3.60		" -vortex	.788	.506		
8.10	4.80		" -no vortex	1.28	.664		
8.03	4.73		" " "	1.84	.826		
8.78	3.82		F.F.-intermittent vortex	2.18	.922		
10.19	4.89		" " "	11.97	5.73	↓	F.F.
11.26	5.78	↓	" -no vortex				

Table 23

Experimental Observations Model 81

Temperature 14° C

$Q/D^{5/2}$	H/D	S	Remarks	$Q/D^{5/2}$	H/D	S	Remarks
1.01	.610	0.0		3.24	1.48	1%	P.F.
1.17	.666			4.36	2.19		P.F.
2.24	.996			5.50	3.04		P.F.
3.96	1.92		P.F.	6.86	4.18		P.F.-vortex
5.98	3.38		P.F.-vortex	8.00	3.84		F.F.-vortex
8.07	3.95		F.F.-intermittent vortex	9.86	5.32		F.F.-no vortex
9.15	4.88		F.F.-no vortex	10.25	5.73		F.F.-vortex
.767	.521			7.43	3.51		" "
.936	.587			1.01	.616	↓	
1.53	.781			1.01	.673	6%	
2.75	1.21		P.F.	1.46	.807		
4.74	2.42		P.F.-vortex	1.88	.925		
6.58	3.97		" "	3.01	1.36		P.F.-intermittent vortex
9.75	5.32		F.F.-no vortex	4.67	2.38		" -vortex
10.21	5.81	↓	" -vortex	6.27	3.72		" -no vortex
.725	.510	1%		8.48	3.53		F.F.-intermittent vortex
1.12	.654			10.25	5.18		" -vortex
1.49	.774	↓		11.30	6.20		" -no vortex
				7.08	4.44	↓	P.F.-intermittent vortex

Table 24

Experimental Observations Model 91

Temperature 23° C

$Q/BD^{3/2}$	H/D	S	Remarks	$Q/BD^{3/2}$	H/D	S	Remarks
.493	.379	0.0		.895	.624	6%	
.808	.508			1.36	.764		
1.22	.667			2.09	.972		
1.94	.883			3.22	1.41		P.F.-small intermittent vortex
2.98	1.41		P.F.	4.45	2.13		P.F.-vortex
.804	.505			5.47	2.82		" "
4.48	2.20		P.F.-vortex	8.91	3.85		F.F.-vortex
5.66	3.00		" "	9.37	4.31		" "
6.78	3.03		F.F.-vortex	11.28	5.79		" -small vortex intermittently
7.40	3.48		" "	.334	.426		
8.28	4.04		" -intermittent vortex	.784	.594		
9.08	4.69	↓	" -small intermittent vortex	1.32	.756	↓	
.380	.338	1%		2.71	1.15	1%	P.F.-small intermittent vortex
.678	.468			3.27	1.46		" " "
.944	.566			.427	.363		
1.17	.646			.770	.508		
1.55	.768			.474	.369	0.0	
2.02	.910			.687	.465		
2.90	1.25		P.F.	.915	.546		
3.96	1.87		" -small intermittent vortex	1.21	.650		
4.70	2.32		" -vortex	3.44	1.55		P.F.-small intermittent vortex
5.57	2.95		" "	4.02	1.84		" " "
6.17	2.58		F.F.-vortex	4.45	2.12		P.F.-vortex
7.02	3.12		" "	3.73	1.74		P.F.-small intermittent vortex
7.79	3.60		" "	3.22	1.42		" " "
8.83	4.33	↓	" "	2.66	1.12		" " "
.566	.521	6%		5.23	2.69	↓	P.F.-vortex

Table 25

Experimental Observations Model 101

Temperature 15.5° C

$Q/D^{5/2}$	H/D	S	Remarks	$Q/D^{5/2}$	H/D	S	Remarks
1.30	.707	0.0		7.78	4.63	1%	P.F.-small vortex
.583	.445			9.01	5.99		" -no vortex
2.22	.995			1.24	.678		
3.33	1.40		P.F.-vortex	1.24	.659	6%	
4.66	2.09		" "	1.76	.826		
5.88	2.94		" "	2.30	.988		
7.04	3.92		" -no vortex	2.99	1.24		P.F.-vortex
8.45	5.42		" " "	3.35	1.36		" "
3.89	1.66		" -vortex	3.80	1.58		" "
1.56	.788			4.62	2.05		" -intermittent vortex
1.56	.786	1%		5.99	2.97		" " "
1.03	.606			7.60	4.51		" -small vortex
2.16	.978			9.19	6.28		" -no vortex
3.28	1.39		P.F.-vortex	.930	.553		
4.36	1.91		" "				

Table 26

Experimental Observations Model 102

Temperature 14° C

$Q/D^{5/2}$	H/D	S	Remarks	$Q/D^{5/2}$	H/D	S	Remarks
.788	.518	0.0		3.45	1.31	1%	P.F.-vortex
1.04	.605			3.73	1.41		" "
1.51	.746			4.09	1.54		" "
2.21	.946			4.76	1.85		" "
3.24	1.23		Slug flow-vortex	6.53	2.90		" "
3.65	1.36		" " "	8.14	4.10		" "
4.43	1.70		P.F.-vortex	8.98	4.92		" "
3.25	1.24		Slug flow-vortex	4.42	1.69		" "
3.86	1.46		P.F.-vortex	12.36	5.44		F.F.-no vortex
4.74	1.83		" "	13.56	6.36		" -intermittent vortex
5.96	2.50		" "	4.82	1.88		P.F.-vortex
7.22	3.36		" -intermittent vortex	1.25	.654	↓	
8.14	4.08		" " "	1.25	.636	6%	
8.94	4.78		" -no vortex	1.94	.838		
10.10	4.07		F.F.-intermittent vortex	3.60	1.32		P.F.
11.26	4.81		" " "	5.18	2.00		P.F.-intermittent vortex
12.71	5.88		" " "	6.90	3.17		P.F.-vortex
.768	.508	↓		6.90	3.14		" -no vortex
.768	.487	1%		7.96	3.92		" -vortex
1.06	.585			8.87	4.80		" "
1.65	.766			10.78	3.65		F.F.-no vortex
2.10	.894			10.78	3.72		" -small vortex
2.81	1.10		P.F.-small vortex	13.45	5.65	↓	" -small intermittent vortex
3.30	1.25	↓	" -vortex				

Table 27

Experimental Observations Model 102-B

Temperature 20° C

$Q/D^{5/2}$	H/D	S	$v_o^2/2gD$	Remarks
.767	.485	0	.026	
1.08	.589		.030	
1.42	.687		.040	
2.25	.916		.045	
2.52	.993		.045	
3.14	1.12		.046	Slug flow
3.54	1.20		.053	F. F.
5.32	2.17			P.F.-strong vortex
7.08	3.39			P.F.-vortex
7.53	3.80			P.F.-small vortex
8.59	4.74			P.F.-no vortex
6.92	3.272			" " "
9.54	5.66	↓		" " "
.703	.450	1%	.025	
1.10	.579		.035	
1.58	.718		.041	
2.02	.839		.048	
2.28	.906	↓	.048	
3.92	1.40	1%	.042	P.F.-strong vortex
5.96	2.58			" -vortex
7.18	3.48			" -small vortex
7.68	3.96			" "
9.14	5.26			" -no vortex
8.08	4.27			" -vortex
8.42	4.60	↓		" "
.838	.457	4%	.037	
1.35	.632		.042	
1.73	.750		.043	
2.16	.863		.049	
4.49	1.64		.017	
6.30	2.84			P.F.-strong vortex
6.97	3.33			" -vortex
7.86	4.10			" -small vortex
9.05	5.23			" -no vortex
3.25	1.16	↓	.05	" " "

Table 28

Experimental Observations Model 103

Temperature 20° C

$Q/D^{5/2}$	H/D	S	Remarks	$Q/D^{5/2}$	H/D	S	Remarks
.739	.501	0.0		3.95	1.50	1%	P.F.-small vortex
1.13	.637			5.56	2.22		" " "
1.59	.780			7.46	3.30		" " "
2.10	.923			10.00	3.87		F.F.-small vortex
2.92	1.16		P.F.-vortex	12.60	5.81		F.F.-small vortex
4.58	1.75		" "	.796	.466	6%	
6.05	2.44		" "	1.16	.608		
7.25	3.20		" "	1.56	.738		
9.79	3.86		F.F.-small vortex	2.11	.888		
11.40	5.00		" " "	3.11	1.18		P.F.-vortex
.577	.437	↓		5.80	2.36		" "
.577	.428	1%		6.98	3.04		" "
1.13	.631			8.59	4.10		" -no vortex
1.58	.771			8.59	4.16		" -vortex
1.90	.865			11.41	4.30		F.F.-intermittent vortex
2.20	.940			12.36	5.02	↓	" " "
2.61	1.05	↓	P.F.-small vortex				

Table 29

Experimental Observations Model 111

Temperature 16° C

$Q/D^{5/2}$	H/D	S	Remarks	$Q/D^{5/2}$	H/D	S	Remarks
.862	.573	0.0		2.25	1.07	1%	P.F.
1.11	.673			3.54	1.69		P.F.-vortex
1.48	.802			5.11	2.86		" "
1.86	.932			6.06	3.79		" "
3.45	1.65		P.F.-vortex	7.08	5.06		" -no vortex
4.38	2.24		" "	7.88	6.06		" " "
5.21	2.95		" -small vortex	4.34	2.19		" -vortex
6.38	4.17		" -no vortex	3.13	1.46		" "
7.50	5.57		" " "	.660	.486	↓	
2.78	1.30		" " "	.660	.475	6%	
1.08	.658	↓		1.01	.616		
1.08	.656	1%		1.31	.724		
.912	.592			1.75	.864		
.740	.514			2.97	1.36		P.F.-vortex
.497	.406			4.45	2.26		" -intermittent vortex
1.30	.736			6.37	4.13		" " "
1.57	.828			7.60	5.68		" -no vortex
1.87	.930	↓		5.30	3.01	↓	" -vortex

Table 30

Experimental Observations Model 111-B

Temperature 22° C

$Q/D^{5/2}$	H/D	S	$v_o^2/2gD$	Remarks
.810	.509	0.0	.026	
1.20	.640	↓	.031	
1.65	.778		.036	
2.11	.916		.039	
3.38	1.44		.029	P.F.
4.86	2.66			"
5.61	3.35			" -vortex
6.16	3.93			" "
7.40	5.44			" -no vortex
6.82	4.68			" " "
3.08	1.28		.041	" " "
4.35	2.17			P.F. -strong vortex
.826	.516	↓	.025	
.826	.515	1%	.025	
1.24	.651	↓	.031	
1.67	.785		.036	
2.22	.946		.040	
3.17	1.33	↓	.032	P.F.

$Q/D^{5/2}$	H/D	S	$v_o^2/2gD$	Remarks
4.31	2.17	1%		P.F. -strong vortex
5.62	3.38	↓		" -vortex
6.24	4.03			" -small vortex
7.27	5.29			" -no vortex
7.96	6.15			" " "
3.72	1.72	↓	.008	" -strong vortex
.854	.519	4%	.025	
1.32	.674	↓	.033	
1.86	.835		.039	
2.22	.934		.041	
3.02	1.24		.044	P.F.
3.74	1.62		.01	" -no vortex
4.76	2.54			" -strong vortex
5.72	3.47			" -vortex
6.27	4.06			" -small vortex
7.18	5.18			" -no vortex
7.74	5.96	↓		" " "

Table 31

Experimental Observations Model 112

Temperature 17.2° C

$Q/D^{5/2}$	H/D	S	Remarks	$Q/D^{5/2}$	H/D	S	Remarks
.634	.488	0.0		1.87	.950	1%	
1.05	.660			3.44	1.67		P.F.-small vortex
1.40	.788			4.94	2.83		" -intermittent vortex
1.75	.910			6.20	4.03		" -no vortex
2.07	1.02		P.F.	7.96	6.38		" " "
3.27	1.58		" -small vortex	.771	.544	↓	
4.30	2.22		" -vortex	.771	.532	6%	
5.04	2.88		" -small vortex	1.281	.708		
6.32	4.22		" " "	1.62	.840		
7.54	5.80		" -no vortex	1.93	.946		
.852	.580			3.52	1.67		P.F.-intermittent vortex
1.24	.725	1%		4.93	2.73		" -vortex
1.55	.836	↓		6.36	4.27		" -no vortex
8.52	.578	↓		7.60	5.91	↓	" " "

Table 32

Experimental Observations Model 113

Temperature 18° C

$Q/D^{5/2}$	H/D	S	Remarks	$Q/D^{5/2}$	H/D	S	Remarks
.803	.547	0.0		2.25	1.04	1%	P.F.-vortex
1.14	.674			2.68	1.20		" "
1.40	.761			3.69	1.65		" "
1.70	.862			3.12	1.40		" "
2.00	.961			4.86	2.14		F.F.-vortex, much air flowing (a)
3.07	1.38		P.F.-vortex	4.86	2.08		F.F.-no vortex (b)
4.73	2.12		(Much air flowing in culvert. Proper designation of type of flow doubtful.)	(a) and (b) alternate with a period of approximately 2 minutes.			
				6.76	2.88	1%	F.F.-intermittent vortex
				8.03	3.84		" " "
5.58	2.46		(F.F. Much air in form of bubbles flowing through pipe. - vortex)	10.00	5.55		" " "
				.814	.539	6%	
7.22	3.33		F.F.-intermittent vortex	1.24	.683		
8.14	4.05		" " "	1.62	.819		
9.78	5.52		" " "	1.89	.908		
10.95	6.71		" -no vortex	3.28	1.46		P.F.-intermittent vortex
				6.16	1.85		F.F. " "
.534	.431			8.00	3.08		" " "
.534	.424	1%		8.00	3.20		" -vortex
.894	.578			9.50	4.53		" -no vortex
1.50	.791			10.81	5.82		" " "
1.72	.872						
1.90	.927						

Table 33

Experimental Observations Model 126

Temperature 23.5° C

$Q/BD^{3/2}$	H/D	S	Remarks	$Q/BD^{3/2}$	H/D	S	Remarks
.331	.294	0.0		.934	.559	1%	
.593	.423			1.12	.630		
.784	.502			1.50	.769		
.949	.565			1.69	.837		
1.27	.687			2.21	1.03		P.F.
1.61	.824			2.87	1.29		" -vortex
2.12	.988			3.36	1.54		" "
2.90	1.31		P.F. -vortex	4.48	2.27		" "
3.60	1.60		" "	4.94	2.70		" -small intermittent vortex
4.44	2.23		" "	6.00	3.67		" " "
5.18	2.88		" -intermittent vortex	6.87	4.59		" " "
5.66	3.31		" " "	7.94	5.85		" " "
2.70	1.30		" -vortex	3.89	1.84	↓	" -vortex
6.15	3.83		" -small intermittent vortex	.386	.331	6%	
7.07	4.84		" " "	.600	.423		
7.79	5.47		" " "	.862	.537		
3.22	1.46		" -vortex	1.19	.643		
2.46	1.12		" "	1.46	.746		
3.05	1.40		" "	2.28	1.02		P.F.
2.95	1.35		" "	3.27	1.44		P.F. -intermittent vortex
3.15	1.43		" "	1.91	.897		
2.72	1.26		" "	2.91	1.28		P.F. -intermittent vortex
3.58	1.65		" "	3.73	1.72		" " "
7.70	5.60		P.F.	4.40	2.19		" -vortex
7.65	5.53	↓	"	4.98	2.67		" "
.385	.322	1%		5.95	3.60		" -small intermittent vortex
.581	.414			7.02	4.70		" -no vortex
.726	.476			7.60	5.50	↓	" -small intermittent vortex
.924	.557	↓					

THE NATIONAL BUREAU OF STANDARDS

Functions and Activities

The functions of the National Bureau of Standards are set forth in the Act of Congress, March 3, 1901, as amended by Congress in Public Law 619, 1950. These include the development and maintenance of the national standards of measurement and the provision of means and methods for making measurements consistent with these standards; the determination of physical constants and properties of materials; the development of methods and instruments for testing materials, devices, and structures; advisory services to Government Agencies on scientific and technical problems; invention and development of devices to serve special needs of the Government; and the development of standard practices, codes, and specifications. The work includes basic and applied research, development, engineering, instrumentation, testing, evaluation, calibration services, and various consultation and information services. A major portion of the Bureau's work is performed for other Government Agencies, particularly the Department of Defense and the Atomic Energy Commission. The scope of activities is suggested by the listing of divisions and sections on the inside of the front cover.

Reports and Publications

The results of the Bureau's work take the form of either actual equipment and devices or published papers and reports. Reports are issued to the sponsoring agency of a particular project or program. Published papers appear either in the Bureau's own series of publications or in the journals of professional and scientific societies. The Bureau itself publishes three monthly periodicals, available from the Government Printing Office: The Journal of Research, which presents complete papers reporting technical investigations; the Technical News Bulletin, which presents summary and preliminary reports on work in progress; and Basic Radio Propagation Predictions, which provides data for determining the best frequencies to use for radio communications throughout the world. There are also five series of nonperiodical publications: The Applied Mathematics Series, Circulars, Handbooks, Building Materials and Structures Reports, and Miscellaneous Publications.

Information on the Bureau's publications can be found in NBS Circular 460, Publications of the National Bureau of Standards ($1.25) and its Supplement ($0.75), available from the Superintendent of Documents, Government Printing Office. Inquiries regarding the Bureau's reports and publications should be addressed to the Office of Scientific Publications, National Bureau of Standards, Washington 25, D. C.


NBS